ABSTRACT

Title of Dissertation: **TLR9 ACTIVATION AS IMMUNOTHERAPY IN A MURINE MODEL OF METASTATIC LYMPHANGIOLEIOMYOMATOSIS**

Oluwamayowa Amosu
Doctor of Philosophy, 2024

Dissertation Directed by: Associate Professor Katharina Maisel
Department of Bioengineering

Pulmonary Lymphangioleiomyomatosis (LAM) is a slow progressing, metastasizing neoplasm primarily affecting women of reproductive age, marked by abnormal growth of smooth muscle-like cells leading to cystic lung destruction. Rapamycin, the only approved treatment for LAM, slows disease progression but ~40% of patients have partial or no response to treatment. There is an urgent need for new treatments. Research shows that LAM has hallmarks of cancer, like expression of immune checkpoint receptors, and is responsive to immune checkpoint inhibition in mouse models. This suggests that other anti-cancer strategies could be effective in treating LAM. In this thesis, we investigated toll like receptor (TLR) activation using intranasal administration of CpG, a TLR9 agonist, as LAM immunotherapy. We used a mouse model of metastatic LAM to determine survival after biweekly intranasal CpG therapy (10μg/ 5μg) with and without systemic α-PD-1, rapamycin, or α-CD317 therapy. We used ELISA to measure the cytokine profile and flow cytometry to quantify cell populations and characterize differences in the immune response between CpG-treated and untreated LAM lungs. We found that CpG treatment enhanced

median survival from 32 to 60 days in murine LAM. Survival benefit of CpG treatment was inversely dose-dependent and more effective during early stages of disease. CpG-treatment was synergistic with both α-PD-1 checkpoint inhibition and rapamycin, with survival increasing from 60 days (CpG) to 71 days (CpG + α-PD-1) and 100 days (CpG + Rapamycin). Histological analysis showed that CpG treatment decreased the LAM nodule burden but inevitably caused tissue inflammation. Efficacy of CpG treatment in LAM is facilitated in part by plasmacytoid dendritic cells through decreased regulatory T cell numbers, priming of Th17 cells, and increased secretion of inflammatory and cytotoxic cytokines by CD8 T cells. Our findings suggest that adjuvant immunotherapy, like CpG, may offer new treatment strategies for LAM that are compatible with the current standard of care, rapamycin.

TLR9 ACTIVATION AS IMMUNOTHERAPY IN A MURINE MODEL OF METASTATIC LYMPHANGIOLEIOMYOMATOSIS

by

Oluwamayowa Amosu

Dissertation submitted to the Faculty of the Graduate School of the
University of Maryland, College Park, in partial fulfillment
of the requirements for the degree of
Doctor of Philosophy
2024

Advisory Committee:

Dr. Katharina Maisel, *Chair*

Dr. Gregg Duncan

Dr. Steven Jay

Dr. Margaret Scull

Dr. Wenxia Song, *Dean's Representative*

Acknowledgements

Completing this dissertation has been a profoundly enriching and demanding journey, one that I could not have embarked on, or completed, without the steadfast support of a community that has nurtured, inspired, and challenged me the entire way.

Firstly, my deepest thanks to my family —my parents, sisters, and the extended chorus of aunties and uncles—your unwavering belief in my potential has been my foundation. You all have infused my life with love and laughter, providing encouragement, support, and prayer at every turn, and anchoring me during the most challenging periods.

To my dearest friends, to my roommates both old and new, to my neighbors and my graduate school colleagues, you all have contributed to this adventure in immeasurable ways. Your companionship, imbued with endless joy, humor, and inspiration has been a source of comfort, rest, and renewal throughout this rigorous academic pursuit. Thank you!

Dr. Katharina Maisel, your guidance as my advisor has been nothing short of transformative. Your patience and insightful mentorship have been crucial to building my confidence as a scientist and helping me find my own way as I start my career. I cannot thank you enough. To all my colleagues in the Maisel Lab, thank you for the collaborative spirit and easy camaraderie— you made the day-to-day of lab a welcoming and supportive space, even when the research was frustrating. A special thanks to Dr. Jake McCright, Bennett Yang, Kaitlyn Moore, Havish Gadde, and Mehul Donthi who supported the research presented in this thesis with long hours, early mornings, and late nights.

To the incredible female role models who believed in my potential and encouraged my career decisions: Dr. Il-Young Hwang, your mentorship at NIH introduced me to the intricate world of flow cytometry and immunology. The skills you taught me have been invaluable to completing this research. Dr. Mary Alice Smith, my first female boss who encouraged me to pursue my interest in immunology, you showed me the impact of leading with kindness. I deeply appreciate your encouragement throughout this journey. Lastly, I must acknowledge Kate Hodges, RN, my first research mentor. Kate, your example as a formidable woman scientist and compassionate human being in the early stages of my career helped me take my first steps into the world of research.

Each of you have made this journey possible for me. You have played different but equally significant roles, weaving a community of support that has carried me through to this point. I am immensely grateful for every challenge you helped me face and the countless ways you have helped me grow both as a scientist and as a person. This dissertation stands not only as a symbol of my academic achievements but also as a monument to the collective effort and support from each of you. Thank you, from the bottom of my heart. Thank you so, so much.

Table of Contents

Chapter 1. Introduction

Lymphangioleiomyomatosis (LAM) is a progressive rare lung disease, primarily affecting women of child-bearing age. The disease is characterized by the persistent abnormal growth of smooth muscle-like cells (LAM cells) predominantly in the lungs, with involvement of the surrounding lymphatics and kidneys. LAM cells grow in clusters and nodules eventually causing damage to healthy lung tissue, obstruction of lymphatic vessels, and the formation of thin walled cysts. LAM patients can experience a range of debilitating symptoms from shortness of breath, lung collapse, and eventual respiratory failure. The median survival of women living with LAM is roughly 30 years after disease onset and 10 years after lung transplantation (1,2).

Epidemiology and Etiology

LAM is caused by the accumulation of random inactivating mutations in both alleles in either of two tumor suppressor genes, tuberous sclerosis complex 1 or 2 (TSC1/TSC2), that encode the proteins hamartin and tuberin respectively. These proteins form a complex to negatively regulate cell growth through inhibition of a signaling pathway called mammalian target of rapamycin (mTOR). The mTOR pathway is a nutrient and energy responsive mechanism that allows cells to adapt to environmental changes and stimuli by regulation of cellular proliferation, growth, metabolism, and survival through either of two protein complexes, mTORC1 or mTORC2. These complexes have distinct but complementary functions. mTORC1 plays a role in protein and lipid synthesis, autophagy, and cellular metabolism and growth, while mTORC2 is involved in

cytoskeletal shape and motility and cell proliferation and survival. In LAM, the loss of functioning TSC1/TSC2 proteins results in insufficient negative regulation of the mTOR pathway. LAM cells are therefore characterized by overactivation of mTOR and unrestrained cellular growth and proliferation that is detached from environmental factors (3). Dysregulation of mTOR is also implicated in other conditions like cancer, diabetes, and tuberous sclerosis complex (TSC), a hereditary condition similar to LAM with in etiology and symptoms. TSC, by contrast, features a germline mutation in TSC1/TSC2 genes whereby acquisition of a random somatic mutation renders the gene non-functional and results in the proliferation of benign tumors in multiple organs and tissues including the kidneys, lungs, heart, and skin (4,5). When these benign tumors affect the lungs in individuals with TSC, the disease is categorized as TSC-LAM. When loss-of-function mutations to TSC1/TSC2 genes are acquired randomly over the course of an individual's life, and not associated with TSC, the resulting pulmonary disease is designated as sporadic LAM.

The prevalence of sporadic LAM ranges from 5 to 8 per million women (6). The prevalence of TSC-LAM is roughly 30-40 per million women (6). The recorded incidence of TSC-LAM is higher likely because patients with tuberous sclerosis are diagnosed early through regular screenings (6), while sporadic LAM isn't usually diagnosed until a patient presents with respiratory symptoms on average between 20 to 40 years old (6). For this reason, sporadic LAM is thought to be significantly underdiagnosed. LAM is difficult to diagnose because of overlapping symptoms with a range of other pulmonary conditions. In the early 2000's, high

resolution computed tomography (HRCT) became the most reliable and non-invasive diagnostic tool able to distinguish LAM from other cystic lung diseases. HRCT allows for visualization of the characteristic thin-walled cysts, also known as LAM nodules, diffused throughout the lungs (7–9). In 2006, researchers found that serum VEGF-D levels were significantly higher in LAM patients compared to healthy individuals and patients with other respiratory conditions (10–12) and elevated serum VEGF-D became a reliable biomarker used both in diagnosis and monitoring of disease progression and response to therapy (13,14). Today, these tools make early detection and accurate LAM diagnoses possible without the need for invasive transbronchial biopsy or video-assisted thoracoscopy.

The main symptom experienced by LAM patients is fatigue and dyspnea, or breathlessness, particularly during exercise or exertion. Other symptoms include persistent cough and chest pain associated with recurrent pneumothorax, or collapsed lung, which affects roughly 60% of patients (15) About 10-20% of LAM patients will require lung transplantation, to prevent respiratory failure as the disease becomes more advanced. The median survival for LAM patients is roughly 29 years from the onset of symptoms with treatment (16), but varies in individuals by disease severity at the time of diagnosis. In more aggressive cases of LAM, lung function can decline at an average rate of 5-10% every year (6).

Research and Treatment

Research into LAM has focused largely on characterizing defining features of LAM cells and investigating potential treatments.

LAM cells are referred to as “smooth muscle-like” cells because they express markers of both smooth muscle and melanocyte lineage and have been identified by diffuse expression of smooth muscle actin and variable expression of melanocyte markers like HMB-45, and receptors for estrogen and progesterone (17,18). In LAM nodules, they appear as elongated, spindle shaped cells or epithelioid cells around the pulmonary vasculature and lymphatics (19). The loss of function mutations in TSC1/TSC2 in LAM cells is associated with abnormally increased cell migration and invasiveness (20). It has been speculated that this migratory feature may allow LAM cells to traverse endothelial barriers and metastasize to other tissues using the lymphatic and circulatory systems (21). Research to determine the origin tissue of LAM cells is ongoing, but recent evidence suggests a uterine origin, which may explain it’s specificity in women (22–24).

Many preclinical studies investigating treatments options for LAM seek to target hormones, VEGF-D, or restore mTOR inhibition using rapamycin. Rapamycin works by binding to a protein subunit of the mTORC1 complex, FKBP12, and preventing the successful assembly of mTORC1 (25). It is important to note that inhibition of mTORC1 with rapamycin does not completely inhibit mTORC2 (26–28).

Research in TSC2 deficient cells lines found that exposure to rapamycin resulted in suppression of mTORC1 hyperactivity as measured by decreased cell proliferation and size, increased autophagy, and decreased secretion of proteins (29,30). Researchers also found that rapamycin reverses some of the disease

phenotypes of TSC2 deficient cells (30,31), allowing for normal cellular functions to resume. Studies using rodent models of LAM, showed that treatment with rapamycin could slow disease progression and reduce tumor sizes (32). These preclinical studies helped pave the way for a pivotal phase III clinical trial: the Multicenter International Lymphangioleiomyomatosis Efficacy and Safety of Sirolimus (MILES). This study provided robust evidence for the efficacy of sirolimus (rapamycin) in stabilizing lung function and reducing serum VEGF-D levels in LAM patients with moderate disease (31–33). As a result , the FDA approved Sirolimus, as the first (and only) treatment for LAM in 2015 (33). This marked a milestone in therapeutic outcomes for LAM and has been instrumental in improving the lives and longevity of patients globally. However, rapamycin treatment only works to slow disease progression and does not induce disease regression, reduce nodule growth or reverse tissue damage (33,34). This means that treatment must be continuous to be effective as suspension in treatment results in increased pulmonary deterioration and worse disease (33). Furthermore, about 40% of patients have partial or no response to treatment with rapamycin and it is not always well tolerated for life-long use (35). *Researchers continue looking for new therapies for LAM because there remains an urgent need for true curative treatments that can both eliminate LAM nodules and restore healthy lung function in patients suffering from LAM.*

Investigating LAM like a cancer

LAM is designated as a neoplastic growth, however, recent research suggests it has many similarities to cancer, particularly immunosuppression. In cancer,

immunosuppression is often mediated by the accumulation of suppressive immune cells such as myeloid derived suppressor cells (MDSCs) and regulatory T cells (14). Cancer cells influence the behavior and responses of immune cells in the surrounding tissue in order to suppress and evade recognition and elimination by the immune system. Mechanisms of immune evasion employed by cancer cells include decreased expression of tumor antigens and major-histocompatibility complex (MHC)-I, increased expression of immune checkpoint inhibitors, and secretion of immunosuppressive exosomes and cytokines (36). These measures along with others that support the growth and metabolic demands of proliferative cells, create and regulate a tumor microenvironment that dampens cytotoxic functions of immune cells while polarizing them towards regulatory and anti-inflammatory activities. For example, increased mTOR activation in lung cancer cells drives surface PD-L1 expression, which results in T cell exhaustion as they arrive in the tissue (37). Downregulation of MHC-1 disrupts proper antigen presentation of tumor antigens and decreased recognition of tumor cells by lymphocytes. Secretion of immunosuppressive exosomes and cytokines like IL-10 and TGF-b help shift the balance towards a local anti-inflammatory Th2 immune response, by recruiting regulatory T cells and inducing M2 polarization of tumor associated macrophages (38). Furthermore, immune cells that mature or differentiate in suppressive environments will go on to support tumor progression. Immature myeloid derived suppressor cells are not intrinsically suppressive but acquire immunosuppressive functions when they mature in the presence of tumor secreted factors. These

cells can differentiate into macrophages, dendritic cells and granulocytes allied with cancerous cells to further frustrate anti-tumor responses. Effective anti-cancer therapies promote robust T cell responses through activated dendritic cells (DCs). Recent work suggests that LAM cells use similar mechanisms as cancerous cells to evade elimination and suppress T cell responses through increased expression of PD-L1 (39). Anti-PD-1/PD-L1 and anti-CTLA-4 therapies that prevent T cell exhaustion in the LAM microenvironment were shown to enhance survival in murine models of LAM, but were not curative (39,40). This suggests that other immune stimulating anti-cancer strategies, like toll like receptor (TLR) activation, could be used to treat LAM. In this dissertation, we investigated intranasal administration of CpG, a TLR9 agonist, as anti-LAM therapy and examined its effects on the dendritic cell and T cell responses in murine LAM. We found that treatment with CpG significantly increased survival, decreased LAM nodule formation, and had additive effects when combined with rapamycin therapy in mice. These findings support immune activation as a therapeutic strategy worthy of further development for the treatment of LAM.

Summary and Dissertation Outline

This dissertation is organized as follows:

Chapter 2 provides a literature review of therapeutic strategies for LAM. This chapter focuses on the immunology of the disease and various therapies studied and tested in LAM. We highlight animal models used to study LAM and review how immune activation performs as a therapeutic strategy in other pulmonary conditions like lung cancer.

Chapter 3 contains studies evaluating the therapeutic efficacy of TRL9 activation as immunotherapy in a mouse model of LAM and characterizes the immune responses that contribute to treatment efficacy.

Chapter 4 investigates CpG in combination with low-dose rapamycin and previously evaluated immune checkpoint inhibition. We also investigate the efficacy of CpG in advanced LAM disease.

Chapter 5 summarizes the conclusions of this dissertation and outlines the ongoing and potential future work to develop TLR activation as immunotherapy for LAM.

In the **Appendices** of this dissertation, we explore alternate strategies to improve treatment outcomes with CpG. We highlight preliminary work into future directions investigating the effect of decreasing treatment by expanding time between doses, and explore nanoparticle drug delivery strategies to target the mediastinal lymph nodes and mitigate inflammation in the lung tissue. We also evaluate another well studied TLR3 agonist, Poly I:C as therapy in LAM. Lastly, I've included work on a semi-automated mechanical device that we developed for reliable dissociation of mucosal tissues, like the lungs, to produce viable single cell suspensions for the cellular analyses carried out in the preceding studies.

Chapter 2. Literature Review: Immunotherapy in LAM

Animal models to study LAM disease

LAM affects a relatively small number of patients, so the pool of patient samples available to conduct research in human cells is understandably limited. Additionally, isolating and culturing Tsc2-null cells from biopsies of LAM lung nodules is particularly difficult because these nodules consist of a mixed population of Tsc2-null disease causing cells and a variety of other wildtype cells like fibroblasts, lymphatic endothelial cells, and mast cells (41–45). A patient-derived TSC2-null cell line (621-101) was successfully cultured from kidney angiomyolipoma (46), and has been used to elucidate cellular pathways (47,48) and interactions with surrounding cells, like fibroblasts, that may contribute to disease (42,49). However, these cells differ substantially from those isolated from lung tissues and are not, on their own, a reliable model to study mechanisms of disease and therapy in pulmonary LAM. Progress in understanding the pathology of LAM disease and researching potential treatments has largely been advanced through the use and development of animal models. Given the genetic etiology of LAM, most models feature rodents with loss of function mutations in one of two Tsc2 alleles and allow researchers the added benefit of studying LAM in a complete immunological system.

Eker Rat Model

One of the earliest animal models used to study TSC and LAM was the Eker rat. This is a strain of purpose bred rats initially discovered in 1954 by Reidar Eker (50) and primarily used to study renal carcinomas. Later the propensity for these

rats to develop spontaneous kidney tumors was characterized and attributed to a germline mutation in the rat homolog of the Tsc2 gene that results in heterozygous adults (Tsc2 +/-) since loss of both alleles (Tsc2 -/-) is fatal during fetal development (51,52). Somatic loss of function mutations in these rats gives rise to Tsc2-null cell proliferation and results in TSC/LAM-like tumor lesions in the kidneys and uterus (53). Spontaneous lung lesions in the Eker rat model are not common and have only been reported at about 15 months of age (23,53). This model has been critical to understanding how Tsc2 mutations contribute to disease pathogenesis, and to studying various treatments for related conditions like uterine leiomyoma (54). For example, mTOR inhibition with rapamycin was first tested in the Eker rat model (32) and later led to clinical trials in LAM patients and eventual FDA approval as a first-line treatment for the disease (33).

Xenograft Models of LAM

Another model that researchers have used to study LAM disease are xenograft models where Tsc2-null cells of human or rodent origin are transplanted into mice or rats, typically as flank tumors, to investigate cellular mechanisms of LAM pathogenesis. From these xenograft models, scientists have uncovered the relationship between estrogen and LAM cell metastasis (55), proliferation (56), and increased prostaglandin production (57). These models have also been used to study the effects of experimental therapy on LAM cell growth (58) and identify potential therapeutic targets for LAM treatment (59).

Mouse models of LAM

Since the discovery of the Eker rat researchers have developed similar mouse models by introducing mutations into both Tsc1 or Tsc2 mouse gene homologs (60,61). Similar to the Eker model, all Tsc1 +/- or Tsc2 +/- genetically modified mice consistently develop legions of Tsc-null cells in the kidney and most feature liver hemangiomas as well (62,63). Many of these models respond favorably to mTOR inhibition and helped further support the determination to assess rapamycin in clinical trials for TSC and LAM patients. These mouse models were critical in connecting the loss of TSC1/TSC2 genes to mTOR dysregulation in affected tissues and elevated levels of the downstream product, phospho-S6 (62,64), which is still used as an identifying marker of LAM cells in current research. However, these mouse models do not readily develop lung legions that reproduce the tissue destruction seen in LAM (65) and so are not ideal for studying pulmonary LAM disease. In a uterine-specific Tsc2 knock-out mouse model that was developed to test the hypothesis of a uterine origin for LAM cells (66), about 50% of mice do eventually develop lung tumors. However, these tumors were not found in the lungs until later in the animal's lifespan (after 6 months) (67). The increased time until the incidence of lung tumor formation in this rodent model increases the chance that early tumor formation in other organs (namely the uterus and kidneys) may require mice to be euthanized long before lung metastases become established, making this a viable but imperfect model of pulmonary LAM.

The mouse model used in our studies was developed in the Krymskaya laboratory (68). Tsc2- null cells were isolated from kidney legions in heterozygous Tsc2+/- mice and injected subcutaneously to form flank tumors in immunodeficient, athymic mice. These flank tumors were then resected, dissociated, and the cells cultured ex-vivo for two days before being injected subcutaneously to form flank tumors in immunocompetent C57BL/6 mice. These flank tumors were again resected, dissociated, and the cells cultured ex-vivo for two days. The cells were designated as “TTJ” and administered via tail vein injection to immunocompetent C57BL/6 mice to reliably induce the LAM-like lung pathology within 7 days of disease induction. This model allows researchers to study Tsc2-null cells in the context of the lung tissue environment, and has been used in the investigation of potential therapies for LAM including anti-PD-1 (39), simvastatin (68), and anti-EGFR Antibody (69).

Approved treatments and therapeutic strategies in clinical trials for LAM

The discoveries from cellular and animal models of LAM have led to clinical trials and approved treatments that have changed the way the disease is managed and increased life expectancy for patients. Most therapeutic strategies involve pathways connected to mTOR signaling, like cell proliferation, and autophagy, while others provide symptom relief and disease management. Generally researchers have strategically opted to study drugs with prior FDA approval, to expedite the process of moving a promising candidate to clinical trials in LAM patients since many parameters like safety and tolerability are already well defined.

mTOR inhibitors

The indisputable link between deficiencies in TSC1/TSC2 gene products and dysregulation of mTOR offered justification for the evaluation of mTOR inhibitors as therapy for LAM. Following the success of clinical trials, the Federal Drug Administration approved the mTOR inhibitor, sirolimus, for treatment of LAM. Sirolimus (rapamycin) has been studied and characterized extensively in LAM patients (33,70–73) and clinical trials are ongoing to understand how best to maximize its therapeutic benefit (NCT03150914, NCT03304678, NCT02432560). Though not approved specifically for the treatment of LAM, everolimus (afinitor), has also been studied in LAM patients with similar results to sirolimus (74,75) and comparatively improved efficacy at reducing angiomyolipomas in TSC patients (76). Both inhibitors work to prevent the formation of the mTOR complex-1 (mTORC1) through binding of FKBP12 and preventing subsequent binding of the protein raptor. They have been invaluable in both suppressing the progression of lung deterioration, stabilizing lung function decline, and markedly improving patient survival (77), despite not performing as remission inducing therapies.

Autophagy Inhibitors

Autophagy is a cellular process that recycles damaged intracellular proteins and organelles in autolysosomes in response to nutrient deficiencies and cellular stress. The role of autophagy is widely debated in the context of cancer (78), and has been linked to both tumor suppression during early stages of cancer initiation (79,80) as well as cancer progression and treatment resistance (81) in

established cancers. Tumors can take advantage of autophagy to replenish nutrients and support continued proliferation and survival (82–84). When mTOR is activated, pathways associated with autophagy are downregulated (85). Consequently, mTOR inhibition with rapamycin has the unfortunate potential to promote autophagy in the LAM microenvironment (86). Autophagy inhibitors like chloroquine and resveratrol have been shown to inhibit growth of Tsc2-null cells *in-vitro* and xenograft tumors *in-vivo* (58,87,88). Clinical trials to test the safety of sirolimus in combination with hydroxychloroquine (89) (NCT01687179) or resveratrol (90) (NCT03253913) reveal that these treatment regimens are well tolerated and safe in LAM patients. Combination therapy with resveratrol significantly decreased blood VEGF-D levels and increased patient's capacity to perform respiratory intensive exercise (6 minutes walking). Although these early-phase clinical trials showed promising results, they enrolled very small patient numbers, so larger studies will be needed to understand the efficacy of autophagy inhibitors and their long-term effects in LAM.

Anti-fibrotic / Anti-angiogenic agents

Inhibition of receptor tyrosine kinases (RTKs) is another therapeutic strategy that is being evaluated for LAM. These are receptors for growth factors such as vascular endothelial growth factor (VEGF), platelet-derived growth factor (PDGF), epidermal growth factor (EGF), fibroblast growth factor (FGF), and insulin-like growth factor (IGF), that are overexpressed in LAM and result in over-activation of mTOR (91–93). Research into RTK inhibitors as therapy for LAM is particularly attractive because a number of these inhibitors already have FDA

approval for the treatment of other conditions like cancer. This could expedite the clinical trial process if found effective for LAM, as their safety profiles are already well characterized. In preclinical models, antibodies targeting these kinases induced cell death in Tsc2-null cells and reduced lung nodules in a mouse model (69,92). Clinical trials evaluating the efficacy and safety of RTKs like Nintedanib (94) (NCT03062943), Imatinib Mesylate (NCT03131999), and Bevacizumab (NCT01552434) in LAM patients are underway. Initial results from the phase-2 study of Nintedanib report no severe treatment responses and durable stabilization of lung function at 12 months post treatment. A thorough evaluation of their efficacy in LAM is needed, but initial results look promising.

Hormone Therapy

Because women of reproductive age are overwhelmingly represented in the LAM patient population and pregnancy tends to worsen disease, many researchers have investigated the involvement of female hormones like estrogen and progesterone in LAM pathogenesis. Research shows that receptors for these hormones are over expressed both in LAM patients and LAM models (95–97). Estrogens have been shown to stimulate increased proliferation in Tsc-deficient cells in-vitro (98), however, tamoxifen, an estrogen inhibitor did not appear to be effective therapy in LAM patients (99). In fact, both tamoxifen and estradiol, an estrogen, were found to stimulate LAM cell growth in angiomyolipomas (100). A retrospective study evaluating the effect of progesterone therapy in LAM patients found that it did not slow the progression of lung function decline (101). Another clinical trial investigating letrozole (NCT01353209), an inhibitor of estrogen

synthesis, was inconclusive in premenopausal women as FDA approval of sirolimus coincided with the study enrollment period (102). More robust studies will be needed to elucidate the effect of estrogen inhibition on LAM disease progression, but taken together, the current available studies do not recommend hormone therapy as an effective treatment strategy.

Other Therapies investigated for LAM

Clinical trials are ongoing for a number of potential drug candidates for LAM including simvastatin, doxycycline, an albuterol.

Simvastatin is a statin, which is a class of drugs that decreases cholesterol production and has potential anti-fibrotic, anti-proliferative, and anti-angiogenic properties. All of those characteristics could be effective in combination with mTOR inhibition for the treatment of LAM. Despite growth-inhibitory and proapoptotic effects of simvastatin on TSC2-null cells in-vitro (103), treatment with simvastatin in LAM patients was associated with a decline in lung function and no significant change in serum VEGF-D levels (104). Thus, simvastatin may not be an ideal candidate for LAM therapy.

Another target for treatment in LAM are matrix metalloproteinases (MMPs), enzymes that degrade extracellular matrix components and are important for tissue remodeling and cell migration. LAM cells are known to produce high levels of MMPs (105,106) and research shows that LAM patients have elevated levels of serum MMP-9 (107). Therefore, inhibition of MMPs in LAM could curb the destructive tissue remodeling and increased cell motility of LAM cells to prevent their spread. Doxycycline is an MMP inhibitor that was evaluated for potential

therapeutic effects in preclinical models of LAM and in LAM patients across several clinical trials (2007-003745-32) (RBR-6g8yz9). In-vitro and xenograft models of LAM showed that doxycycline had no effect on MMP expression in cells or tumor growth in rodents (108). Similarly, treatment with doxycycline in LAM patients did not have an effect on clinical benchmarks like lung function or progression of disease, nor did it reduce serum MMP levels (109,110) despite significant reduction in urinary MMP (111). Consequently, MMP inhibition does not appear to be an effective therapy for the treatment of LAM.

Pulmonary rehabilitation is a guided therapeutic exercise training program for individuals with chronic lung conditions to help them improve lung function and reduce symptoms related to physical activity through endurance and resistance training. In addition to exercise training patients receive psychological and social support that can equip them with coping strategies to better manage their condition. Fatigue and exercise intolerance are the most common symptoms experienced by LAM patients, so this type of therapy is often recommended to improve stamina. When evaluated in a clinical trial (NCT02009241), pulmonary rehabilitation proved to be a safe intervention and improved exercise capacity, dyspnea, daily physical activity, quality of life and muscle strength in LAM patients (112). While this therapeutic approach is wholistic, safe, and tailored to each patient's needs, it is likely most effective as an early intervention to preserve lung function. More studies are needed to evaluate its efficacy in patients with more severe disease.

Another therapeutic approach being studied for LAM is bronchodilation using common beta-agonist inhalers like albuterol. Bronchodilators work by relaxing the smooth muscle tissues surrounding the airways, allowing them to widen and improve airflow through the lungs. In LAM, this would offer relief from respiratory symptoms like, dyspnea and shortness of breath. A retrospective study examined lung function decline in LAM patients using bronchodilators and found that treatment with beta-agonists in combination with sirolimus significantly stabilized lung function (113). This study lead to an ongoing clinical trial to determine the effects of Albuterol, a short-acting beta-2 agonist, on pulmonary function in LAM patients (NCT01799538). More studies are needed to thoroughly evaluate inhaled beta-agonists as supportive therapy and symptom management in LAM.

Immune response to treatment in LAM disease

Not much is known about the specific immune response to treatment in LAM disease. Researchers have only seriously considered and investigated the involvement of the immune system in the pathogenesis of LAM since the late 1990s when increased lymphatics, immune cells, and other hallmarks of immune activity were observed as methods in immunology advanced. We might infer from what is known about how mTOR affects the immune system (114) that inhibition of the mTOR pathway using rapamycin could negatively affect the activation and activity of innate immune cells, since mTORC1 is involved in many processes related to cell growth, proliferation and metabolism (115). However contradictory studies report results showing that mTOR inhibition is associated with the

increased expansion of central memory T cells and increase NF-KB activity, which is a common pathway utilized in immune activation (116,117).

Many cells in the pulmonary LAM microenvironment express higher levels of the immune checkpoint inhibitor, PD-L1, than in healthy lungs (39). Over expression of immune checkpoint inhibitors is one mechanism of immunosuppression used by a variety of cancers to evade cytotoxic T cell responses. When PD-1 receptors on T cells bind PD-L1 on other cell types, it leads to T cell exhaustion and deactivation. Immune checkpoint inhibition (ICI) is a form of immunotherapy that blocks these receptors from interacting and prevents activated T cells from becoming exhausted when they arrive in tumor tissues. This helps them resist immunosuppression and remain activated to carry out their effector functions that eliminate tumor cells. The finding that ICI increases survival in a mouse model of pulmonary LAM suggests that activated T cell responses could be a critical component to effective treatments and immunotherapies in LAM.

Immune activation as a therapeutic strategy

Immune activation using Toll Like Receptors

Toll like receptors (TLRs) are highly conserved transmembrane pattern recognition protein receptors primarily found in and on innate immune system cells like macrophages and dendritic cells that help them to recognize and quickly respond to microbial pathogens that the body encounters. There are various receptors and they each recognize different patterns. For example, TLR4 recognizes lipopolysaccharide (LPS), a bacterial surface protein, while TLR9

recognizes bacterial and viral DNA containing unmethylated cytosine–phosphate–guanine (CpG) DNA motifs that aren't present in human DNA.

When a TLR is activated in an innate immune cell, it immediately triggers a signaling cascade that usually results in the secretion of pro-inflammatory cytokines, increased phagocytic activity, and eventually the activation of T lymphocytes that can launch a more targeted adaptive immune response a few days later. All of this alters the tissue environment where the microbial threat was detected and recruits immune cells to the area to eliminate it (inflammation).

TLRs are used most often as vaccine adjuvants (118), where they are delivered alongside antigens and help train the immune system response against antigens found in the surrounding tissue where the TLR signal was first encountered. These immune activating properties of TLRs have led scientists to explore their potential as cancer immunotherapy. The Federal Drug Administration (FDA) has approved several TLR agonists for treatment of specific cancers. For example, the BCG vaccine is a TLR4 agonist approved for treatment of non-metastatic bladder cancer (119).

Immune activation in Cancer

Immunotherapy in the cancer field has had many breakthrough in the last few decades. For example, CAR-T cell therapy, where a patient's T cells are genetically engineered and expanded ex-vivo before being readministered as therapy, has been particularly successful in treating deadly blood cancers. Researchers are also working to develop cancer vaccines that can help train the

immune system to recognize cancer antigens and eliminate them without the need for less targeted approaches like chemotherapy.

Most FDA-approved immunotherapies for lung cancers fall under the umbrella of immune checkpoint inhibitors, specifically anti-PD-1/PD-L1 antibodies. As described above, this form of therapy help T cells remain activated in immunosuppressive tumor tissues. Toll like receptor agonists have been extensively studied in mouse models of lung cancer with promising results. However, these outcomes have not yet been recapitulated in clinical trials due to adverse effects that aren't well tolerated in humans.

TLR agonists are being tested alongside checkpoint inhibition for the treatment of solid tumors. ICI may be more effective in treating "hot" tumors, or tumors where an active immune response is already established, but may be susceptible to tumor immunosuppression. In "cold" tumors, injecting TLR agonists has the effect of activating immunosuppressed cells in the tumor microenvironment and inducing an inflammatory immune response to transform a tumor from "cold" to "hot". And because hot tumors readily respond to ICI therapy, the combination of TLR activation and ICI work well as immune activating therapy (120).

Chapter 3. Efficacy of CpG treatment in a mouse model of LAM

Acknowledgements:

This work was completed with the help of Dr. Jacob McCright, Bennett Yang, Juan Grano de Oro Fernandez, Kaitlyn Moore, Havish Gadde, Mehu Donthi, Michele Kaluzienski, and Katharina, Maisel. Their contributions made this chapter possible and I am deeply grateful for the time, effort, and care dedicated by each individual to making these studies successful.

This chapter is partially reproduced from the Biorxiv self-published manuscript available online: Mayowa M Amosu, Jacob C McCright, Bennett E Yang, Juan Grano de Oro Fernandez, Kaitlyn A Moore, Havish S Gadde, Michele L Kaluzienski, Katharina Maisel. bioRxiv 2023.02.06.527331; doi: https://doi.org/10.1101/2023.02.06.527331

Introduction

Lymphangioleiomyomatosis (LAM) is a progressive rare lung disease, primarily affecting women who are diagnosed in their 20-40s (121). LAM patients can experience a range of debilitating symptoms from shortness of breath, lung collapse, and eventual respiratory failure. LAM is characterized by the persistent abnormal growth of smooth muscle-like cells (LAM cells) and the formation of thin-walled cysts predominantly in the lungs, with involvement of the lymphatic system and kidneys. LAM is caused by inactivating mutations in tumor suppressor genes tuberous sclerosis complex 1 and 2 (TSC1 / TSC2) that negatively regulate cell growth through inhibition of a signaling protein complex called mechanistic target of rapamycin (mTOR). Currently, sirolimus (rapamycin)

is the only FDA approved drug for LAM (122), which inhibits the constitutively activated mTOR complex thus slowing disease progression (123,124). However, rapamycin does not promote disease regression or lung regeneration (33,34). Furthermore, patient responses to rapamycin are incomplete and not always well tolerated for life-long use (33). Therefore, there is an urgent need for other curative treatments that can eliminate LAM nodules and restore healthy lung function in patients suffering from LAM.

LAM is designated as a neoplastic growth, and recent research suggests it has similarities to cancer (23). Immunosuppression is a common feature of many cancers, including lung cancers (125,126), which over time conditions immune cells to ignore the tumor cells thus promoting cancer progression (127–129). In human LAM tissues, a lack of T-cell infiltration suggests immunosuppression due to unresponsiveness of lymphocytes to LAM antigens (130). LAM lungs also typically have elevated levels of secreted factors like monocyte chemoattractant protein 1 (MCP-1) (131), which may contribute to recruitment of immunosuppressive cells (132,133). Prior work by us and others has also shown that human LAM nodules have elevated expression of PD-L1, an immune checkpoint inhibitor that causes T cell suppression, and LAM causes overexpression of checkpoint molecules PD-1 and CTLA-4 on T cells in a mouse model (39,40). Anti-PD1/PD-L1 and anti-CTLA-4 therapies were shown to enhance survival in mouse models of LAM (39,40), suggesting that countering immunosuppression in LAM could be an effective strategy for treating LAM.

In addition to the previously investigated checkpoint inhibitor treatments, reducing immunosuppression in LAM could be accomplished by reactivating antigen presenting cells (APCs) in the local tumor environment. Recent studies investigating targeted activation of APC's in cancer show enhanced anti-tumor immunity through improved T cell responses (134), and increased responsiveness of immunosuppressed myeloid cells to immunotherapy (135). Local tumor treatments inducing APC activation have also been shown to stimulate systemic anti-tumor immunity and regression of distant tumors (136). Treatments that mimic microbial pathogens to stimulate toll-like receptors (TLRs) on APCs have been explored for this purpose. When engaged through TLR activation, APCs like dendritic cells and macrophages secrete inflammatory cytokines and promote the differentiation of cytotoxic T cells, reduce regulatory T cells, and can lead to increases in pro-inflammatory helper T cells (137,138). Several TLR agonists have received FDA approval for cancer treatment. For example, BCG is a TLR4 agonist that is used as immunotherapy for bladder cancer and there are at least 8 additional clinical trials are investigating TLR adjuvants as cancer therapeutics (NCT04364230, NCT04819373, NCT04278144, NCT03486301, NCT04840394, NCT02668770, NCT05607953, NCT04935229). TLR9 agonists, like CpG, have been explored as therapy in multiple cancers including non-small cell lung cancer and are FDA approved vaccine components (139–141). TLR9 agonists have also been shown synergize with immune checkpoint inhibition, leading to increased therapeutic responses (142–146). Given the current efforts to leverage the TLR9 agonist CpG in cancer

therapy, we investigated its potential for therapy in LAM. We assessed the therapeutic efficacy of CpG and the immune mechanisms involved in its therapeutic action.

Materials and Methods

Mice

7 to 9-week old female C57BL6/J mice (Jackson Laboratory) were used for all studies. Study protocols were approved by the UMD Institutional Animal Care and Use Committee (IACUC).

LAM induction

TSC2-null kidney-derived epithelial tumor (TTJ) cells, were provided by the Krymskaya Lab at the University of Pennsylvania (39). TTJ cells (5.0×10^5) were administered in 100 µL of PBS via tail vein injection to induce LAM disease in 8-9 week old female mice. Lung lesions typically develop within 3-7 days.

Survival Studies

Mice received CpG class B (5 µg/10 µg) 2x/week (Invivogen, tlrl-1826-5), in 50 µL of PBS, intranasally starting 4 days post LAM induction. Mice receiving combination therapy, received intranasal CpG and 300 µg anti-PD-1 antibody (BioXCell, BE0146-A0) or 1 µg/g Rapamycin (Selleck Chemicals, S1039) in 200 µL of PBS via intraperitoneal (IP) injection 2x/week. Control groups received 50 µL of PBS intranasally or 200 µL PBS with or without 300 µg of rat IgG isotype

control (BioXCell, BE0089) by IP injection. Mice were monitored for symptoms of disease and body weight changes and removed from studies based on experimental timing or humane endpoints. At endpoint, mice were euthanized and lung tissues collected for histological analysis.

Histology

Tissues were fixed overnight in 4% PFA at 4ºC, embedded in paraffin wax, sectioned at 5 µm, and stained with hematoxylin and eosin (H&E). LAM nodule counts, average nodule diameters, and general tissue inflammation were quantified using QuPath Imaging software.

Flow Cytometry

After LAM induction, mice received 6 intranasal treatments (twice weekly for 21 days) of CpG (5 µg or 10 µg) in 50 µL PBS or 50 µL of PBS as a vehicle control. 24 hours after the final treatment, lung tissues were perfused and collected for flow cytometric analysis. Left lung lobes were dissociated by enzymatic digestion with 1 mg/mL collagenase D (Roche, 11088882001), and 1 mg/mL collagenase IV (Worthington Biochemical, LS004188) in DMEM with 5% FBS for 1 hour. Single cell suspensions were stained to identify eosinophils (CD64-, Siglec F+, Ly6G-), neutrophils (CD64-, Siglec F-, Ly6G+) dendritic cells (CD11c+, MHC-II^{high}), plasmacytoid dendritic cells (CD11c+, PDCA-1+, MHC-II^{high}), alveolar macrophages (CD64+, SiglecF^{high}, CD11b-), interstitial macrophages (CD64+, SiglecF^{low}, CD11b+, MHC-II+), B Cells (CD19+ or B220+), T Cells (CD3+, CD4+ or CD8+), regulatory T Cells (CD3+, CD4+, FoxP3+), Th1 T cells (CD3+, CD4+,

FoxP3-, Tbet+), Th2 T cells (CD3+, CD4+, FoxP3-, Gata3hi), and Th17 T Cells (CD3+, CD4+, FoxP3-, ROR-γt+). To stain intracellular markers and cytokines, cells were fixed and permeabilized (BD Cytofix/Cytoperm Plus, 554715), before staining for cytokines (IFN-γ , perforin, granzyme B, TNF-α). Cells were analyzed by flow cytometry using a BD FACSCelesta (BD Biosciences) and FlowJo (FlowJo LLC).

APC Uptake

After LAM induction, mice received 6 intranasal treatments (twice weekly for 21 days) of CpG (5 μg) in 50 μL PBS or 50 μL of PBS as a vehicle control. For the 6^{th} treatment dose, mice received intranasal treatments of CpG (5 μg) with 25 μg DQ™ Ovalbumin (ThermoFisher Scientific, D12053) in 50 μL PBS or 25 μg DQ™ Ovalbumin with 50 μL of PBS as a vehicle control. DQ Ovalbumin is a substrate that emits green fluorescence (515 nm) upon proteolytic degradation and is designed for the study of antigen processing and presentation. 18 hours after the final treatment, mice were administered 250 μg Brefeldin-A (BioLegend, 420601) by IP injection. Brefeldin-A inhibits the secretion of cytokines, allowing them to accumulate within immune cells for detection by flow cytometry. 6 hours after the Brefeldin-A treatment, lung tissues were perfused and collected for flow cytometric analysis. All buffers used henceforth contained 3.0 μg /mL Brefeldin-A (Invitrogen, 00-4506) until cells were fixed. Left lung lobes were dissociated by enzymatic digestion with 1 mg/mL collagenase D (Roche, 11088882001), and 1 mg/mL collagenase IV (Worthington Biochemical, LS004188) in DMEM with 5% FBS for 1 hour. Single cell suspensions were stained to identify antigen

presenting cells like dendritic cells (CD11c+, MHC-II^{high}), plasmacytoid dendritic cells (CD11c+, PDCA-1+, MHC-II^{high}), alveolar macrophages (CD64+, SiglecF^{high}, CD11b-), and interstitial macrophages (CD64+, SiglecF^{low}, CD11b+, MHC-II+). Cells were analyzed by flow cytometry using a BD FACSCelesta (BD Biosciences) and FlowJo (FlowJo LLC). Gating strategies can be found in the data supplement (**Fig E1**).

DC Migration

14 days after LAM induction, mice received a single intranasal treatment dose of CpG (10 μg) with 100 μg fluorescent 40 nm polystyrene beads (Invitrogen, F8795) in 50 μL PBS, 100 μg fluorescent polystyrene beads in 50 μL of PBS with 25 μg anti-CCR7 antibody via IP injection, or 100 μg fluorescent polystyrene beads in 50 μL of PBS as a vehicle control. At 1 and 3 days post treatment, lung tissues were perfused and collected for flow cytometric analysis. Left lung lobes were dissociated by enzymatic digestion with 1 mg/mL collagenase D (Roche, 11088882001), and 1 mg/mL collagenase IV (Worthington Biochemical, LS004188) in DMEM with 5% FBS for 1 hour. Single cell suspensions were stained to identify conventional dendritic cells (CD11c+, MHC-II^{high}) and plasmacytoid dendritic cells (CD11c+, PDCA-1+, MHC-II^{high}). Cells were analyzed by flow cytometry using a BD FACSCelesta (BD Biosciences) and FlowJo (FlowJo LLC).

ELISA

For cytokine analysis, lungs (smallest right lobe) were snap-frozen and stored at -80°C. For tissue homogenates, snap-frozen lungs were homogenized at 4°C at 20% w/v in protein extraction reagent (T-PER, Thermo Fisher Scientific) containing Halt™ Protease Inhibitor Cocktail (Thermo Fisher Scientific). Lung tissue homogenates were centrifuged at 15,000 g for 10 min at 4°C. Supernatants were aliquoted and stored at -80°C. Supernatants were diluted 1:10 with 1% BSA ELISA assay diluent and ELISA was performed according to manufacturer's instruction (ELISA MAX™ Standard Set, Biolegend).

Statistical Analysis

Data were analyzed using Graphpad Prism (GraphPad, La Jolla, CA). Survival studies were assessed using the log-rank (Mantel-Cox) test. Unpaired Welch t tests were used to compare pairs of samples or groups. Mann–Whitney test was used to compare the groups of data that failed to satisfy parametric assumptions. Brown-Forsythe and Welch One-way ANOVA were used for comparisons between ≥3 groups. Differences were considered statistically significant when $p < 0.05$. *p<0.05, **p<0.01, ***p<0.001, ****p<0.0001.

Results

Treatment with intranasal CpG increases survival in LAM

To determine the therapeutic benefit of TLR9-agonist CpG in LAM disease, we performed survival studies comparing the effect of two doses of intranasal using our metastatic mouse model of LAM. We found that intranasal CpG significantly increases survival in mouse LAM, with median survival increasing 1.4-fold from 32.5 to 45 days (**Fig 1A**). We found that a lower dose of CpG (5mg) resulted in higher survival than higher dose CpG (10mg), with median survival increasing further from 45 to 60 days, an almost 2-fold increase compared to untreated mice. We conducted a cross sectional study after 3 weeks (Day 22) to assess treatment effect on LAM nodule formation. Histological analysis showed that treatment with CpG reduced LAM-like nodules in both size and number in treated vs untreated lungs (**Fig 1B**). Higher dose CpG (10ug), significantly decreased the nodule count, more that the lower dose (5ug), which was surprising given the improvement in overall survival with lower dose CpG (**Fig 1C**). However, the overall abnormal tissue fraction is similar for both doses of CpG, even though the higher dose has a lower nodule burden (**Fig 1C**), suggesting that negative side effects of CpG may contribute to the increased morbidity with higher dose CpG. In addition, we found that treatment with higher dose CpG results in similar levels of immune cell infiltration to untreated LAM, while treatment with lower dose CpG results in less CD45+ cells than untreated LAM (**Fig 2**).

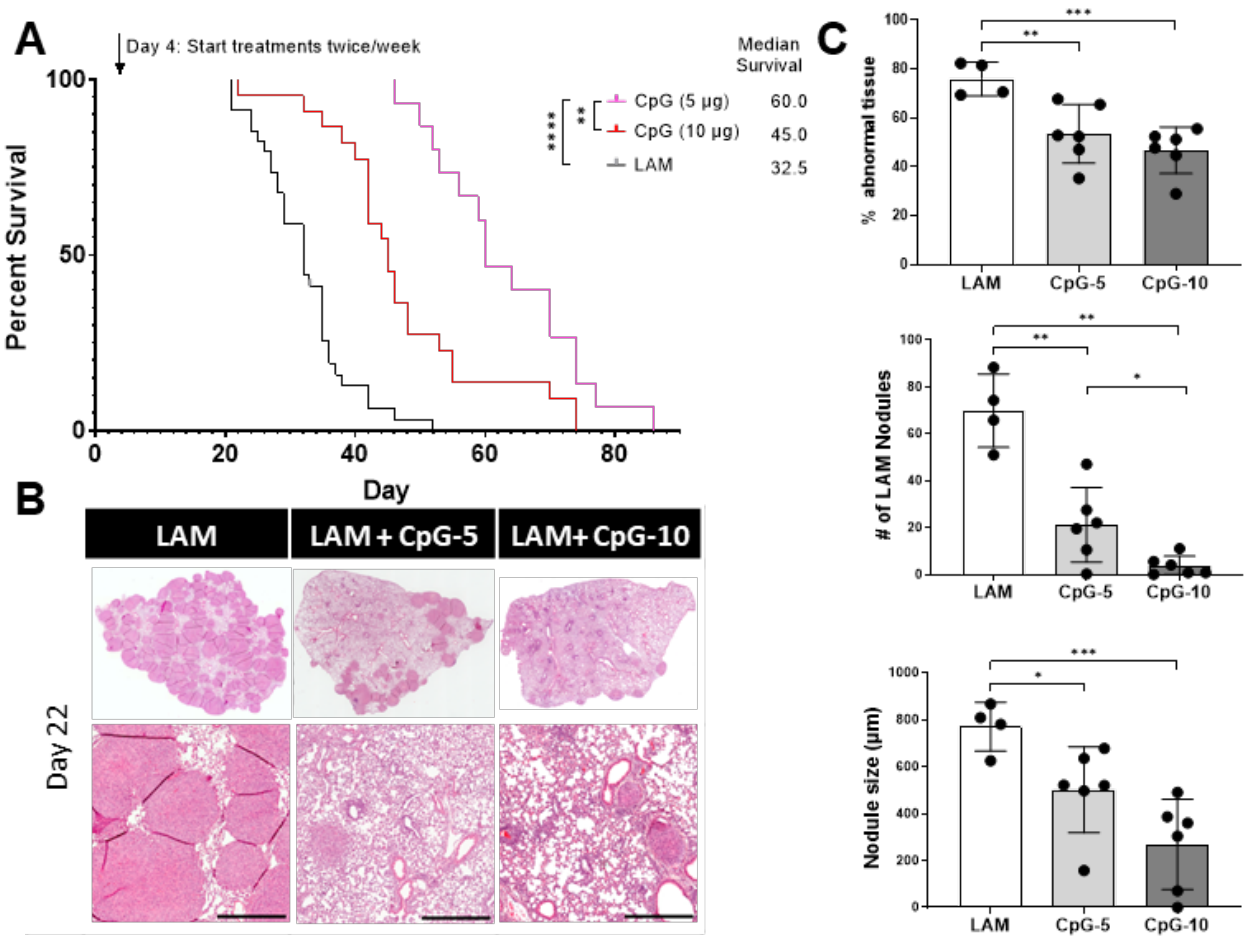

Figure 1. *Intranasal CpG increases survival in murine model of metastatic LAM, decreases tissue-wide inflammation and overall LAM nodule burden*. **A)** Aggregate data from three survival experiments LAM n=34, CpG (10ug) n=22, CpG (5ug) n=15. **B)** Representative H&E stained histological images of mouse lungs from treatment groups: untreated LAM control, CpG 5 µg, and CpG 10 µg. Scale bar = 500 µm. **C)** Quantification of LAM nodules and Inflamed tissue regions between treatment groups 22 days post LAM induction and after 6 total treatment administrations. 3 sections analyzed per mouse. Statistical analysis was performed using log-rank test (survival studies) and one-way ANOVA (histological analysis). * $p<0.05$, ** $p<0.01$, *** $p<0.001$, **** $p<0.0001$.

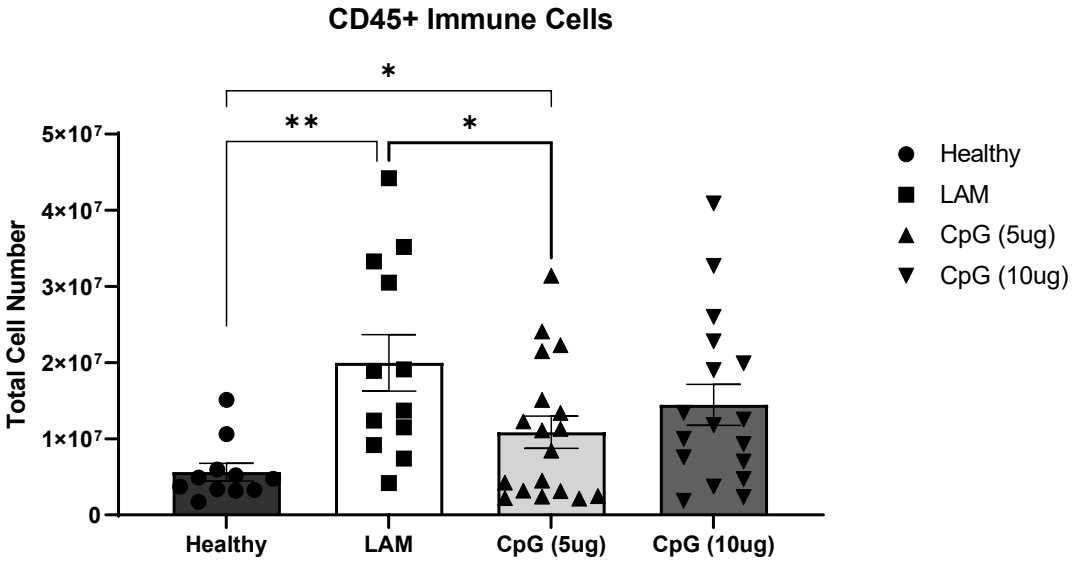

Figure 2: Total immune cell counts in lungs of mice on day 22 in early stage disease with or without CpG treatment. Data is representative of n=2+ experiments with n>4 mice. Statistical analysis was performed using two-way ANOVA. * p<0.05, ** p<0.01, *** p<0.001, **** p<0.0001.

Dendritic Cells in CpG treated lungs have increased migration and antigen presentation

Antigen Presentation

We hypothesized that treating with CpG in the lungs would first stimulate antigen presenting cells to take up antigen to be presented to T cells in the lymph node. To assess whether CpG treatment induced increased activation, and antigen uptake and presentation in antigen presenting cells in the LAM microenvironment, measured surface expression of CD80 and MHC-II markers. We also measured antigen presentation in ex-vivo APCs using DQ-Ovalbumin. We found increased MHC-II+ cells that had successfully taken up and processed DQ-Ovalbumin, in CpG treated lungs compared to untreated LAM controls (**Fig.**

3), suggesting increased antigen processing and presentation. We also found that untreated LAM lungs had higher antigen processing that untreated healthy lungs (**Fig. 3**), suggesting that APCs in the LAM microenvironment are activated and potentially already processing LAM associated antigens. With the introduction of CpG in the tissue, those antigens could be presented alongside an inflammatory PAMP that would skew the immune response against LAM associated antigens. Among conventional dendritic cells, we found decreased MHC-II and CD80 expression in CpG treated lungs compared to untreated controls (**Fig. 4**), while plasmacytoid dendritic cells had significantly increased expression of both markers (**Fig 5.)** This suggests that plasmacytoid dendritic cells are more activated (CD80) in response to CpG and likely drive increased antigen presentation (MHC-II). We also found increased PD-L1 expression across all dendritic cells in CpG treated lungs. Although upregulation of PD-L1 is commonly interpreted as evidence of immunosuppression, this increase in response to TLR9 activation is consistent with the literature (147) and likely indicative of an immunoregulatory response to prevent excessive tissue damage as a result of inflammation.

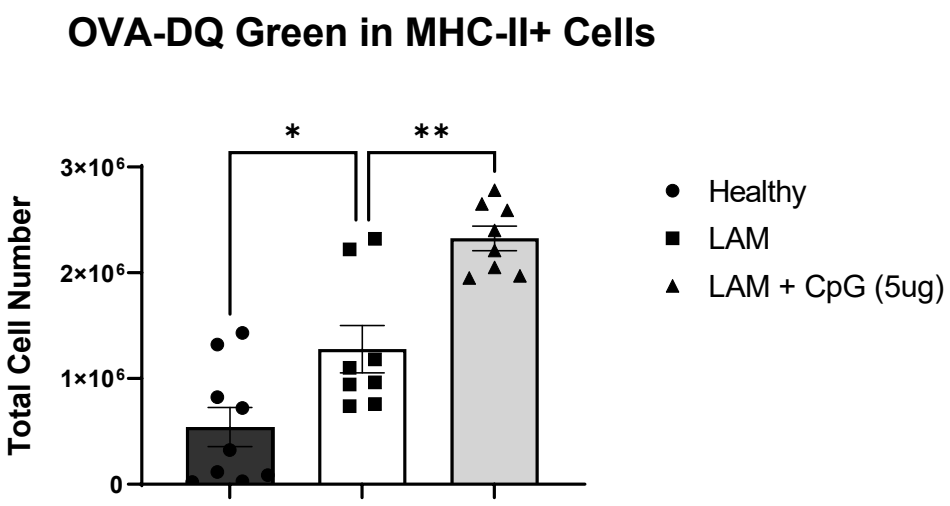

Figure 3: *CpG increases antigen presentation and processing in CpG-treated LAM lungs.* Data shows total cell numbers in the left lung lobe of OVA-DQ Green fluorescence in antigen presenting cells (MHC-II+) at day 22 post LAM induction and 24hrs after intranasal treatment with CpG and OVA-DQ. Data is representative of n=2 experiments with n>4 mice. Statistical analysis was performed using two-way ANOVA. * p<0.05, ** p<0.01, *** p<0.001, **** p<0.0001.

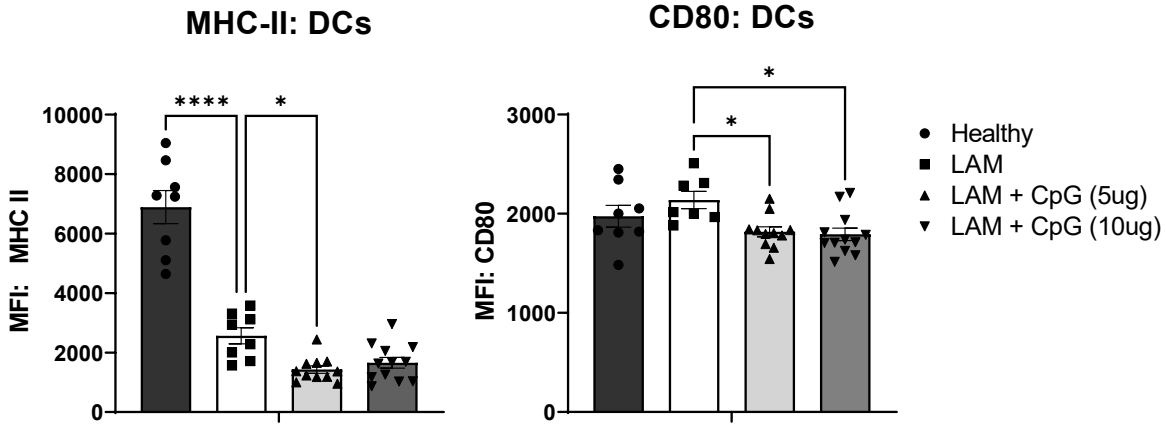

Figure 4: *CpG decreases antigen presentation and activation in conventional dendritic cells of CpG-treated LAM lungs*. Data shows mean fluorescence intensity of CD80 and MHC-II antibodies in conventional dendritic cells ($CD11C^{high}$, MHC-II+) at day 22 post LAM induction and 24hrs after intranasal treatment with CpG. Data is representative of n=2 experiments with n>4 mice. Statistical analysis was performed using two-way ANOVA. * p<0.05, ** p<0.01, *** p<0.001, **** p<0.0001.

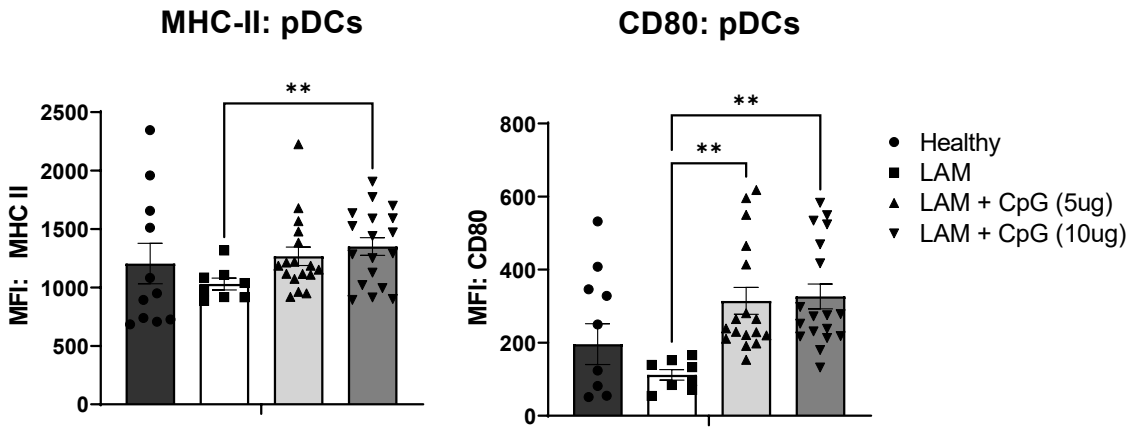

Figure 5: *CpG increases antigen presentation and activation in plasmacytoid dendritic cells of CpG-treated LAM lungs*. Data shows mean fluorescence intensity of CD80 and MHC-II antibodies in plasmacytoid dendritic cells (pDCA-1+, MHC-II+) at day 22 post LAM induction and 24hrs after intranasal treatment with CpG. Data is representative of n=2 experiments with n>4 mice. Statistical analysis was performed using two-way ANOVA. * $p<0.05$, ** $p<0.01$, *** $p<0.001$, **** $p<0.0001$.

DC Migration

We consistently found that treating with CpG in the lungs resulted in a significant decrease in lung dendritic cells within 24 hours (**Fig. 6**). This was unexpected, as conventionally TLR activation results in recruitment of dendritic cells to the tissue (148). However, exposure to CpG DNA can stimulate upregulation of CCR7 in dendritic cells and T cells (149,150) which is critical for migration to lymph nodes via lymphatic vessels.We hypothesized that perhaps the decline in the population of lung dendritic cells could be explained by CCR7 mediated migration out of lung tissues and to lung draining lymph nodes for antigen presentation and T cell activation.

To determine if intranasal CpG results in increased CCR7 mediated migration, we needed to distinguish lung tissue resident DCs from lymph node resident

DCs. This is not easily accomplished phenotypically, so we used fluorescent polystyrene beads to label tissue resident dendritic cells. We administered the beads intranasally to target the lung tissues so that any DCs that internalized fluorescent beads and migrated to the lymph node were distinguishable from lymph node DCs by their acquired fluorescence. To investigate the role of CCR7 binding, we used an anti-CCR7 antibody to block CCR7 receptors on immune cells and prevent them from leaving the tissue.

We conducted a study where we induced LAM in mice and allowed 14 days of disease progression before dosing according to the treatment groups outlined in Table 3. One and three days post treatment, we harvested lungs and mediastinal lymph node tissues and quantified populations of fluorescently labelled DCs in lymph node samples by flow cytometry as a measure of lung DC infiltration in lung draining lymph nodes.

When we examined dendritic cells, we found an increased number of fluorescently labelled DCs in lymph nodes from CpG-treated LAM mice compared to those in nodes from LAM control mice (**Fig. 6**). Mice receiving anti-CCR7 antibody had decreased migration compared to CpG treated mice. This suggests that lung dendritic cells are leaving the tissue after being activated by CpG and migrating to the lung draining lymph node through binding interactions with CCR7.

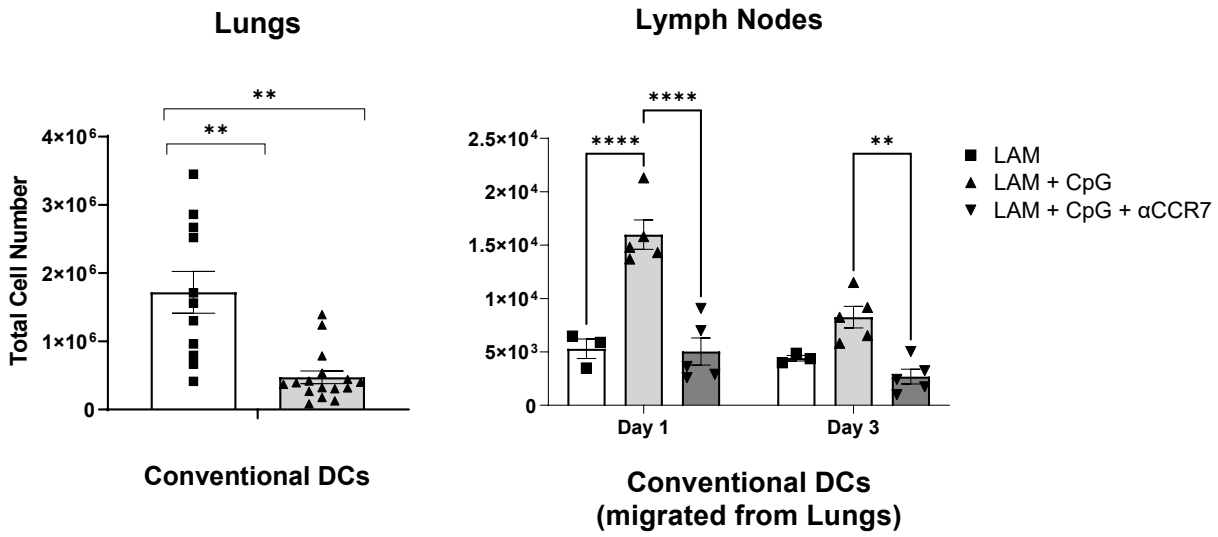

Figure 6: *Conventional dendritic cells in CpG-treated LAM lung tissues migrate to lung draining LNs.* Data compares total cell numbers of lung resident cDCs in the lungs vs lymph nodes of CpG-treated vs untreated mice at day 22 post LAM induction and 24hrs after intranasal treatment with CpG and anti-CCR7 antibody. Data is representative of n=2 experiments with n>4 mice. Statistical analysis was performed using two-way ANOVA. * $p<0.05$, ** $p<0.01$, *** $p<0.001$, **** $p<0.0001$.

Intranasal CpG modulates Immune cell infiltration in LAM Lungs and shifts T Cells toward inflammatory phenotypes and reduces regulatory T cells

We next sought to determine the immune mediators of CpG treatment that could be responsible for the treatment efficacy. We assessed immune cell subsets early during intervention at day 5 and later at day 22. On day 5, populations of eosinophils, alveolar macrophages, dendritic cells, and B and T cells were significantly decreased at both low and higher dose CpG. In contrast, neutrophils and interstitial macrophages, and monocytes were increased in response to CpG treatment (**Fig 7A, Figure 8**). By day 22, CpG treatment in LAM mice resulted in decreased cell counts in all identified immune populations except B cells and

interstitial macrophages when compared to counts in untreated LAM controls (**Fig 7B**). Between Day 5 and Day 22, untreated mice had the greatest expansion of interstitial macrophages and cDCs, while CpG treated mice had greatest expansion in cDCs and T Cells (**Figures 8-9**). We also found up to 5-fold increases in T and B cell numbers in CpG treated mice compared to up to 10 fold increases in disease controls (**Figures 8-9**). B cells in untreated mice were the only cell population with little expansion from Day 5 to 22. In CpG treated lungs, there was no expansion in eosinophil, alveolar macrophage and monocyte populations. This suggests that CpG stimulates inflammation in the tissue, but recruits a different assortment of cells while restraining the level of inflammation seen in untreated LAM.

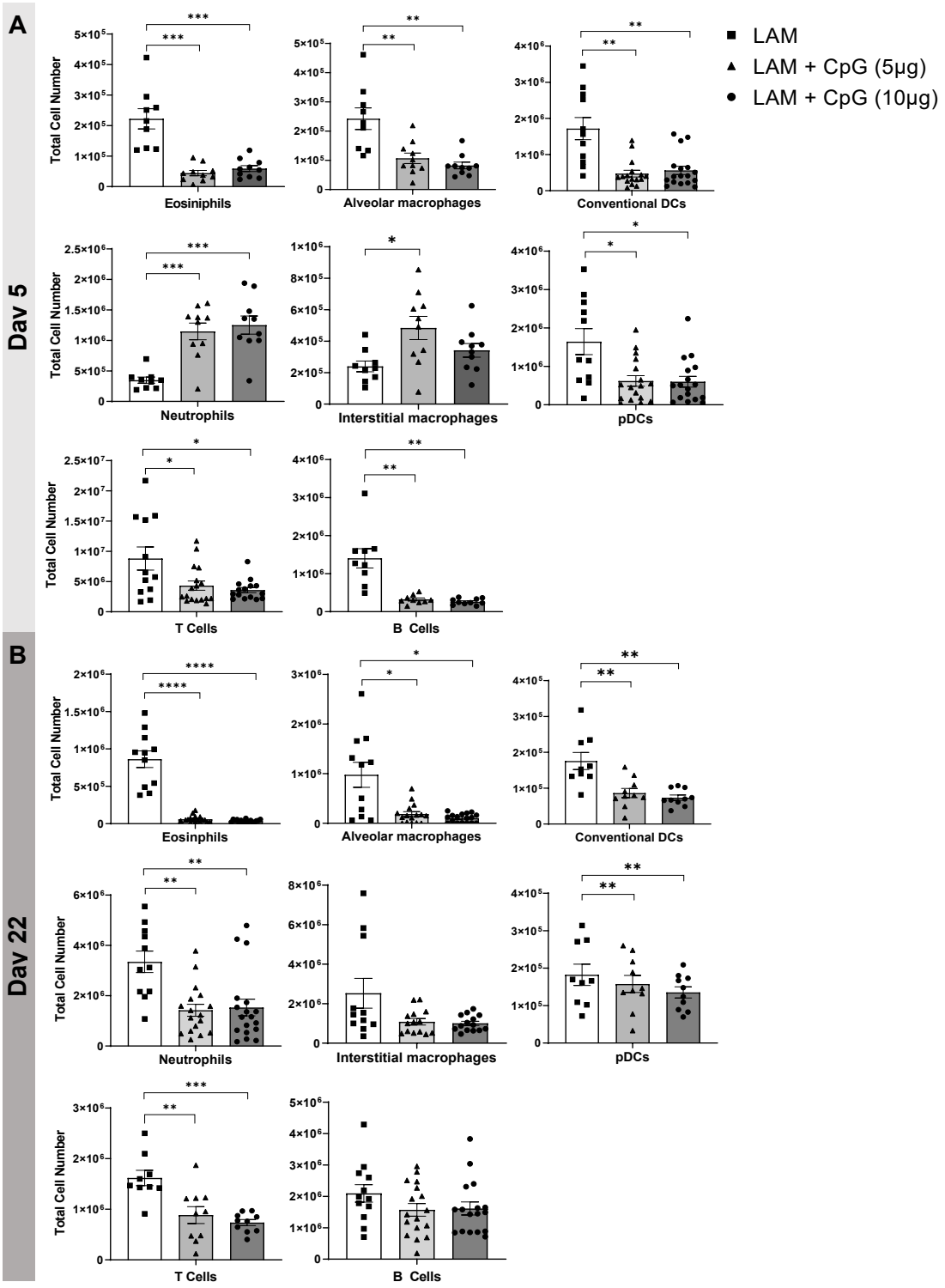

Figure 7. *CpG treatment modulates immune cell infiltration in LAM.* Data shows total cell numbers in the left lung lobe of granulocytes and antigen presenting cells at day 5 or day 22 after LAM induction and 1 or 18 days respectively after CpG treatment has started. Data is representative of n= 2+ experiments and n>8 mice. Statistical analysis was performed using one-way ANOVA. * p<0.05, ** p<0.01, *** p<0.001, **** p<0.0001.

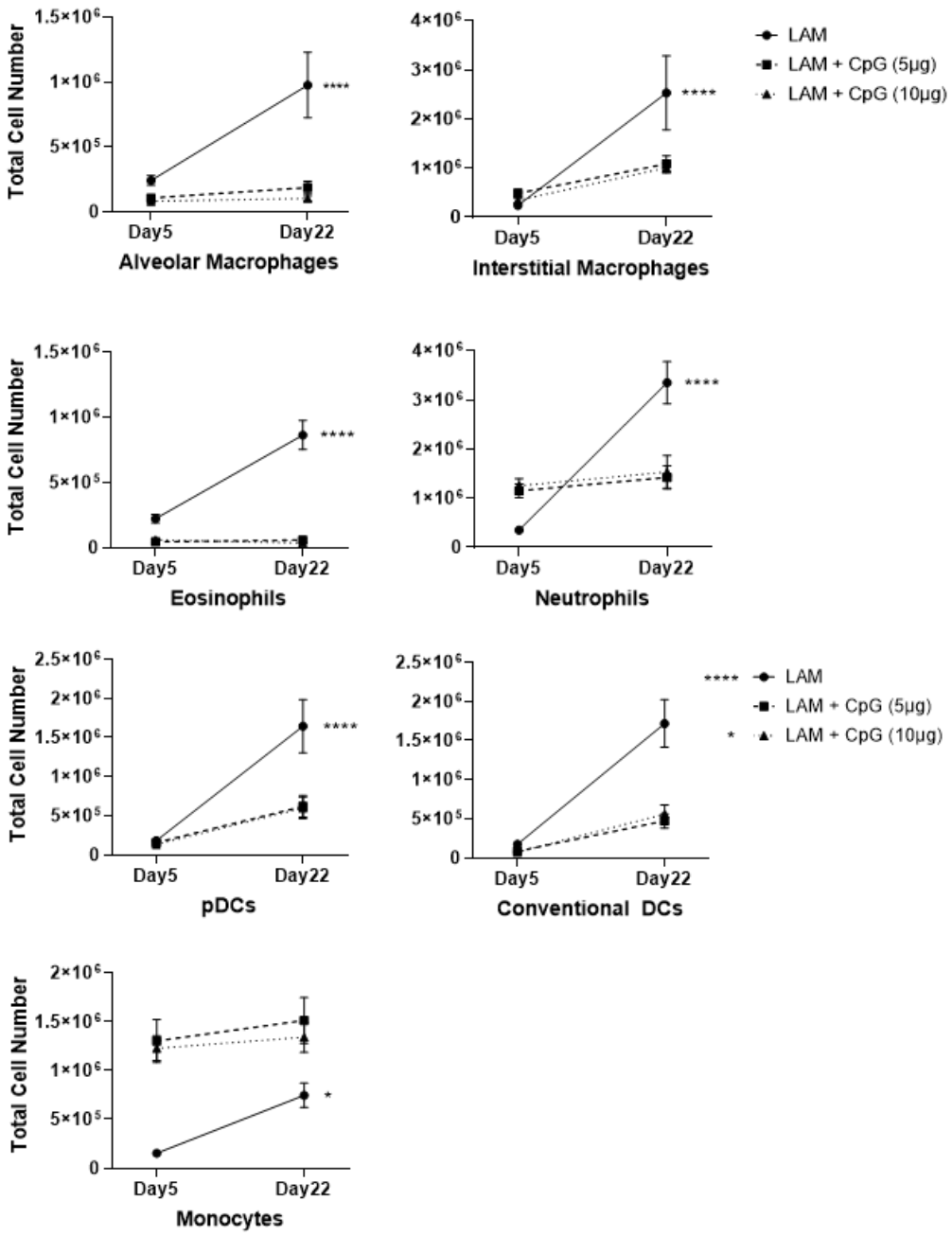

Figure 8: Total cell counts of granulocytes and antigen presenting cells on day 5 and 22 in early stage disease with or without CpG treatment . Data is representative of n=2+ experiments with n>4 mice. Statistical analysis was performed using two-way ANOVA. * $p<0.05$, ** $p<0.01$, *** $p<0.001$, **** $p<0.0001$.

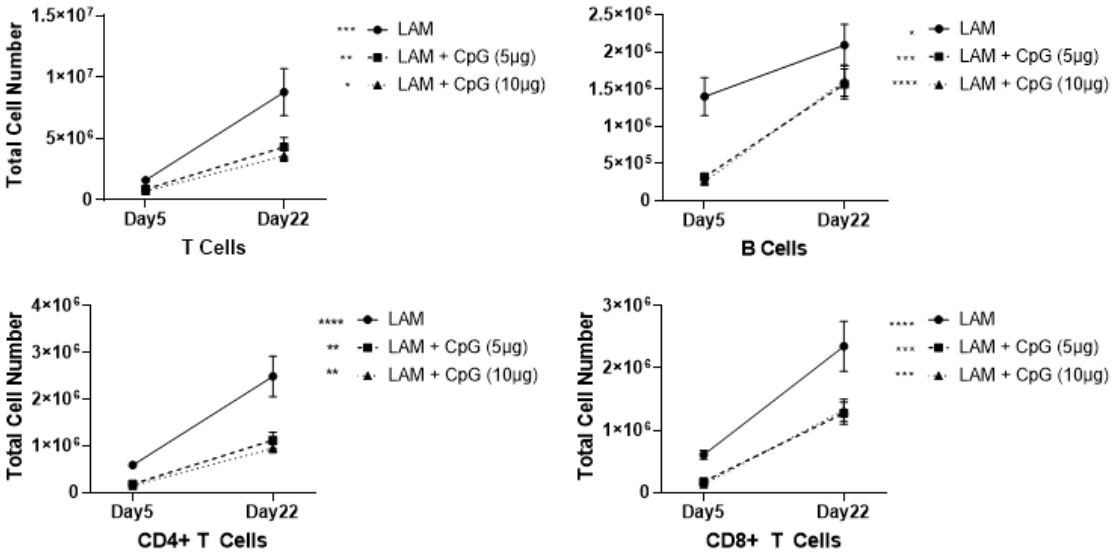

Figure 9: Total cell counts of T and B cells on day 5 and 22 in early stage disease with or without CpG treatment . Data is representative of n=2+ experiments with n>4 mice. Statistical analysis was performed using two-way ANOVA. * p<0.05, ** p<0.01, *** p<0.001, **** p<0.0001.

While we saw an overall reduction in CD4+ and CD8+ T cell numbers with CpG treatment in LAM lungs (**Fig. 10**), we found a shift in the activation and skewing of both CD8+ and CD4+ T cells in the lungs. Flow cytometry analysis revealed that CD8+ T cells have increased expression of activation marker ICOS (**Fig. 10**) and the proportion of effector memory CD8+ T cells is significantly increased with CpG treatment (**Fig. 11A**), while naïve CD8+ T cells are reduced with the highest dose CpG. This suggests that CpG treatment activates cytotoxic CD8+ T cells. We also observed increased secretion of perforin, granzyme b, and TNF-α in CD8+ T cells from CpG treated LAM lungs (**Fig. 11B**) suggesting increased cell-mediated cytotoxicity and decreased T cell exhaustion, as exhausted cells do not secrete these effector cytokines (151).

We found signs of reduced immunosuppression as indicated by the significantly decreased regulatory CD4 T cell numbers in CpG treated mice (**Fig. 12A**) and decreased expression of the immune checkpoint inhibitor PD-1 on both CD8+ and CD4+ T cells (**Fig. 13**). This suggests that these cells are less susceptible to immunosuppression through T cell exhaustion mediated by upregulation of PD-L1 on cells in the LAM microenvironment (39).

Furthermore, we found increased proportions of Th1 and Th17 cells (**Fig. 12A**), suggesting that T cells in CpG treated LAM lungs are polarized towards more proinflammatory phenotypes. We also found an increase in IL12/23 in LAM lung tissues after CpG treatment (**Fig. 12B**), which are important mediators of CD4+ T cell differentiation, with IL-23 pushing Th17 differentiation, which is consistent with the increased proportion of Th17 cells found in LAM lungs after CpG treatment. These data suggests that intranasal CpG stimulates an immune response in T lymphocytes that is associated with anti-tumor responses.

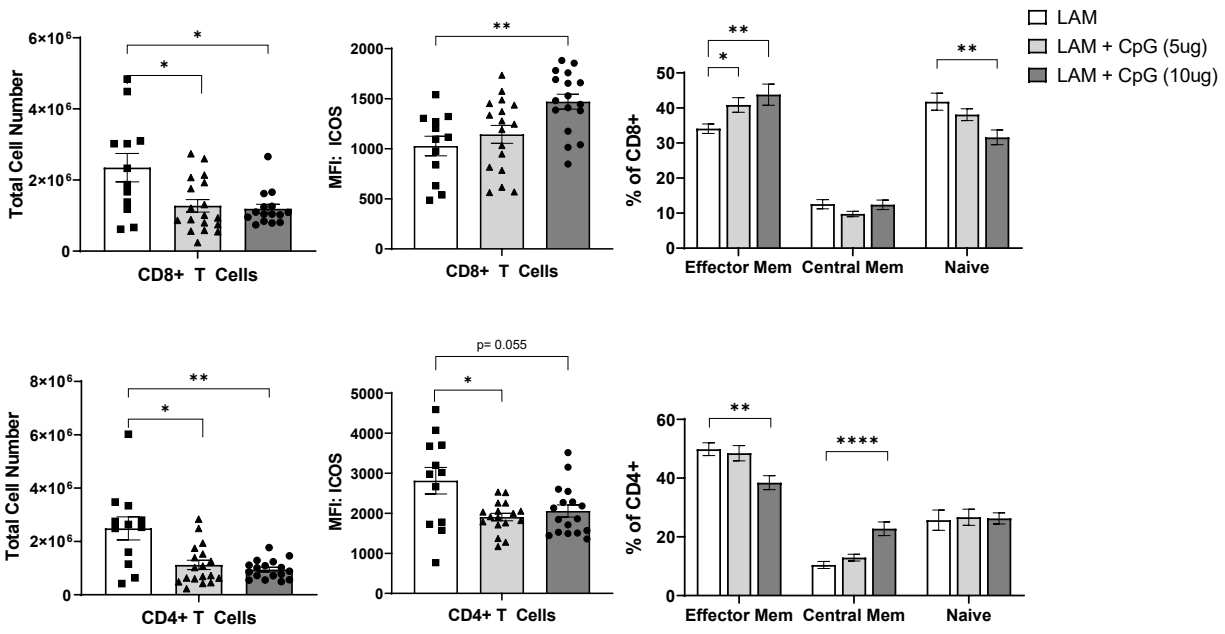

Figure 10: T cells after CpG treatment on day 22 in early stage disease with or without CpG treatment. Data shows CD4+ and CD8+ T cell numbers, ICOS expression, and cell population distribution between effector memory, central memory and naïve subsets. Data is representative of n= 3 experiments and n>10 mice. Statistical analysis was performed using one-way ANOVA. * $p<0.05$, ** $p<0.01$, *** $p<0.001$, **** $p<0.0001$.

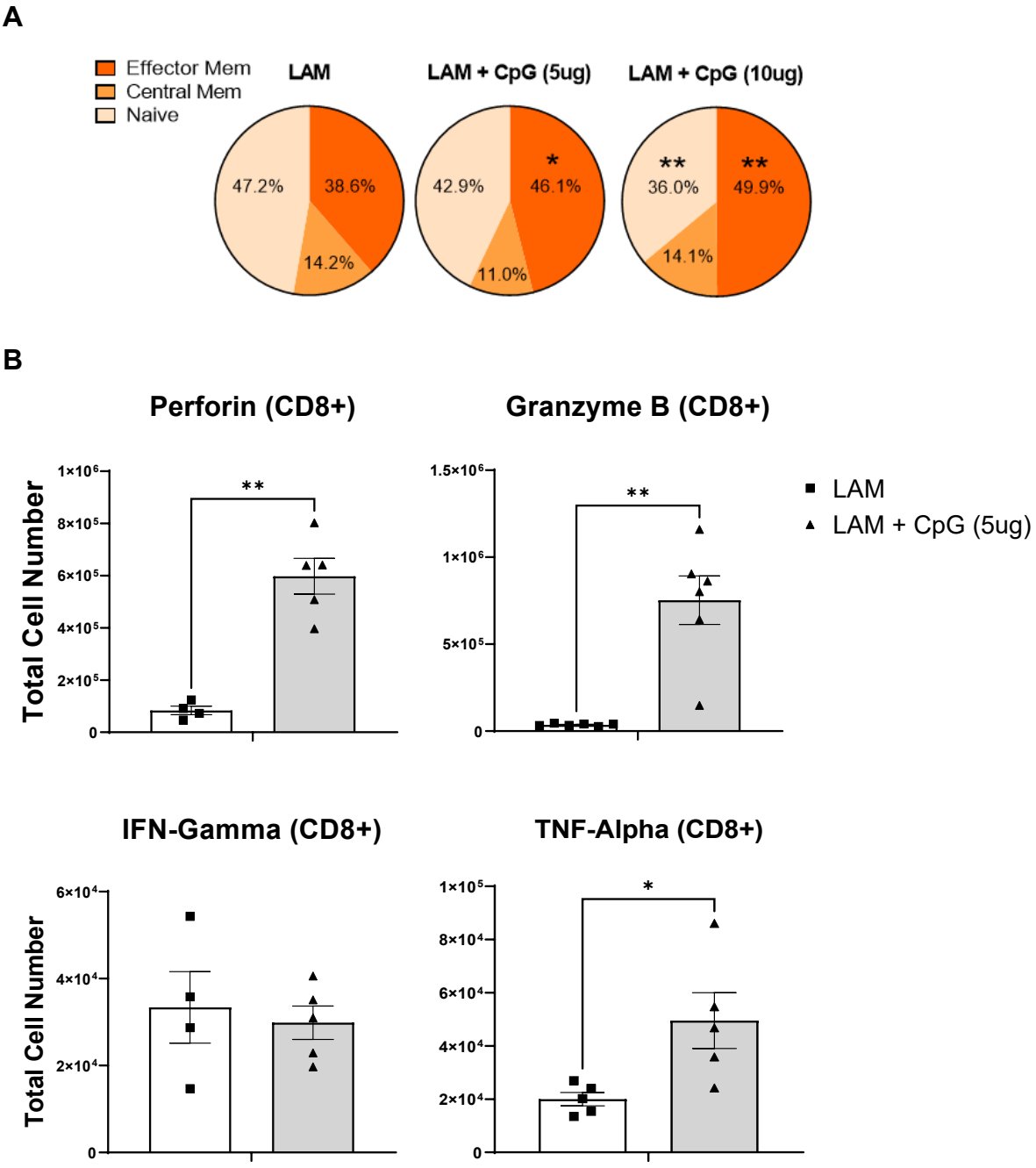

Figure 11. *CD8T cells in CpG treated LAM lungs are activated and secrete inflammatory and cytotoxic cytokines.* Data shows T cell populations in the left lung lobe 22 days after LAM induction. **A)** Effector memory, central memory, and naïve CD8+ T cell subsets. **B)** Intracellular staining of CD8+ T cells for inflammatory cytokines perforin, granzyme b, IFN-γ, TNF-α.Data is representative of n= 2+ experiments and n>5 mice. Statistical analysis was performed using one-way ANOVA. * $p<0.05$, ** $p<0.01$, *** $p<0.001$, **** $p<0.0001$.

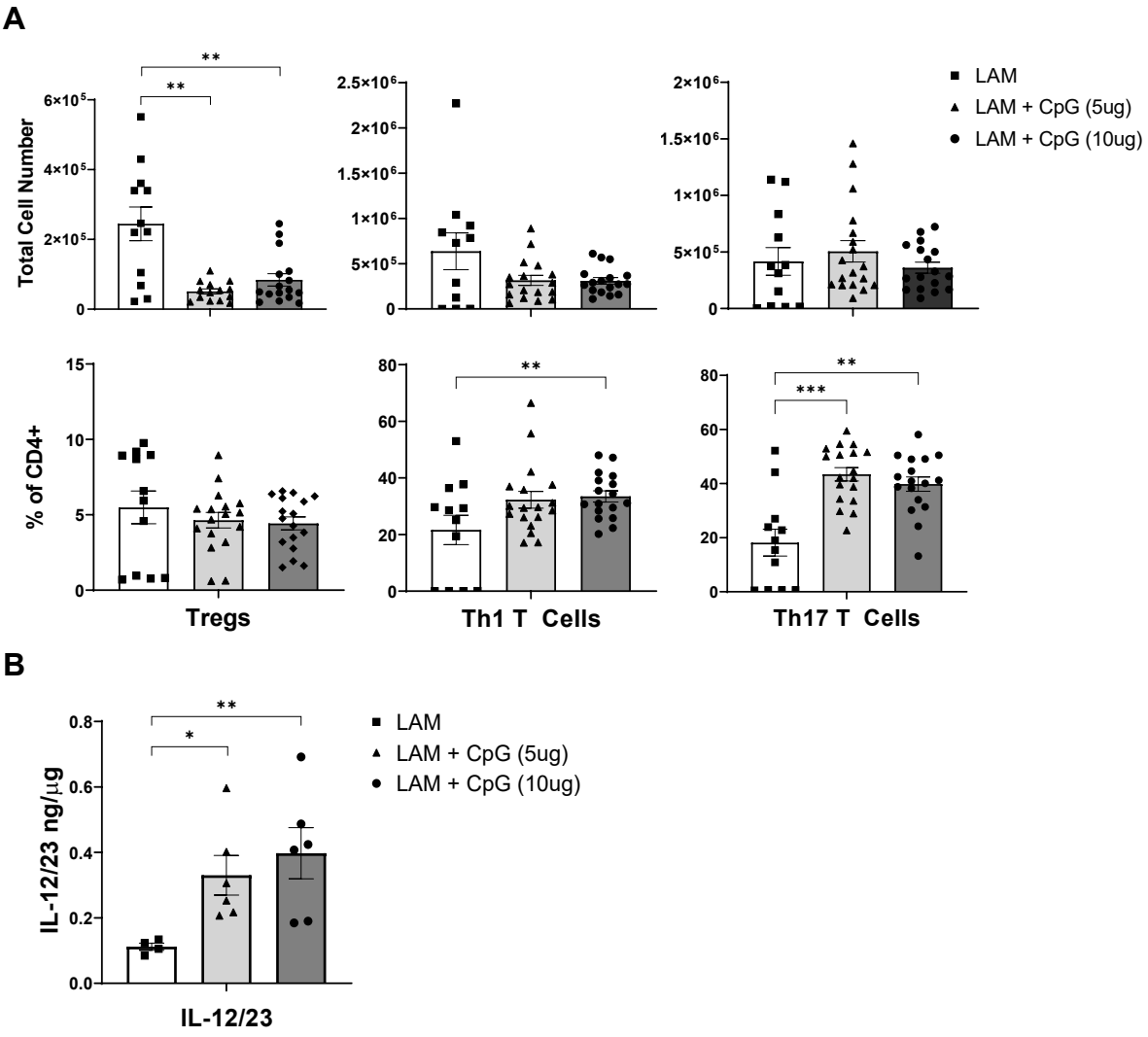

Figure 12. *CD4 helper T cells in CpG treated LAM lungs shift away from immunosuppressive phenotypes.* **A)** CD4 helper T cell subsets: Tregs, Th1, and Th17 total cell numbers and frequency of CD4+ cells. **B)** IL12/23 cytokine levels in LAM lungs. Data is representative of n= 2+ experiments and n>5 mice. Statistical analysis was performed using one-way ANOVA. * p<0.05, ** p<0.01, *** p<0.001, **** p<0.0001.

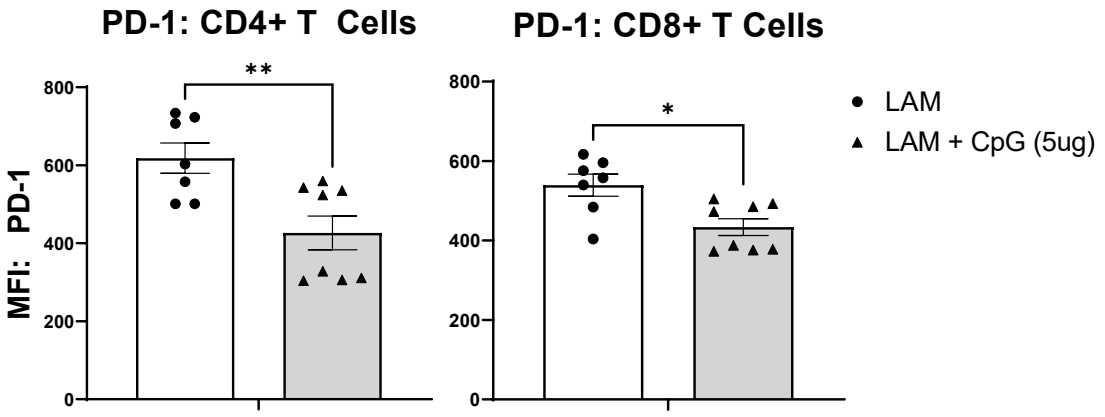

Figure 13. *CpG treatment in LAM decreases expression of immune checkpoint receptors in T cells.* Data shows MFI of PD-1 expression in CD4+ and CD8+ T Cells. Data is representative of n= 2+ experiments and n>5 mice. Statistical analysis was performed using one-way ANOVA. * p<0.05, ** p<0.01, *** p<0.001, **** p<0.0001.

Therapeutic efficacy of CpG is mediated in part by plasmacytoid dendritic cells.

Plasmacytoid dendritic cells (pDCs) express high levels of TLR9 in both mouse and human lungs. Therefore, we hypothesized that pDCs would mediate CpG treatment efficacy by activating and skewing T cells. We depleted pDCs using anti-PDCA-1 antibodies (**Fig. 14**) and examined treatment outcome and immunity. We found that pDC depletion in CpG treated mice with LAM significantly reduced survival, with a decreased median survival from 60 days to 56 days (**Fig. 15**), suggesting that pDCs are involved in the immune response that makes CpG treatment beneficial.

We used flow cytometry to investigate the affect of pDC depletion on other cells in the LAM microenvironment during CpG treatment and found that depleting pDCs significantly effect reduced the number of monocytes and interstitial

macrophages in CpG-treated LAM lungs **(Fig. 16)**. This suggests that part of the mechanism may involve pDC mediated recruitment of monocytes to the lung tissues and an interaction with interstitial macrophages that is yet to be understood.

To assess the effect of pDCs on T cell immunity in LAM, we also assessed CD4+ T cell subsets after pDC depletion and found that the number of Treg cells remained reduced but the proportion of Th17 cells was no longer increased compared to CpG treatment alone (**Fig 17A**). Additionally, we found that pDC depletion abrogated the increase in IL-12/23 and IL-6 that are caused by CpG treatment (**Fig 17B**), both key cytokines that promote Th17 differentiation, suggesting that pDCs are at least in part required for inducing beneficial Th17 responses after CpG treatment in LAM. In CD8+ T cells, pDC depletion resulted in a significant decrease in the secretion of inflammatory cytokines, perforin, granzyme B, and TNF-α (**Fig. 17C**), suggesting that pDCs play a role in activating these cytotoxic responses stimulated by CpG-treatment in LAM.

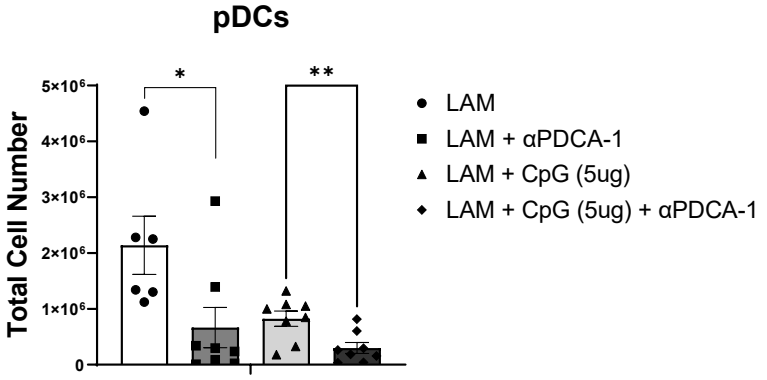

Figure 14: Total pDC counts on day 22 in early stage disease with or without CpG treatment. Data is representative of n=2+ experiments with n>4 mice. Statistical analysis was performed using two-way ANOVA. * p<0.05, ** p<0.01, *** p<0.001, **** p<0.0001.

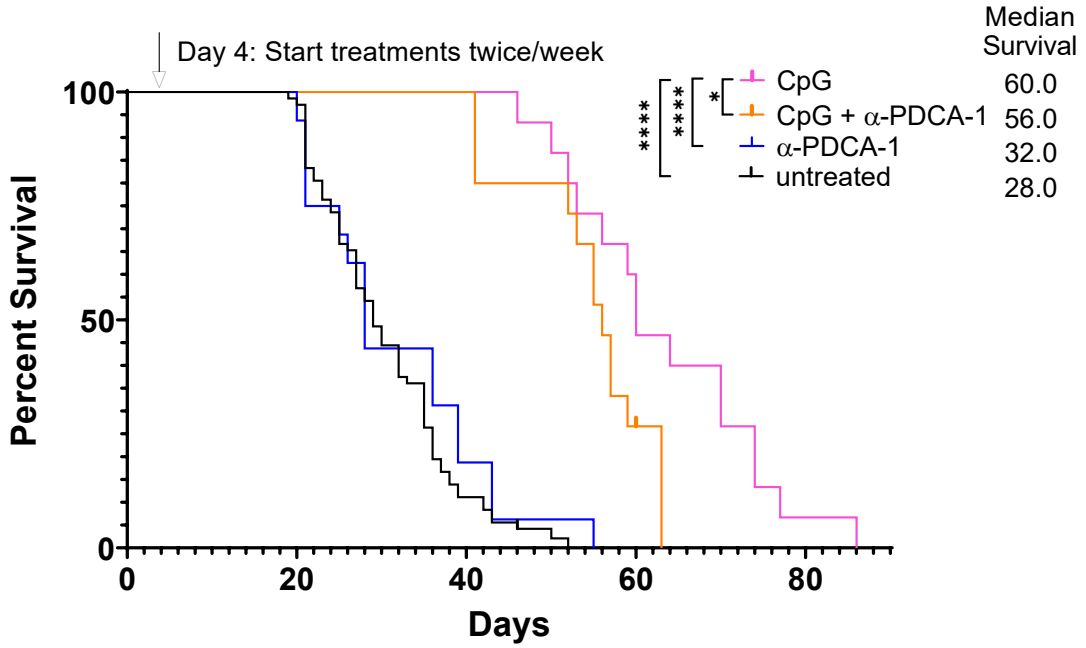

Figure 15. *pDC depletion in CpG-treated LAM decreases survival.* Survival curve showing pDC depletion reduces survival after CpG treatment. Data is representative of n=2+ experiments and n>6 mice. Statistical analysis was performed using log-rank test * p<0.05, ** p<0.01, *** p<0.001, **** p<0.0001.

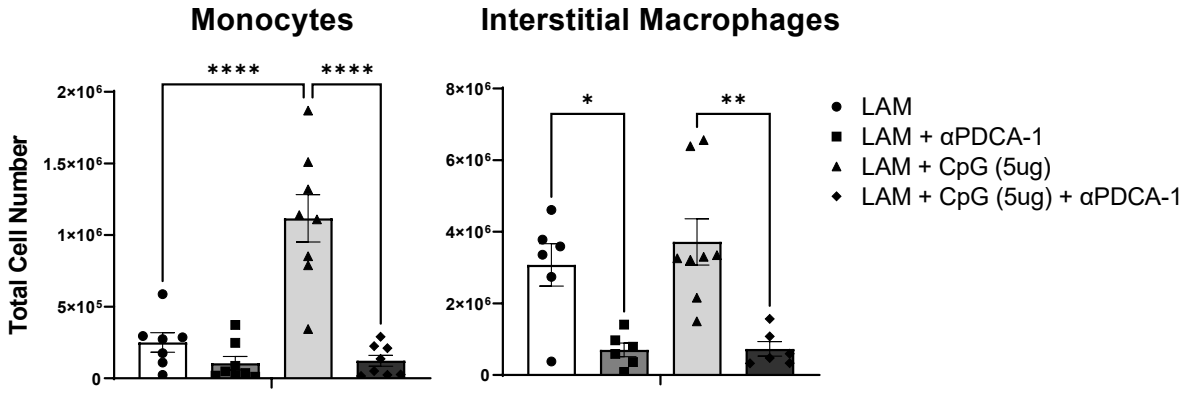

Figure 16: pDC depletion in CpG-treated LAM decreases monocytes and interstitial macrophages. Total cell counts of monocytes and interstitial macrophages in LAM lungs being treated with or without CpG treatment or anti-pDCA-1 antibody depletion. Data is representative of n=2+ experiments with n>4 mice. Statistical analysis was performed using two-way ANOVA. * p<0.05, ** p<0.01, *** p<0.001, **** p<0.0001.

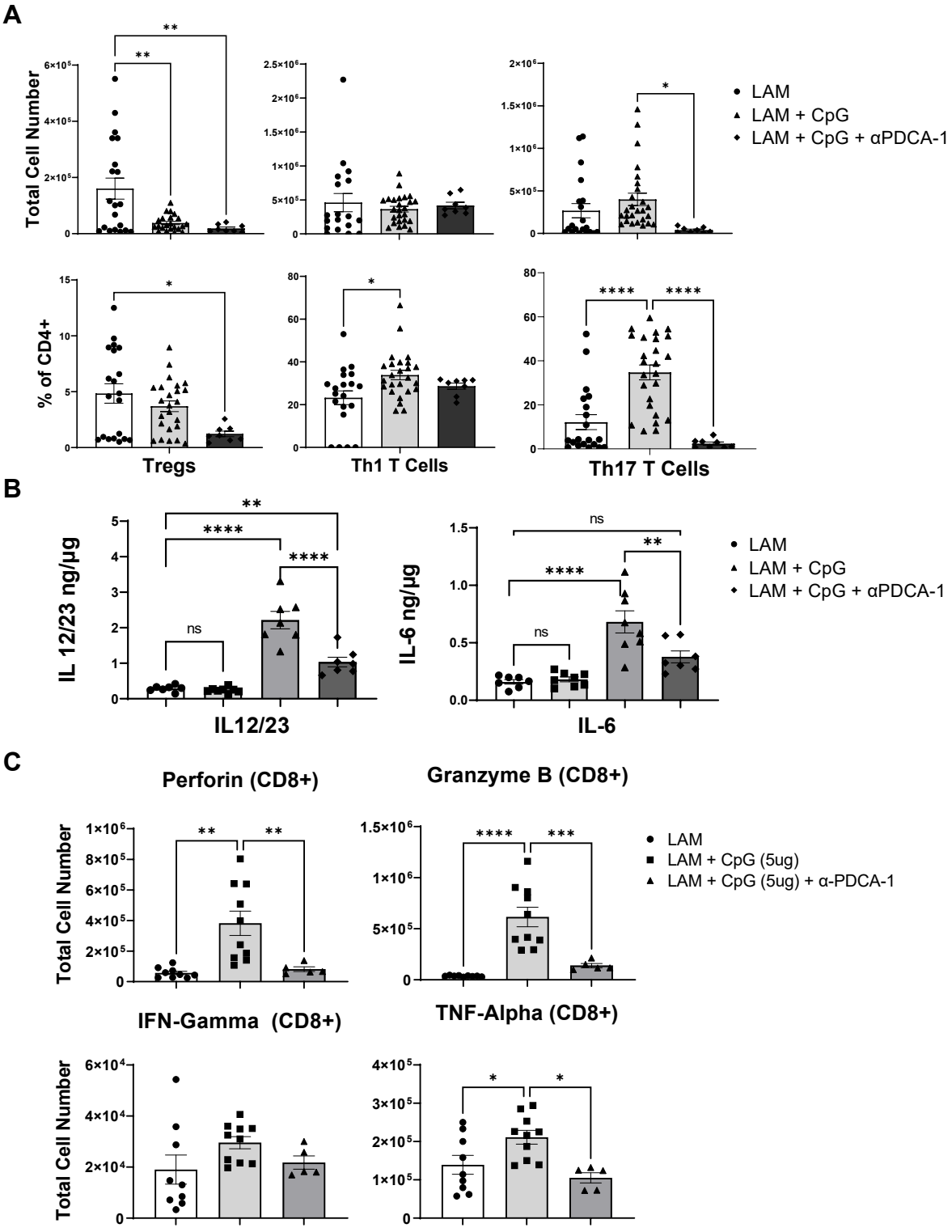

Figure 17. *pDC depletion in CpG-treated LAM affects T cell responses.* **A)** CD4 helper T cell subsets: total cell numbers and % of CD4+ cells. **B)** IL12/23 and IL-6 cytokine levels in LAM lungs. Data is representative of n=2+ experiments and n>6 mice. Statistical analysis was performed using one-way ANOVA . * p<0.05, ** p<0.01, *** p<0.001, **** p<0.0001.

Discussion

Our research offers preclinical evidence to support the benefit of adjuvant-mediated immunotherapy in the treatment of LAM. We found that intranasal treatment with CpG at early-stage disease increased survival in mice with LAM. This treatment slowed the progression of disease in the lungs and decreased the LAM nodule burden in treated mice. CpG treatment also increased the population of cytotoxic and effector CD8+ T cells and decreasing the population of Treg cells in the LAM microenvironment. We found that pDC mediated induction of Th17 cells is in part responsible for CpG treatment efficacy. We also observed synergistic effects of both systemic checkpoint inhibition and low-dose rapamycin when combined with local CpG adjuvant therapy. This finding suggests that immune activating therapies, particularly combination therapies, could be an effective strategy to treat LAM.

Our data suggest that CpG efficacy is mediated in part by cytotoxic CD8+ T cells and Th17s that are activated through pDCs. CpG-stimulated pDCs have been shown to promote Th17 differentiation through increased secretion of cytokines like IL-6, IL-23 and TGF-β (152)), which can induce tumor regression in mice (153)In alignment with this, the depletion of pDCs from the lung microenvironment in our CpG-treated LAM mice results in decreased IL-6 and IL-23 production in the tissue and is correlated with decreased expansion of Th17 cells. Th17 cells are associated with both pro-tumor and anti-tumor immunity as a result of their ability to switch between pro-inflammatory Th17-Th1 and immunoregulatory Th17-Treg phenotypes. In anti-tumor immune responses,

Th17 cells are involved in tumor infiltration (154) and the activation of cytotoxic CD8+ T cells(155). CpG stimulation has been shown to inhibit Tregs and promote Th17 differentiation in a mouse model of leukemia(156). Authors found that CpG tumor vaccine prolonged survival of mice with leukemia and suggest that this is due to both the reduction in Tregs and increased Th17 response. Additionally, Tregs can be skewed to generate IL-17 in the presence of pro-Th17 IL-6 and IL1β(157), and these Tregs are less effective at inhibiting effector Th17 and cytotoxic CD8+ T cells in autoimmune arthritis(158). Thus, our findings that Th17s are mediators of anti-LAM immunity after CpG treatment aligns with existing literature demonstrating the importance of inflammatory Th17s in anti-tumor immunity.

pDCs have also been implicated in mediating immune responses against viruses and cancer. pDCs have been shown to induce IFNy producing CD8+ and CD4+ T cells, crucial to resolving LCMV infection in the lungs(159). Additionally, in the lungs, pDCs were shown to affect Th17 differentiation in a mouse model of Bordetella pertussis infection. Interestingly, in B. pertussis infection pDCs reduced Th17 differentiation and blocking pDC produced IFNa resulted in reduced bacterial loads and increased Th17s(160). Overall, literature suggests that pDCs can have beneficial or detrimental effects, depending on the context. Our findings show that in LAM, depleting pDCs inhibits the Th17 cell response and reduces survival after CpG-mediated TLR9 activation, suggesting that pDCs play a beneficial role in this disease.

A sophisticated balance of pro- and anti-inflammatory signals helps regulate immune responses in the body. Immunotherapies influence these pathways, tipping the scale towards inflammation to produce impressive anti-tumor responses. Our work here has shown that this balance is also disturbed in LAM and anti-LAM immunity can be activated using TLR9 adjuvant CpG. However, the inflammation induced can also lead to adverse effects and inflammatory toxicities. Choosing the right dose and treatment schedule to maintain equilibrium between treatment efficacy and runaway inflammation could be key to avoiding undesirable tissue damage and severe symptoms. Our finding that lower dose CpG therapy produces less inflammation in the lungs and increases survival in LAM mice despite the increase in nodule count (compared to higher dose CpG), suggests that too much inflammation may cause damage in an already delicate tissue environment like the LAM affected lungs and thus high levels of CpG have reduced treatment efficacy. A recent clinical trial looking at inhaled TLR9 agonist for the treatment of lung cancer reported several adverse events in patients all related to inflammatory immune responses (NCT03326752) (161), suggesting that TLR9 activation while potent may require more targeted delivery strategies that prevent exposure to all tissues. Our data suggest that this is true also for CpG treatment in LAM. A potential strategy to mitigate CpG side effects is to encapsulate CpG into a nanoparticle system that can deliver the TLR9 agonist directly to antigen presenting cells or the lymph nodes, where adaptive immunity is shaped. Encapsulation of CpG could reduce tissue-wide inflammation and thus reduce local toxicity effects, while maintaining the anti-LAM immune activation so

crucial to inhibit LAM nodule proliferation. In addition, activation of stromal cells is correlated with tumor progression (162) and immunotherapy strategies inhibiting activated fibroblasts have been successful in promoting anti-tumor immunity in several preclinical cancer models (163–165). Because LAM nodules are composed of many cell types including fibroblasts that may contribute to LAM pathology (42,166,167), targeting activating treatments to immune cells in the lymph nodes while inhibiting activation of stromal cells in the tissue could help curb tissue remodeling (168).

Several immunotherapies are currently approved for treatment of lung cancer and may be considered for LAM. These include monoclonal antibodies against EGFR and VEGF/VEGFR pathways and immune checkpoint inhibitors targeting PD-1/PD-L1 or CTLA-4. Clinical trials for adoptive T cell therapy and lung cancer vaccines are ongoing (169) and several immunotherapies are approved for advanced lung cancers (170). Similarly, clinical trials for LAM therapies have explored the use of FDA-approved anti-angiogenic and anti-fibrotic therapies targeting pathways involved in the progression of lung cancer and idiopathic pulmonary fibrosis (Bevacizumab, Nintedanib, Saracatinib), but so far with limited success. Immune checkpoint inhibitors have not yet been tested in LAM patients, but there is promising research in mouse models to support this treatment strategy (39,40). Furthermore, our work showing TLR9 agonist treatment can enhance survival in murine LAM could be translated into the clinic in future, particularly since TLR9 agonists have been approved for several cancers and are explored in clinical trials for lung cancer. Given that our mouse model of LAM

does not fully represent human LAM, we checked the presence of pDCs and TLR9 expressing antigen presenting cells in LAM tissues using the LAM Cell Atlas (171). The LAM Cell Atlas confirmed that TLR9 expressing pDCs are present in human LAM lung tissues, suggesting that a TLR9 stimulating treatment could be successfully translated to humans. Finally, results from lung cancer studies suggest that combination of immune checkpoint inhibitors and TLR9 agonists lead to successful anti-lung cancer immune re-activation. Our data suggests that this strategy could be successful in LAM as well and thus there is potential for designing LAM combination immunotherapies in the future.

Significance

The findings presented in this chapter introduce a novel therapeutic strategy for LAM: TLR9 activation through inhaled CpG treatment. The documented benefits of this treatment strategy lays the justification for future clinical investigations of adjuvant therapy in LAM. We have also identified key players in the immune response generated by this response: plasmacytoid dendritic cells, and T cells. These could be important targets for future immunotherapy in LAM. In addition, these data contribute to the body of work suggesting immunosuppression play a role in the pathogenesis of LAM, because immune activation yields beneficial outcomes.

Chapter 4. Investigating CpG as therapy during Late Stage LAM Disease and in Combination with Existing Treatments

Acknowledgements:

This work was completed with the help of Dr. Jacob McCright, Bennett Yang, Juan Grano de Oro Fernandez, Kaitlyn Moore, Havish Gadde, Mehu Donthi, Michele Kaluzienski, and Katharina Maisel. Their contributions made this chapter possible and I am deeply grateful for the time, effort, and care dedicated by each individual to making these studies successful.

This chapter is partially reproduced from the Biorxiv self-published manuscript available online: Mayowa M Amosu, Jacob C McCright, Bennett E Yang, Juan Grano de Oro Fernandez, Kaitlyn A Moore, Havish S Gadde, Michele L Kaluzienski, Katharina Maisel. bioRxiv 2023.02.06.527331; doi: https://doi.org/10.1101/2023.02.06.527331

Introduction

Our initial results suggest that treatment with CpG in LAM lungs has a therapeutic benefit when treatment begins early in the course of disease. However, most women are not diagnosed with LAM until they present with clinical symptoms and have likely begun to lose some amount of pulmonary function. Therefore, it is worth investigating whether CpG treatment can be effective when administered at a later stage of LAM disease and how this might affect the immune microenvironment in the lungs. Here, we hypothesized that CpG treatment would increase survival in mice and counter LAM immunosuppression when administered later in the course of LAM disease.

The combination of checkpoint inhibition and TLR activation has been well studied in models of cancer with encouraging results (172–174). CpG activates cells within the tumor and stimulates anti-tumor immune responses and antigen presentation. It can also induce increased expression of PD-L1 on cells (147), which would make tumor cells more susceptible to checkpoint inhibition. Anti-PD-1 therapy makes the T cell response more resistant to immunosuppression and was shown to have potential as immunotherapy for pulmonary LAM based on results in our mouse model (39). Here we investigate the combination of CpG with checkpoint inhibition for synergism in LAM.

There are conflicting results around the proinflammatory vs anti-inflammatory effects of mTOR inhibition in various settings. Inhibition of mTOR in macrophages and monocytes has been shown to promote proinflammatory cytokines and inhibit anti-inflammatory IL-10 production (175,176). In dendritic cells, ex-vivo exposure to rapamycin during TLR activation increases the antitumor immunity of autologous DC vaccination in mice (177). However, rapamycin is generally known to be an immunosuppressive drug that can promote immune tolerance through the induction of tolerogenic dendritic cells and the expansion of regulatory T cells. Research shows that rapamycin therapy inhibits some key inflammatory immune responses in plasmacytoid dendritic cells (178). The mTOR complex 1 is also involved in TLR9 activation through the myD88 signaling pathway, so inhibition of mTOR with rapamycin may attenuate the inflammatory response induced by CpG treatment. These seemingly contradictory responses may exist on a spectrum dependent on dose

administered. Recent work investigating how dose of rapamycin induces different immune responses, found that low-dose rapamycin results in the expansion of central memory T cells while higher doses of rapamycin tend to be immunosuppressive/immunoregulatory (116).

Recent work has also shown the efficacy of combination ICI and mTOR inhibition in the treatment of various cancers (179,180). However, the effect of TLR9 activation in this therapeutic setting has not yet been documented. Given that checkpoint inhibition is synergistic with both CpG (in murine LAM) and rapamycin (in cancer models), We hypothesized that CpG-ICI-rapamycin triple combination treatment will work synergistically to increase survival in mice with LAM. Here we investigate CpG in various combinations in an attempt to maximize the therapeutic benefit of this treatment strategy.

Materials and Methods

Mice

7 to 9-week old female C57BL6/J mice (Jackson Laboratory) were used for all studies. Study protocols were approved by the UMD Institutional Animal Care and Use Committee (IACUC).

LAM induction

TSC2-null kidney-derived epithelial tumor (TTJ) cells, were provided by the Krymskaya Lab at the University of Pennsylvania (39). TTJ cells (5.0×10^5) were

administered in 100 µL of PBS via tail vein injection to induce LAM disease in 8-9 week old female mice. Lung lesions typically develop within 3-7 days.

Survival Studies

Mice received CpG class B (5 µg/10 µg) 2x/week (Invivogen, tlrl-1826-5), in 50 µL of PBS, intranasally starting 4 days post LAM induction. Mice receiving combination therapy, received intranasal CpG and 300 µg anti-PD-1 antibody (BioXCell, BE0146-A0) and / or 1 µg/g Rapamycin (Selleck Chemicals, S1039) in 200 µL of PBS via intraperitoneal (IP) injection 2x/week. Control groups received 50 µL of PBS intranasally or 200 µL PBS with or without 300 µg of rat IgG isotype control (BioXCell, BE0089) by IP injection. Mice were monitored for symptoms of disease and body weight changes and removed from studies based on experimental timing or humane endpoints. At endpoint, mice were euthanized and lung tissues collected for histological analysis.

Histology

Tissues were fixed overnight in 4% PFA at 4ºC, embedded in paraffin wax, sectioned at 5 µm, and stained with hematoxylin and eosin (H&E). LAM nodule counts, average nodule diameters, and general tissue inflammation were quantified using QuPath Imaging software.

Flow Cytometry

14 days after LAM induction, mice received a single intranasal treatment dose of CpG (5 µg or 10 µg) in 50 µL PBS or 50 µL of PBS as a vehicle control. At 1 and 3 days post treatment, lung tissues were perfused and collected for flow

cytometric analysis. Left lung lobes were dissociated by enzymatic digestion with 1 mg/mL collagenase D (Roche, 11088882001), and 1 mg/mL collagenase IV (Worthington Biochemical, LS004188) in DMEM with 5% FBS for 1 hour. Single cell suspensions were stained to identify eosinophils (CD64-, Siglec F+, Ly6G-), neutrophils (CD64-, Siglec F-, Ly6G+) dendritic cells (CD11c+, MHC-II^{high}), plasmacytoid dendritic cells (CD11c+, PDCA-1+, MHC-II^{high}), alveolar macrophages (CD64+, SiglecF^{high}, CD11b-), interstitial macrophages (CD64+, SiglecF^{low}, CD11b+, MHC-II+), B Cells (CD19+ or B220+), T Cells (CD3+, CD4+ or CD8+), regulatory T Cells (CD3+, CD4+, FoxP3+), Th1 T cells (CD3+, CD4+, FoxP3-, Tbet+), Th2 T cells (CD3+, CD4+, FoxP3-, Gata3hi), and Th17 T Cells (CD3+, CD4+, FoxP3-, ROR-γt+). Cells were analyzed by flow cytometry using a BD FACSCelesta (BD Biosciences) and FlowJo (FlowJo LLC). Gating strategies can be found in the data supplement (**Fig E1**).

Statistical Analysis

Data were analyzed using Graphpad Prism (GraphPad, La Jolla, CA). Survival studies were assessed using the log-rank (Mantel-Cox) test. Unpaired Welch t tests were used to compare pairs of samples or groups. Mann–Whitney test was used to compare the groups of data that failed to satisfy parametric assumptions. Brown-Forsythe and Welch One-way ANOVA were used for comparisons between ≥3 groups. Differences were considered statistically significant when $p < 0.05$. *p<0.05, **p<0.01, ***p<0.001, ****p<0.0001.

Results

CpG treatment is less effective in late stage disease

Given the encouraging results we found with CpG treatment in early LAM, and since LAM can be diagnosed at a variety of disease stages, we next evaluated CpG's therapeutic potential in more advanced disease. We induced LAM in mice and allowed disease to develop for 14 days, before beginning intranasal treatment with CpG. We found that the previously beneficial lower dose CpG (5 μg) had no significant effect on survival, but a high dose of CpG (20 μg) showed some therapeutic benefit (**Fig 18A**), increasing median survival from 32 days to 40 days. Despite the increased survival, we found that CpG treatment did not improve abnormal tissue fractions, nodule count, or nodule size in more advanced disease (**Fig. 18B-C**). However, we did observe that nodules in CpG-treated mice showed histological signs of necrosis in LAM nodules, unlike untreated LAM controls (**Fig 18B**). We then determined the effect of CpG on the immune response in late stage LAM mice 1 and 3 days following the first intranasal treatment of CpG (days 15 and 17 after disease induction). Unlike the striking responses seen during early intervention, CpG given later in disease did not significantly affect immune cell infiltration in LAM lungs. There were no differences in total CD45+ immune cell populations between CpG treated and untreated LAM lungs (**Fig. 19**). We found only a decrease in eosinophils and cDCs at day 15; all other populations of identified immune cells remained unchanged (**Fig. 20**). Overall, our data suggest that CpG treatment, while increasing survival, only has a minor beneficial effect in late stage disease.

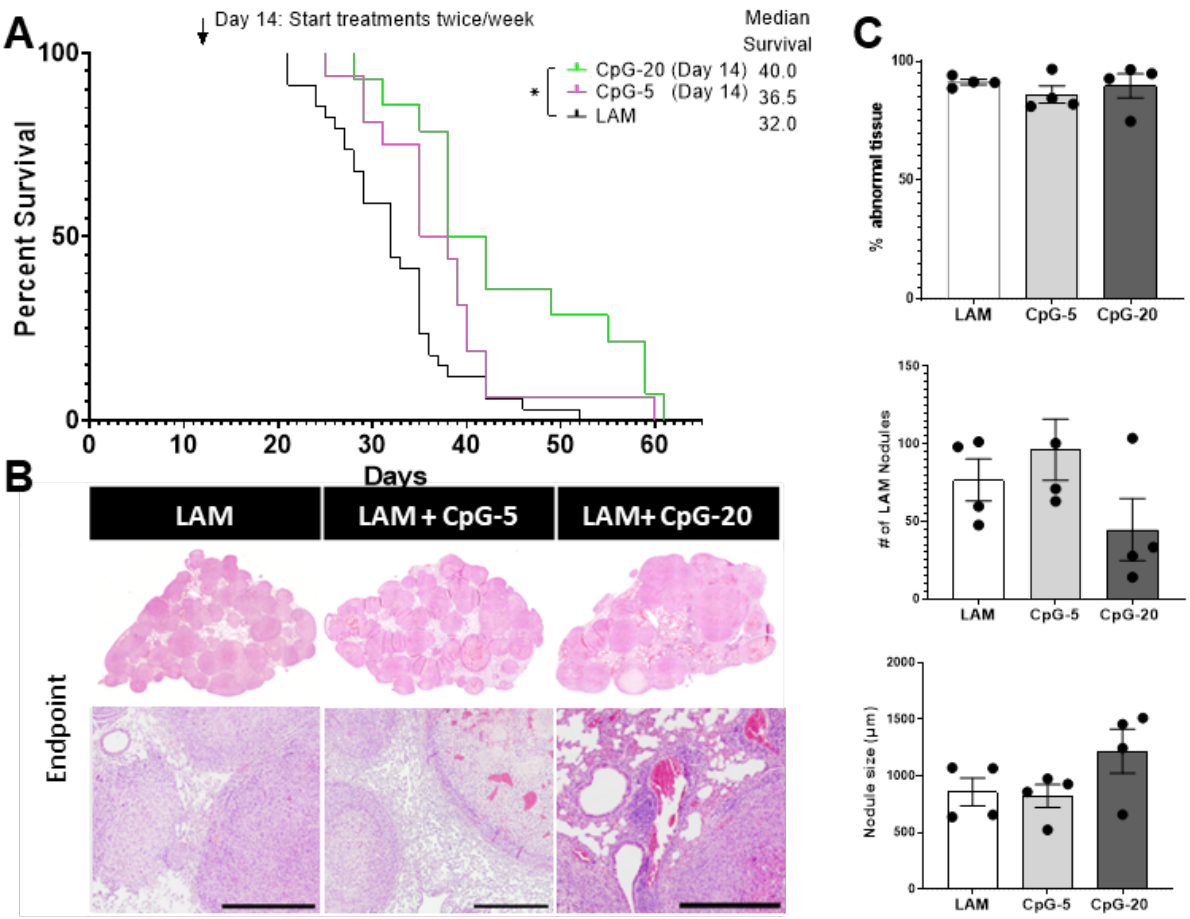

Figure 18. *Late intervention intranasal CpG increases survival in murine model of metastatic LAM at higher dose.* **A)** Survival studies showing 20 µg and 5 µg CpG treatments in late stage disease. **B)** Representative H&E images of mouse lungs from treatment groups: untreated LAM control, CpG 5 µg, and CpG 20 µg. Scale bar = 500 µm. **C)** Quantification of LAM nodules and abnormal tissue regions for treatment groups of mice at symptomatic endpoints from survival studies. Data is representative of n=2+ experiments and n>4 mice. Statistical analysis was performed using log-rank test (survival studies) and one-way ANOVA (histological analysis). * $p<0.05$.

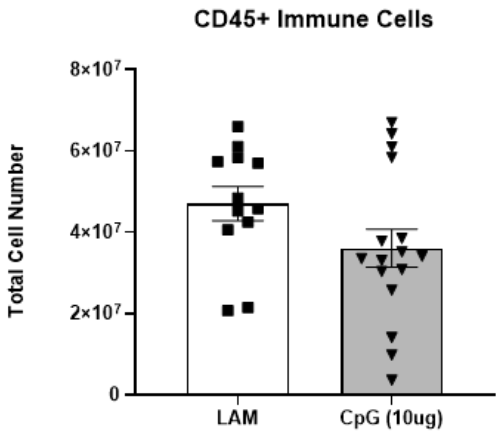

Figure 19: Total immune cell counts on day 15 after late intervention CpG treatment on day 14. Data is representative of n=2+ experiments with n>4 mice. Statistical analysis was performed using two-way ANOVA. * $p<0.05$, ** $p<0.01$, *** $p<0.001$, **** $p<0.0001$.

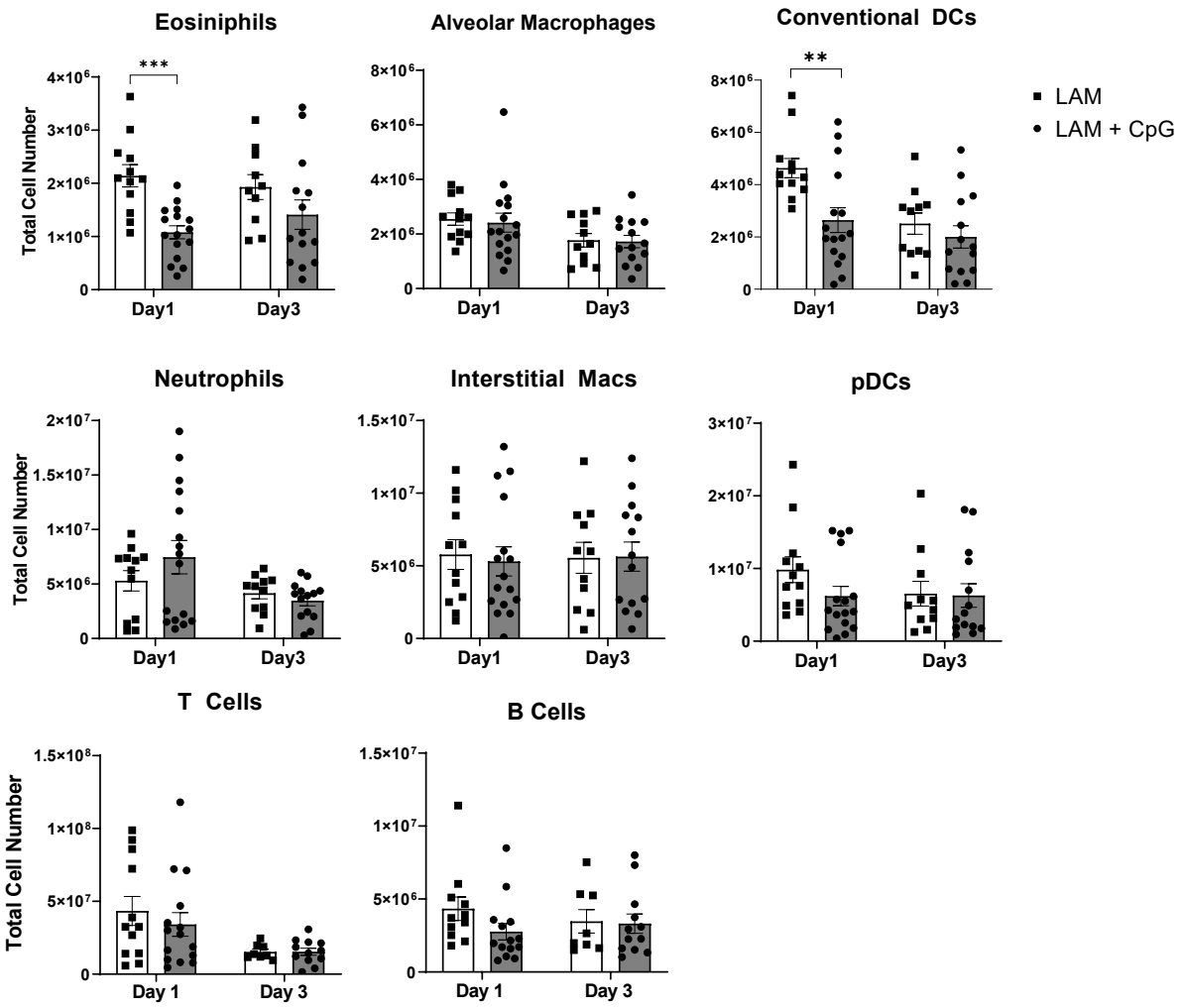

Figure 20. *CpG treatment modulates immune cell populations in response to late intervention (starting at day 14) intranasal CpG in LAM lungs (Day 1 & Day 3 after CpG treatment).* Total cell numbers of granulocytes and antigen presenting cells infiltrating the lungs 1 and 3 days after CpG treatment obtained via flow cytometry. Data is representative of n= 3 experiments and n = 8+ mice. Statistical analysis was performed using one-way ANOVA. * $p<0.05$, ** $p<0.01$, *** $p<0.001$.

Combination therapy of CpG with anti-PD1 or rapamycin synergizes to increase survival in mouse LAM

Rapamycin is the only treatment currently available to LAM patients, so it is crucial to evaluate combination therapy of CpG with low-dose rapamycin for clinical translation. We found that combination CpG with low-dose Rapamycin therapy significantly increased survival in mice (**Fig. 21A**) compared to CpG or Rapamycin treatments alone, increasing median survival more than 3-fold, from 29 days in untreated mice to 100 days in mice receiving combination therapy. Median survival for combination therapy was 1.6 times higher than either monotherapy, and mice treated with CpG had the same median survival as those receiving low-dose rapamycin (60 days). Histological analysis of tissues collected at endpoints from survival studies showed that combination of CpG with Rapamycin therapy significantly reduced LAM nodule counts and size, and abnormal lung tissue compared to CpG monotherapy (**Fig. 21B-C**).

We have also previously shown that treatment with anti-PD-1 antibody prolongs survival in our mouse model of LAM (39). CpG has been shown to synergize with checkpoint inhibition in pre-clinical cancer models (181–183) and thus we sought to evaluate combination therapy of CpG with checkpoint inhibition to determine synergistic effects in LAM. We found that combination CpG and anti-PD-1 therapy increased survival in mice (**Fig. 22A**) compared to CpG or anti-PD1 treatment alone, increasing survival to 65 days for combination therapy compared to 45 and 49 days for the monotherapies, respectively. This is consistent with recent work showing synergism for this approach in treating solid

tumors (144), and suggests that TLR9 activation can make LAM more responsive to checkpoint inhibition. CpG and anti-PD-1 therapy also resulted in reduced LAM nodule counts and lower abnormal tissue fractions, but did not reduce LAM nodule size (**Fig. 22B-C**). We observed signs of necrosis in the larger LAM nodules of mice receiving checkpoint inhibition with and without CpG (**Fig. 22B**) that were not present in nodules of untreated LAM controls or rapamycin treated mice. Tumor necrosis is often associated with enhanced cytotoxic T-cell responses as a result of immune checkpoint inhibition.

To establish that combination rapamycin and anti-PD-1 therapy are compatible for treatment in LAM, we conducted a survival study and found the combination to be synergistic, increasing median survival to 77 days from 49 and 60 days for anti-PD1 and rapamycin respectively (**Fig. 23**). Triple combination therapy of CpG with low-dose rapamycin and anti PD-1 therapy also proved to be synergistic, with a median survival of 95 Days (**Fig. 24**). It is interesting to note that only the combinations that included both CpG and rapamycin resulted in the highest survival across all survival experiments (100 and 95 days), suggesting that the interaction between the two is the primary driver of these treatment outcomes.

Taken together, our data suggests that that TLR9 activation may be beneficial as co-treatment with current clinical LAM therapy, rapamycin, and may also be combined with checkpoint inhibitors for increased efficacy.

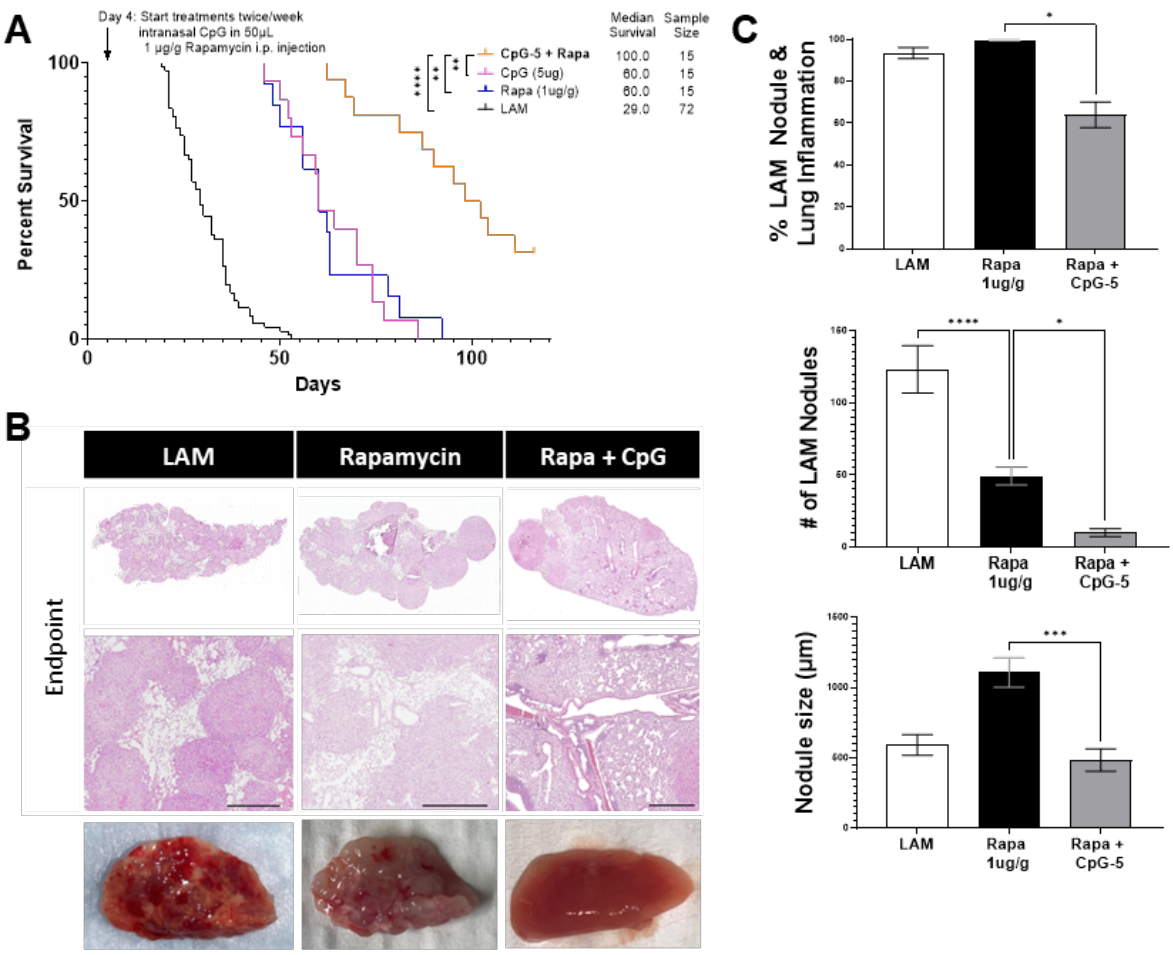

Figure 21. *CpG treatment is synergistic with Rapamycin Therapy.* **A)** Aggregate data from four survival experiments. LAM n=34, CpG (10 µg) n=22, α-PD-1 n=16, CpG (10 µg) + α-PD-1 n=20. **B)** Representative H&E stained histological images of mouse lungs from treatment groups: untreated LAM control, CpG (10 µg), α-PD-1, CpG (10 µg) + α-PD-1 . Scale bar = 500 µm. **C)** Quantification of LAM nodules and Inflamed tissue regions between treatment groups of mice at symptomatic endpoints from survival studies in (A). 3 sections analyzed per mouse. Statistical analysis was performed using log-rank test (survival studies) and one-way ANOVA (histological analysis). * $p<0.05$, ** $p<0.01$, *** $p<0.001$, **** $p<0.0001$.

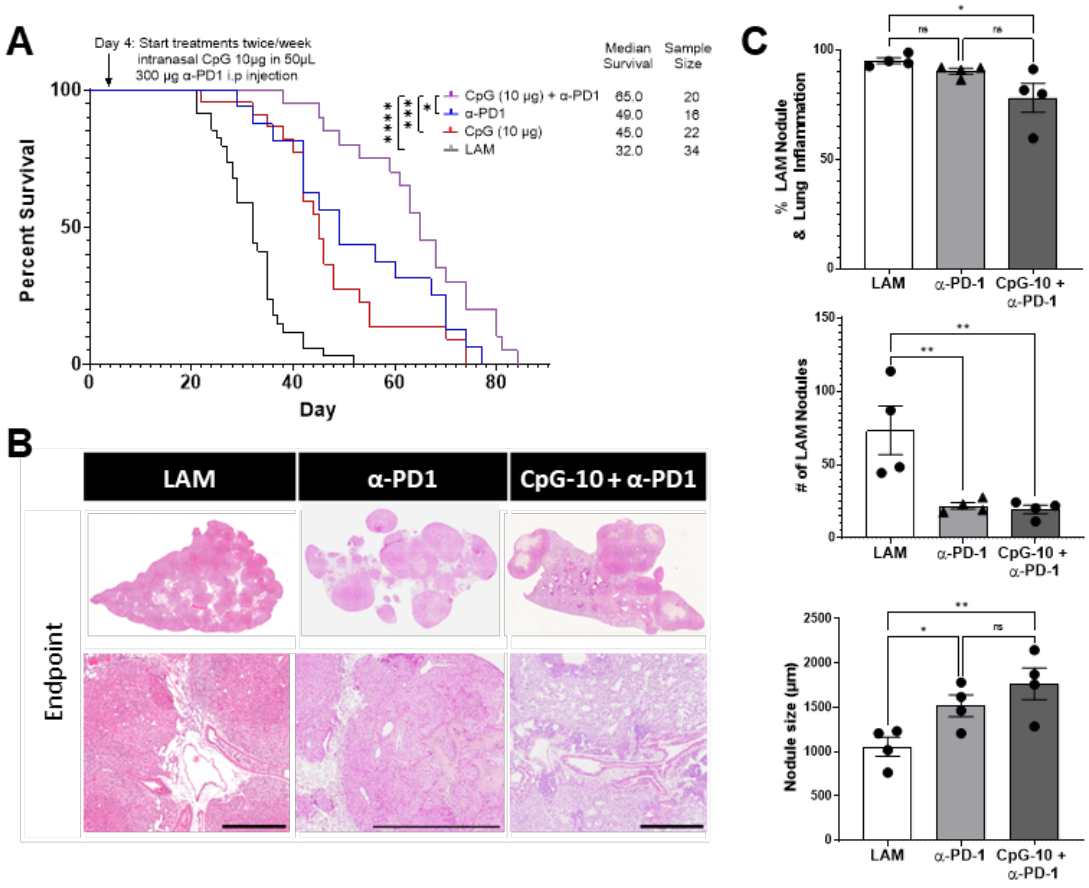

Figure 22. *CpG treatment is synergistic with ICI Therapy.* **A)** Aggregate data from four survival experiments LAM n=34, CpG (10 µg) n=22, α-PD-1 n=16, CpG (10 µg) + α-PD-1 n=20. **B)** Representative H&E stained histological images of mouse lungs from treatment groups: untreated LAM control, CpG (10 µg), α-PD-1, CpG (10 µg) + α-PD-1 . Scale bar = 500 µm. **C)** Quantification of LAM nodules and Inflamed tissue regions between treatment groups of mice at symptomatic endpoints from survival studies in (A). 3 sections analyzed per mouse. Statistical analysis was performed using log-rank test (survival studies) and one-way ANOVA (histological analysis). * p<0.05, ** p<0.01, *** p<0.001, **** p<0.0001.

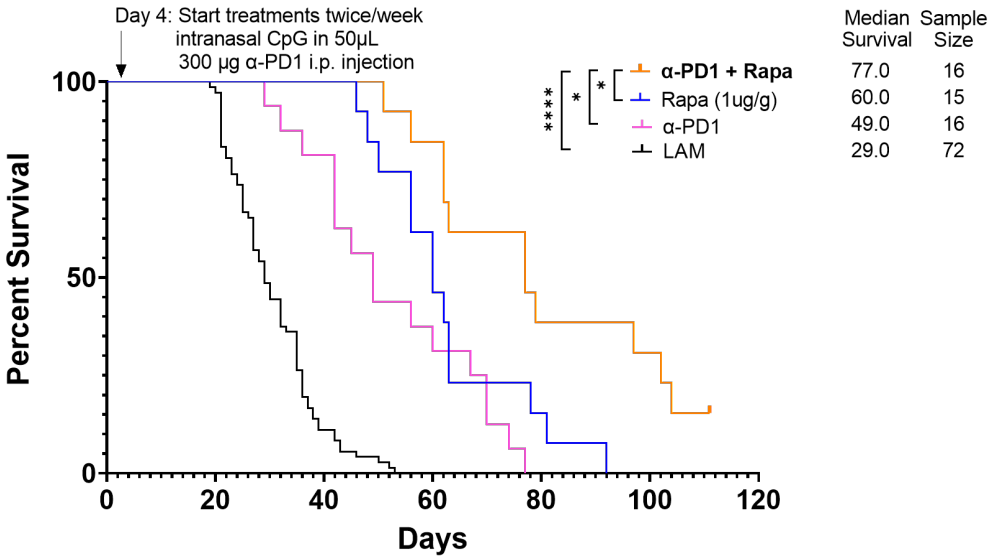

Figure 23. *Anti-PD-1 therapy is synergistic with Rapamycin in LAM.* Aggregate data from n>2 survival experiments LAM n=72, α-PD-1 n=16, Rapamycin n=15, Rapamycin + α-PD-1 n=16. Statistical analysis was performed using log-rank test (survival studies). * p<0.05, ** p<0.01, *** p<0.001, **** p<0.0001.

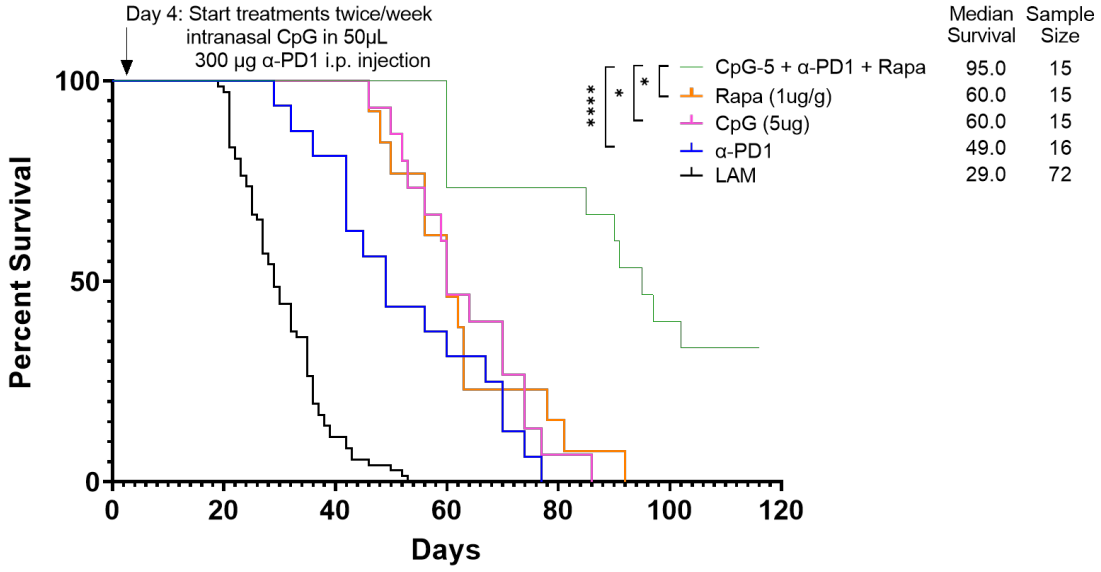

Figure 24. *Triple combination CpG-Rapamycin- Anti-PD-1 therapy is synergistic in LAM.* Aggregate data from n>2 survival experiments LAM n=72, α-PD-1 n=16, CpG n=15, Rapamycin n=15, Rapamycin + CpG + α-PD-1 n=15. Statistical analysis was performed using log-rank test (survival studies). * p<0.05, ** p<0.01, *** p<0.001, **** p<0.0001.

Discussion

Our finding that CpG treatment was not as effective for treating LAM at a more advanced stage of disease is consistent with evidence showing that patients diagnosed later in the course of their disease progression are not as responsive to therapy (184). It is possible that the stage of disease chosen for intervention in our mouse model was too advanced to be rescued by TLR activation or did not reflect the level of disease typical for a late stage human diagnosis. However, it is worth noting that even with early intervention CpG therapy, mice eventually develop lung lesions and respiratory symptoms. Additionally, it is unlikely that patients with advanced LAM would be able to tolerate the inflammatory effects of CpG in an already delicate tissue. CpG, like rapamycin, seems to be most effective when given early in the course of disease.

Despite mTOR inhibition, we found that TLR-9 activation with CpG was synergistic with low-dose rapamycin therapy in our mouse model. This could be due to incomplete mTOR inhibition, as rapamycin reliably blocks mTORC1, but not mTORC2 (185). The effect of rapamycin on mTORC1 vs mTORC2 is dose dependent. Concentrations of rapamycin required to inhibit mTORC2 are much higher than those necessary to inhibit mTORC1 (186–188) and are not well tolerated for clinical intervention. Chronic inhibition of mTOR with rapamycin does eventually sequester enough free mTOR proteins to partially hinder a cell's ability to assemble new mTORC2 complexes (26). However, low-dose rapamycin is not sufficient to completely suppress mTORC2 activity (189). In fact, evidence suggests that inhibition of mTORC1 can lead to activation of mTORC2 (190) and

vice versa (191–193), potentially as a means to rescue proliferative functions through a parallel pathway.

In LAM patients, treatment with rapamycin is not curative but significantly slows the proliferation of LAM cells and disease progression (33,34,122). This is recapitulated in our model showing LAM nodules dispersed throughout the lungs at symptomatic endpoints despite increased survival when treating with low-dose rapamycin (**Fig. 21B**). Research points to activity of mTORC2 as a driver of persistent proliferation and nodule formation seen in LAM lungs despite inhibition of mTORC1 (57,194), and could explain incomplete patient responses to treatment with rapamycin alone.

Our finding that the benefit of CpG treatment was further enhanced with low-dose rapamycin is consistent with results showing that increased mTORC2 activity or mTORC1 inhibition work alongside TLR activation to generate pro-inflammatory immune responses. One research group found that mTORC2 activation increases TLR-4 induced proinflammatory cytokine production in human dendritic cells (82), and increases their capacity to prime T cells. Another study found that low-dose rapamycin alongside TLR activation increases TNF-α production in macrophages (83). In addition, mTORC1 inhibition significantly increases NF-KB activity and blocks the secretion of IL-10, an anti-inflammatory cytokine (176). (All TLRs, with the exception of TLR-3, signal through the MyD88-NFKB pathway to produce proinflammatory cytokines). This suggests that low-dose rapamycin treatment may not affect the ability of antigen presenting cells in the LAM microenvironment to respond to CpG and initiate inflammatory immune

responses. In fact, low-dose rapamycin therapy has been shown to regulate and even increase the expansion of central memory T cells (116).

Rapamycin is the only FDA-approved treatment currently available to LAM patients, and its compatibility with CpG in our studies suggests this treatment strategy could merit consideration in clinical applications. It is possible that Rapamycin's cytostatic effect on LAM cell proliferation, combined with the immune infiltration mediated by CpG, alters the tissue microenvironment in the lungs in a way that synergistically restrains LAM nodule formation. More investigation into how this combination works will help in understanding how other immunotherapies may work in tandem with rapamycin. In addition, our finding that treatment with CpG alone is just as effective at increasing survival as low-dose rapamycin is further justification for its assessment in clinical trials. Given that 40% of LAM patients have partial or no response to treatment with Rapamycin (35), TLR9 activation could offer these individuals a therapeutic strategy with similar benefits to standard of care.

Significance

The findings presented in this chapter advance our understanding of potential immunotherapeutic strategies for LAM and their combined outcomes with standard of care. We present a novel approach (TLR9 activation) that may be as effective as rapamycin and seems to have additive effects when combined. This is important, because it shows that immune-modulation is possible in the LAM microenvironment, and works to significantly improve relevant outcomes in our preclinical models of disease.

Chapter 5. Conclusions and Future Directions

Thesis Summary and Conclusions

With each new therapeutic strategy deployed in the search for a curative treatment for LAM, more is uncovered about the way this disease interacts with the immune system and responds to treatment induced stresses. Targeting the mTOR pathway has been a reliable strategy to slowing disease progression, but it is clear that other strategies and interventions are needed to induce remission and promote lung tissue restoration. The immune system is the primary mechanism through which the body identifies threats to the organism and maintains homeostasis and health by responding to and removing destabilizing agents. Harnessing the adaptive immune system with surgical precision against LAM cells has been frustrated by the lack of uniquely identifying cellular targets. Given these limitations, the work undertaken in this dissertation focused instead on a method to exploit the non-specificity of innate immunity and the types of reliable inflammatory immune responses generated against toll like receptor activation to transform the tissue microenvironment into one that is less hospitable for the proliferation of LAM cells. We have demonstrated that treatment with CpG, a TLR9 agonist used most commonly as a vaccine adjuvant, has on its own, significant beneficial treatment outcomes in a preclinical model of pulmonary LAM. Not only was CpG intervention found to be compatible with rapamycin therapy, but it also further improved the treatment outcomes observed with rapamycin alone by inhibiting LAM nodule formation and size. Although the precise mechanism by which CpG activates Th17 and cytotoxic CD8+ T cells in

LAM lungs requires further investigation (pDCs appear to be just one of many cellular players), it is clear that an adaptive immune response is generated in the course of CpG treatment. This has promising implications for the use of CpG as an adjuvant in the development of vaccines against LAM specific antigens, when markers for these disease cells can be identified.

Significance

This thesis explores TLR9 activation as a potential treatment for LAM and advances LAM research by offering a new strategy for treatment other than mTOR inhibition that appears to be as effective in mice as the only approved therapy. The body of work presented provides rationale to support future research into the development and optimization of this treatment strategy to increase tolerability for clinical use. This treatment strategy also has the potential to meet the need the in 40% of patients who don't respond well to rapamycin. This thesis also draws new parallels between LAM and cancer to strengthen consideration of LAM in the cancer field, which could grant LAM researchers better access to the wealth of funding available for cancer research. Making the connection between LAM and cancer could allow LAM patients to participate in clinical trials for cancer related research. This could open the door for more therapeutic cross-talk and treatment options for LAM patients. This thesis has implications beyond LAM, as it also contributes to lung cancer research by investigating mechanisms of immunosuppression in the lung tumor microenvironment. Scientists have been researching ways to alter tumor microenvironments in cancer with varying success. Progress in this area is

significant because lung cancer is the leading cause of cancer related deaths (25% of all cancer deaths). This work also supports research into treatments for other cystic lung diseases with poor treatment options by providing justification for preclinical assessment of TLR activation as therapy for other chronic lung diseases.

Future Directions

In our earlier studies, we observed that higher dose CpG (10 μg) resulted in significantly fewer LAM nodules than lower dose CpG (5 μg) but also resulted in 15 days lower median survival comparatively (**Fig. 1A**). This could be due to the increased inflammation induced generally in the tissue. Because LAM patients already experience declining lung function, it is not ideal for any proposed treatments to exacerbate the condition of already fragile tissue structures. There are several approaches that should be investigated to optimize CpG treatment and minimize detrimental tissue effects like tissue-wide inflammation.

Firstly, a dose response study to determine the lowest possible dose of CpG that can be administered in the lungs without affecting treatment outcomes would be useful. Based on our findings with CpG at 10 μg vs 5 μg, it is possible that even lower doses of CpG could be sufficient to generate an effective immune response while simultaneously lowering the extent of inflammation.

There are also many cell types present in the lung tissue like fibroblasts, endothelial cells, and epithelial cells that may not respond favorably to chronic TLR9 activation. For these stromal cells, inhibition of activation pathways, like fibroblast activation protein inhibitor (195), could help prevent these cells from

inadvertently contributing to tumor proliferation and preserving healthy lung tissue by preventing tissue reconstruction, fibrosis, and treatment resistance (196).

Given the conflicting evidence surrounding the interactions between CpG, Rapamycin and their combined effect in cancer therapy, characterizing the immune response to Rapamycin + CpG combination therapy in LAM would help identify the major cell types and mechanisms that contribute to treatment efficacy. This knowledge could point towards new treatment targets and provide justification for moving strategies involving immune activation and mTOR inhibition to clinical trials.

Another potential strategy to mitigate CpG's inflammatory side effects is to encapsulate CpG into a nanoparticle system that can deliver the TLR9 agonist directly to antigen presenting cells or the lymph nodes. Encapsulation and targeted delivery of CpG to draining lymph nodes, the site where most immune responses are orchestrated, could protect the tissue from widespread inflammation. Targeting antigen presenting cells like macrophages or dendritic cells could be done through surface modifications like antibody conjugation on encapsulating nanoparticle systems (197). Targeted delivery to the lymph nodes may be achieved through a variety of methods like surface PEGylation (198,199) or formulation of lipid- based particles that can take advantage of chylomicron processing to shuttle cargo to lymphatics.

In the following preliminary studies, we begin to explore alternate treatment strategies for the development of CpG as therapy for LAM. We attempt dosing

regimens that feature increased timing between treatments in an effort to decrease the total amount of CpG administered to mice over the course of a survival experiment (effectively reducing the dose). We also explore delivery of inhaled CpG encapsulated in nanoparticle formulations designed to target the lung draining lymph nodes.

Appendix I: Preliminary Data for Future Directions:

Alternate Treatment Strategies

Acknowledgements:

This work was completed with the help of Dr. Jacob McCright, Bennett Yang, Juan Grano de Oro Fernandez, Kaitlyn Moore, Havish Gadde, Mehu Donthi, Michele Kaluzienski, and Katharina Maisel. Their contributions made this chapter possible and I am deeply grateful for the time, effort, and care dedicated by each individual to making these studies successful.

Introduction

Earlier we found that intranasal CpG treatment in LAM lungs enhances survival. However, this strategy on its own is not curative as even treated lungs eventually develop lung nodules. Here we explored various alternative treatment strategies to improve the efficacy of CpG-treatment in LAM lungs or mitigate its inflammatory side-effects.

The timing of drug administration is another variable in optimizing treatment efficacy. In cancer treatment, immunotherapies like immune checkpoint inhibitors are commonly administered to patients at a high dose every 2-3 weeks, while researchers typically administer these drugs to mice twice weekly. In our earlier study, we found that high dose CpG (10 µg) administered twice weekly resulted in decreased survival in mice despite reducing LAM nodule count and size compared to lower dose CpG (5 µg) (**Fig. 1A**). Here we investigated whether high doses given less frequently in mice would result in improved treatment outcomes.

Studies investigating TLR tolerance and dosing regimens indicate that reactivating TLRs within 5 days of a prior stimulation, can induce TLR tolerance in vivo (200). TLR tolerance is characterized by a transient unresponsiveness of immune cells to re-exposure of TLR agonists and reduced pro-inflammatory cytokine production (201–206). Researchers found that delaying a secondary stimulation until after the refractory period (5 days) avoided the induction of TLR tolerance (207). Since our initial treatment regimen involved twice weekly administration of CpG, it is possible that the frequency of treatment could induce and maintain immune tolerance, eventually contributing to a protumor environment that supports disease progression**.** We hypothesized that adjusting the timing of CpG administration to once weekly, would further increase survival in mice with LAM by circumventing TLR tolerance.

Evidence also suggests that alternating stimulation of two different TLRs that signal through separate pathways can also circumvent TLR tolerance and maintain a pro-inflammatory response if weekly stimulation of a single TLR is insufficient (208). We hypothesized that alternating between CpG (TLR9) and Poly I:C (TLR3) staggered in such a way that each agonist was given once a week, but mice were dosed twice weekly, would result in increased survival over twice weekly dosing with CpG alone.

In our earlier studies, we observed that higher dose CpG (10 μg) resulted in significantly fewer LAM nodules than lower dose CpG (5 μg) but also resulted in 15 days lower median survival comparatively (**Fig. 1A**). This could be due to the increased inflammation induced generally in the tissue. Because LAM patients

already experience declining lung function, it is not ideal for any proposed treatments to exacerbate the condition of already fragile tissue structures. Encapsulation and targeted delivery of CpG to draining lymph nodes, the site where most immune responses are orchestrated, could protect the tissue from widespread inflammation. Here we explore drug delivery techniques to target lung draining lymph nodes for CpG stimulation in an effort to mitigate general inflammation potentially caused by delivering CpG directly to the lung tissues.

Materials and Methods

Mice

7 to 9-week old female C57BL6/J mice (Jackson Laboratory) were used for all studies. Study protocols were approved by the UMD Institutional Animal Care and Use Committee (IACUC).

LAM induction

TSC2-null kidney-derived epithelial tumor (TTJ) cells, were provided by the Krymskaya Lab at the University of Pennsylvania (39). TTJ cells (5.0×10^5) were administered in 100 µL of PBS via tail vein injection to induce LAM disease in 8-9 week old female mice. Lung lesions typically develop within 3-7 days.

Survival Studies

Mice received CpG class B twice per week (5 µg /10 µg), once per week (5 µg), or once every two weeks (10 µg). (Invivogen, tlrl-1826-5), in 50 µL of PBS, intranasally starting 4 days post LAM induction. Control groups received 50 µL of PBS intranasally or 200 µL PBS. Mice were monitored for symptoms of disease

and body weight changes and removed from studies based on experimental timing or humane endpoints. At endpoint, mice were euthanized and lung tissues collected for histological analysis.

Flow Cytometry

14 days after LAM induction, mice received a single intranasal treatment dose of Poly I:C (10 μg) in 50 μL PBS or 50 μL of PBS as a vehicle control. At 1 and 3 days post treatment, lung tissues were perfused and collected for flow cytometric analysis. Left lung lobes were dissociated by enzymatic digestion with 1 mg/mL collagenase D (Roche, 11088882001), and 1 mg/mL collagenase IV (Worthington Biochemical, LS004188) in DMEM with 5% FBS for 1 hour. Single cell suspensions were stained to identify eosinophils (CD64-, Siglec F+, Ly6G-), neutrophils (CD64-, Siglec F-, Ly6G+) dendritic cells (CD11c+, MHC-II^{high}), plasmacytoid dendritic cells (CD11c+, PDCA-1+, MHC-II^{high}), alveolar macrophages (CD64+, SiglecF^{high}, CD11b-), interstitial macrophages (CD64+, SiglecF^{low}, CD11b+, MHC-II+), B Cells (CD19+ or B220+), T Cells (CD3+, CD4+ or CD8+), regulatory T Cells (CD3+, CD4+, FoxP3+), Th1 T cells (CD3+, CD4+, FoxP3-, Tbet+), Th2 T cells (CD3+, CD4+, FoxP3-, Gata3hi), and Th17 T Cells (CD3+, CD4+, FoxP3-, ROR-γt+). Cells were analyzed by flow cytometry using a BD FACSCelesta (BD Biosciences) and FlowJo (FlowJo LLC). Gating strategies can be found in the data supplement (**Fig E1**).

Nanoparticle Encapsulation and Delivery

CpG encapsulated in PEG-coated, PLGA particles (at 0.1 μg, 1.0 μg, 5 μg, 10 μg, and 20 μg) were delivered intranasally to healthy mice. Empty PLGA coated in ionic liquids at varying rations were delivered by intratracheal administration to healthy mice. 6 hours post treatment, lung and mediastinal lymph node tissues were collected for IVIS imaging and analysis.

Statistical Analysis

Data were analyzed using Graphpad Prism (GraphPad, La Jolla, CA). Survival studies were assessed using the log-rank (Mantel-Cox) test. Unpaired Welch t tests were used to compare pairs of samples or groups. Mann–Whitney test was used to compare the groups of data that failed to satisfy parametric assumptions. Brown-Forsythe and Welch One-way ANOVA were used for comparisons between ≥3 groups. Differences were considered statistically significant when $p < 0.05$. *p<0.05, **p<0.01, ***p<0.001, ****p<0.0001.

Results

Alternate Dosing Regimens do not improve therapeutic efficacy

We conducted survival studies to assess the effects of these various dosing schedules on the efficacy of CpG in LAM, and found no significant differences in survival benefit between them. Weekly dosing of CpG at 5 μg did not result in a survival benefit over twice weekly dosing. **(Fig. 25)**. Similarly, survival of mice given higher dose CpG (10ug) every two weeks, was not different from that of mice treated twice weekly at the same dose (**Fig. 26**). Lastly, alternating TLR

activation between CpG (5 µg) and Poly I:C (5 µg) also did not result in a survival benefit over weekly or twice weekly dosing of CpG (5 µg) alone (**Fig. 25**).

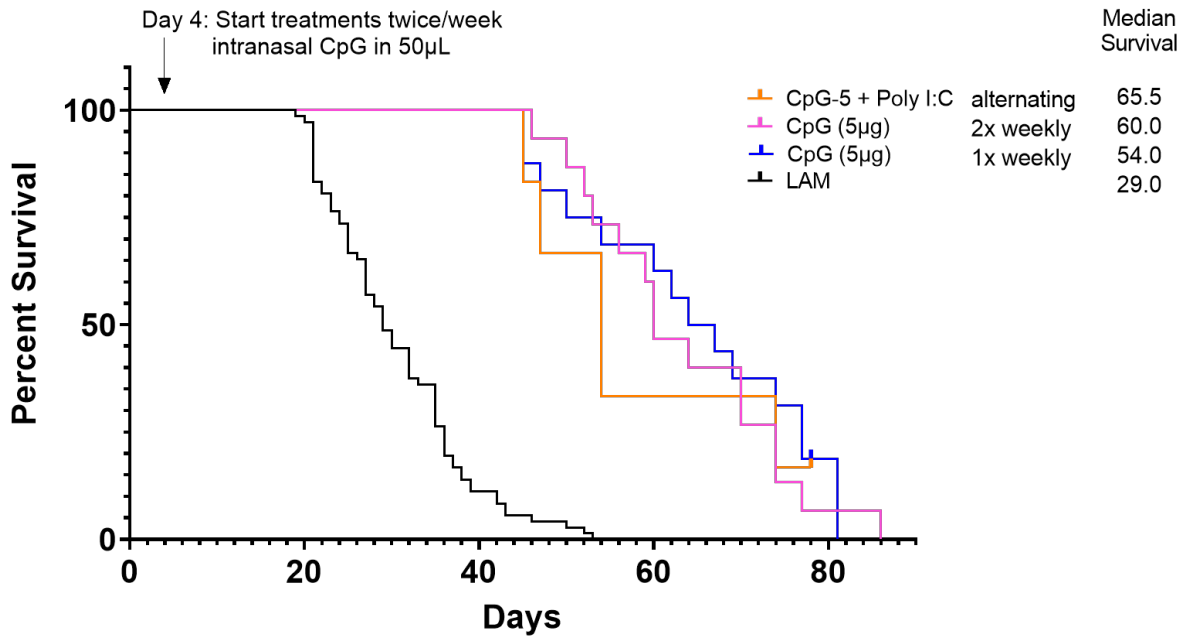

Figure 25. *Alternative Dosing Schedules: CpG-5 + TLR Switching have no effect on efficacy of CpG Therapy in LAM.* Aggregate data from n>2 survival experiments. LAM n=72, CpG 2x weekly n=15, CpG 1x weekly n=16, CpG + Poly I:C n=15. Statistical analysis was performed using log-rank test (survival studies).

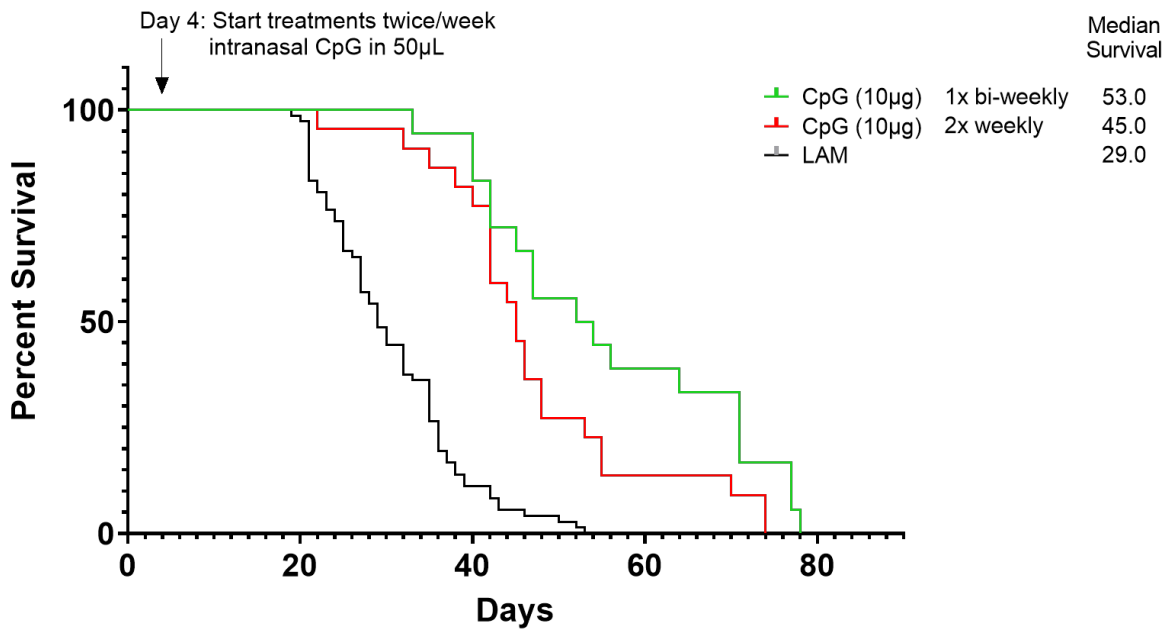

Figure 26. *Alternative Dosing Schedules: CpG-5 have no effect on efficacy of CpG Therapy in LAM.* Aggregate data from n>2 survival experiments LAM n=72, CpG 2x weekly n=22, CpG 1x bi-weekly n=18. Statistical analysis was performed using log-rank test (survival studies).

Nanoparticle Delivery of CpG and LN targeted nanoparticles.

We investigated the capacity of PEG-coated PLGA particles loaded with CpG DNA to reach the lung draining lymph nodes when delivered intranasally and assessed the delivery of these fluorescently labeled particles using IVIS imaging. We observed increasing fluorescence of particles in lungs with increasing dose of particles (**Fig. 27**). However, no fluorescence in the lung draining lymph nodes was observed regardless of dose (**Fig. 27**). We then attempted intratracheal delivery of empty PLGA particles coated in ionic liquids designed to target immune cells. We found that intratracheal delivery successfully allowed all formulations to reach the lung draining lymph nodes (**Fig. 28**).

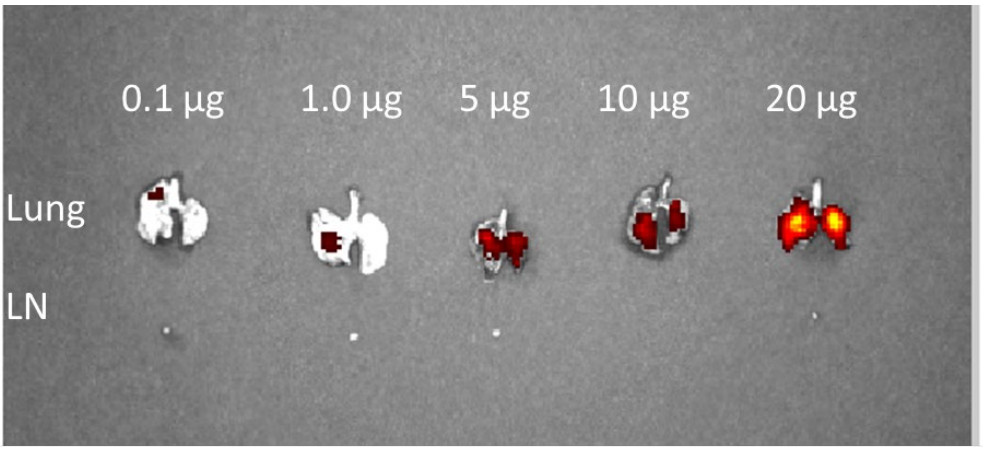

Figure 27. *CpG encapsulated in PEG-coated PLGA particles delivered intranasally to healthy mice.* IVIS imaging of lungs and lymph nodes at 6 hours post intranasal dosing at multiple doses of particles.

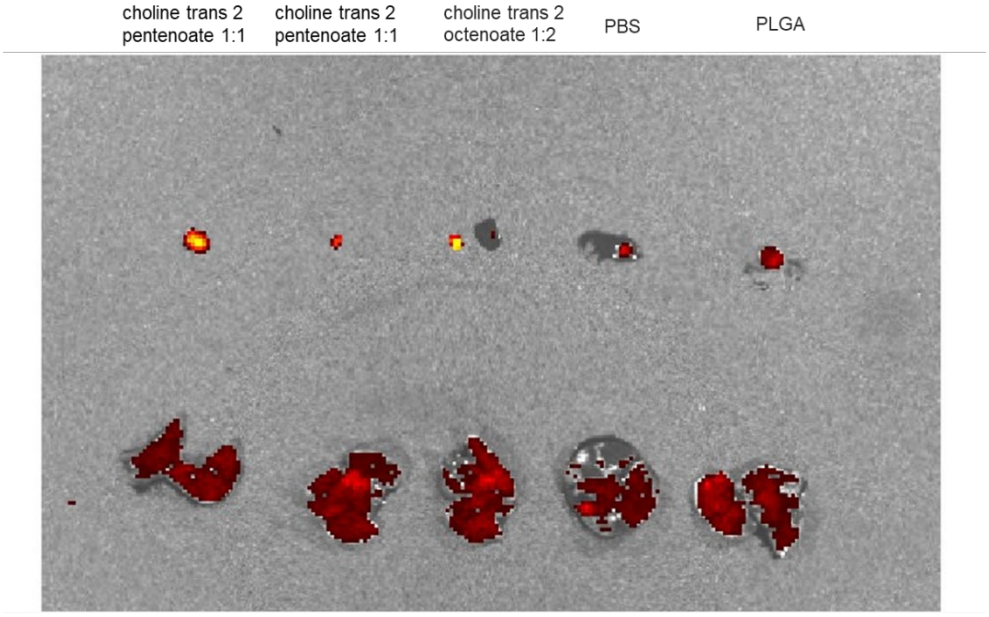

Figure 28. *Lymph node targeting of PLGA particles coated in ionic liquids designed to target immune cells.* IVIS imaging of lungs and lymph nodes at 6 hours post intratracheal administration at multiple doses of particles.

Discussion

Survival studies to assess the effects of various dosing regimens on the efficacy of CpG in LAM, found no significant differences in survival benefit. This suggests that the effect of a singular low dose of CpG given weekly in mice is effective and that less treatment is needed to achieve similar survival benefit. Immune response to low dose CpG appears durable and perhaps treating with even lower doses or treating every two weeks could also be effective. High dose CpG seems to limit survival regardless of how infrequent the administration, which suggests that the inflammation or detrimental effects from high dose CpG cannot be overcome and should not be considered for future treatments. Given our results, TLR tolerance does not appear to be a major barrier to improving treatment efficacy, as we did not observe a marked improvement in treatment when dosing outside of the refractory period of 5 days for a single TLR. Interestingly Poly I:C given at a lower dose (5 μg) alternated with low dose CpG did not negatively affect overall survival like we saw when combined with checkpoint inhibition. This suggests that the effects of Poly I:C may also be inversely dose dependent like with CpG.

The mediastinal lymph nodes are crucial for orchestrating immune responses against respiratory antigens. Direct lymph node delivery is not yet possible because they are located deep in the chest cavity. The ability to target the lung draining lymph nodes through non-invasive procedures like inhalation of nanoparticles opens the possibility to more precisely manipulate the desired immune response that optimizes all the positive aspects of CpG therapy while

minimizing side effects. However, a significant portion of the particles delivered intratracheally were still retained in the lung tissue. Provided that the cell targeting function of the ionic liquid formulation is reliable, we could improve the delivery of particles by targeting migratory dendritic cells or lymphatic endothelial cells 9(LECs). DCs readily take up antigen and travel to the lymph nodes, while LECs form the lymphatic vessels that lead to the lymph node.

Appendix II: Poly I:C as LAM Immunotherapy

Acknowledgements:

This work was completed with the help of Dr. Jacob McCright, Bennett Yang, Juan Grano de Oro Fernandez, Kaitlyn Moore, Havish Gadde, Mehu Donthi, Michele Kaluzienski, and Katharina Maisel. Their contributions made this chapter possible and I am deeply grateful for the time, effort, and care dedicated by each individual to making these studies successful.

Introduction

Poly I:C is another TLR agonist that has been studied as an adjuvant in lung cancer models with varying success (209,210). TLR3 stimulation promotes similar pro-inflammatory immune responses as TLR9 activation, but through different signaling pathways. We explored the use of intranasal Poly I:C, a TLR-3 agonist, and the combination of intranasal Poly I:C with checkpoint inhibition as LAM therapy.

Materials and Methods

Mice

7 to 9-week old female C57BL6/J mice (Jackson Laboratory) were used for all studies. Study protocols were approved by the UMD Institutional Animal Care and Use Committee (IACUC).

LAM induction

TSC2-null kidney-derived epithelial tumor (TTJ) cells, were provided by the Krymskaya Lab at the University of Pennsylvania (39). TTJ cells (5.0×10^5) were

administered in 100 µL of PBS via tail vein injection to induce LAM disease in 8-9 week old female mice. Lung lesions typically develop within 3-7 days.

Survival Studies

Mice received Poly I:C (10 µg 2x/week or 5 µg weekly) (Invivogen, tlrl-pic), in 50 µL of PBS, intranasally starting 4 days post LAM induction. Mice receiving combination therapy, received intranasal Poly I:C and 300 µg anti-PD-1 antibody (BioXCell, BE0146-A0) in 200 µL of PBS via intraperitoneal (IP) injection 2x/week. Control groups received 50 µL of PBS intranasally or 200 µL PBS with or without 300 µg of rat IgG isotype control (BioXCell, BE0089) by IP injection. Mice were monitored for symptoms of disease and body weight changes and removed from studies based on experimental timing or humane endpoints. At endpoint, mice were euthanized and lung tissues collected for histological analysis.

Histology

Tissues were fixed overnight in 4% PFA at 4ºC, embedded in paraffin wax, sectioned at 5 µm, and stained with hematoxylin and eosin (H&E). LAM nodule counts, average nodule diameters, and general tissue inflammation were quantified using QuPath Imaging software.

Flow Cytometry

14 days after LAM induction, mice received a single intranasal treatment dose of Poly I:C (10 µg) in 50 µL PBS or 50 µL of PBS as a vehicle control. At 1 and 3 days post treatment, lung tissues were perfused and collected for flow cytometric

analysis. Left lung lobes were dissociated by enzymatic digestion with 1 mg/mL collagenase D (Roche, 11088882001), and 1 mg/mL collagenase IV (Worthington Biochemical, LS004188) in DMEM with 5% FBS for 1 hour. Single cell suspensions were stained to identify eosinophils (CD64-, Siglec F+, Ly6G-), neutrophils (CD64-, Siglec F-, Ly6G+) dendritic cells (CD11c+, MHC-II^{high}), plasmacytoid dendritic cells (CD11c+, PDCA-1+, MHC-II^{high}), alveolar macrophages (CD64+, SiglecF^{high}, CD11b-), interstitial macrophages (CD64+, SiglecF^{low}, CD11b+, MHC-II+), B Cells (CD19+ or B220+), T Cells (CD3+, CD4+ or CD8+), regulatory T Cells (CD3+, CD4+, FoxP3+), Th1 T cells (CD3+, CD4+, FoxP3-, Tbet+), Th2 T cells (CD3+, CD4+, FoxP3-, Gata3hi), and Th17 T Cells (CD3+, CD4+, FoxP3-, ROR-γt+). Cells were analyzed by flow cytometry using a BD FACSCelesta (BD Biosciences) and FlowJo (FlowJo LLC). Gating strategies can be found in the data supplement (**Fig E1**).

Statistical Analysis

Data were analyzed using Graphpad Prism (GraphPad, La Jolla, CA). Survival studies were assessed using the log-rank (Mantel-Cox) test. Unpaired Welch t tests were used to compare pairs of samples or groups. Mann–Whitney test was used to compare the groups of data that failed to satisfy parametric assumptions. Brown-Forsythe and Welch One-way ANOVA were used for comparisons between ≥3 groups. Differences were considered statistically significant when $p < 0.05$. *p<0.05, **p<0.01, ***p<0.001, ****p<0.0001.

Results

TLR3 activation in LAM lungs is not effective as therapy

To evaluate the effectiveness of Poly I:C, we conducted a survival experiment where we induced LAM in mice and administered intranasal Poly I:C twice weekly beginning 4 days post induction. We observed that PolyI:C did not offer any survival benefit compared to untreated control mice. Mice treated with Poly I:C lost weight and reached symptomatic endpoints at the same rate as untreated mice (**Fig. 29A**).

Histological analysis of lung tissues from treated vs untreated mice shows that treatment with Poly I:C results in similar levels of tissue inflammation and LAM tumor burden as in disease controls. Additionally, treatment with Poly I:C did not significantly decrease the number of LAM nodules present in lungs at study endpoints (**Fig 29B**).

We hypothesized that combination therapy would increase survival in mice with LAM compared to individual treatments. We conducted a survival study to evaluate the effect of combination Poly I:C and anti-PD-1 vs either treatment alone. We found that combination therapy showed an increased survival benefit over Poly I:C alone (**Fig. 29A**). However, this benefit was significantly lower than that seen with anti-PD1 treatment, so it is possible that repeated Poly I:C treatment in LAM lungs has a detrimental effect that decreases the efficacy of anti-PD1 therapy.

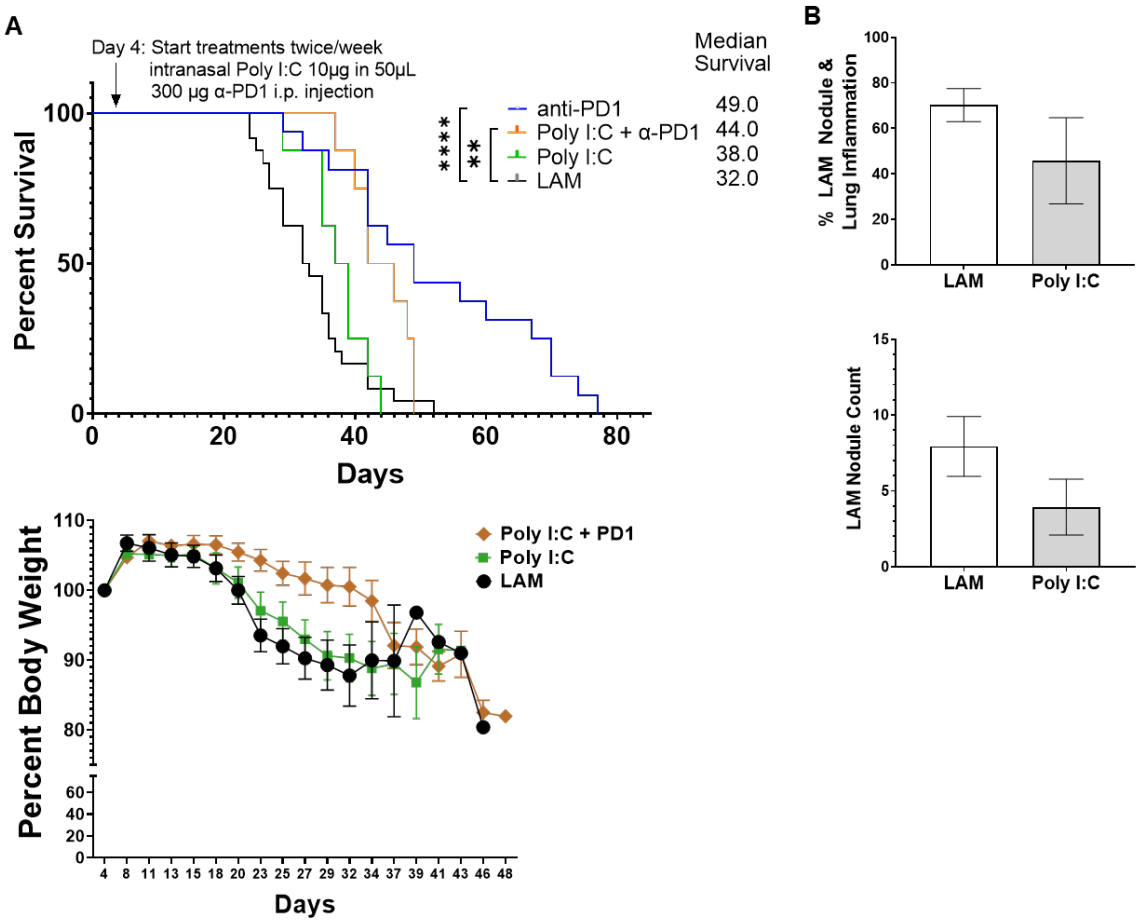

Figure 29. *TLR3 activation in LAM lungs is not effective as therapy.* **A)** Aggregate data from n>2 survival experiments LAM n=24, α-PD-1 n=16, Poly I:C n=8, Poly I:C + α-PD-1 n=8. **B)** Quantification of LAM nodules and Inflamed tissue regions between treatment groups of mice at symptomatic endpoints from survival studies in (A). 3 sections analyzed per mouse. Statistical analysis was performed using log-rank test (survival studies). * p<0.05, ** p<0.01, *** p<0.001, **** p<0.0001.

Immune Characterization: Poly I:C

We hypothesized that similar to CpG, adjuvant immunotherapy with Poly I:C would enhance cytotoxic T cell responses against LAM and reduce immune regulatory cells such as regulatory T cells in the lungs. To characterize the effect of Poly I:C on the tissue microenvironment, we induced LAM in mice, allowed disease to develop for 14 days before administering a single dose of intranasal Poly I:C. We harvested lung tissues at 1 and 3 days post treatment and analyzed cells using flow cytometry.

T Cells

We found that overall T cell numbers between treated and untreated groups were not significantly different (**Fig 30**). Poly I:C activates TLR3 which allows cells to recognize viral double stranded RNA. We anticipated that introducing this mimic into the pulmonary space could trigger an inflammatory immune response that would result in an increase of effector and memory T cells in the lungs even if overall T cell numbers remained comparable to disease controls. When we looked at T cell subsets, we found that Poly I:C treated mice had increased populations of central and effector memory CD4+ T cell subsets at 1 and 3 days post treatment respectively. However, Poly I:C did not significantly affect CD4 T cell polarization, as we did not find any changes in populations of Tregs, Th1, or Th17 CD4+ helper T cells between treated and untreated groups. In addition, subsets of CD8+ T cells were unaffected by treatment at either day post treatment (**Fig. 31**). This suggests that Poly I:C in LAM lungs does not stimulate lasting effector T cell responses.

Granulocytes

We found that innate immune cell populations normally associated with tumor growth and inflammation decrease in response to intranasal CpG treatment in LAM lungs. The total number of lung eosinophils was also lower in Poly I:C treated LAM mice 1 day post treatment compared to disease controls (**Fig. 32**). However, this decline was not maintained at day 3. There was no significant change in neutrophil lung infiltration between treatment groups at either day. This suggests that the effect of Poly I:C treatment in LAM lungs is not durable.

Antigen Presenting Cells

Typically during pulmonary viral infection, monocytes are recruited to the alveolar cavity, where they eventually differentiate into macrophages or dendritic cells. We found that treatment with Poly I:C did not significantly affect the population of lung alveolar or interstitial macrophages (**Fig. 32**). Our results suggest that introducing Poly I:C in LAM lungs does not stimulate infiltration of monocytes to the tissue or differentiation in the alveolar cavity, as alveolar macrophage populations remain similar to that of disease controls post treatment.

We did find a significant decrease in conventional dendritic cells (CD11b+ and CD103+ DCs) at 1 day post treatment in Poly I:C treated LAM mice compared to controls (**Fig. 32**). Again, this effect was not sustained, as DC populations were trending up by day3 in treated mice. We did not find that Poly I:C had any effect on the population of plasmacytoid dendritic cells in the lungs.

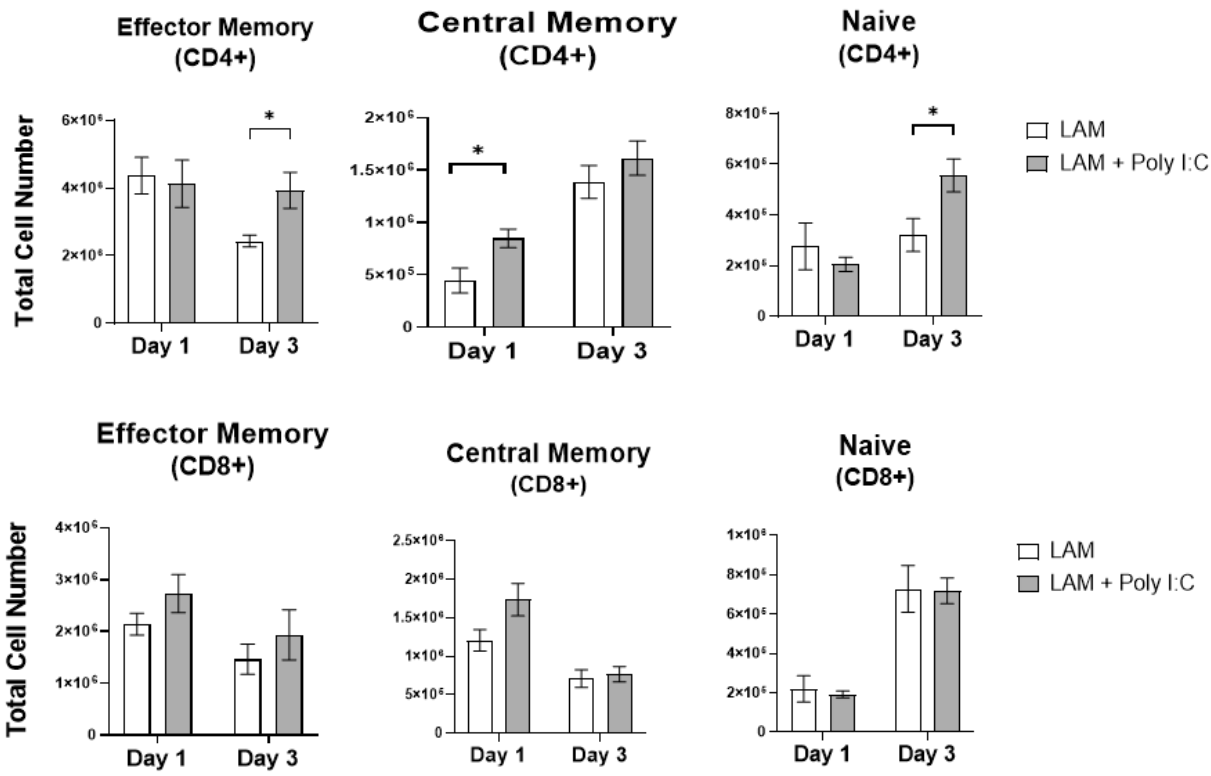

Figure 30. *Effect of Poly I:C treatment on subsets of CD4+/CD8+ T Cells.* Data shows CD4+ and CD8+ T cell numbers of effector memory, central memory and naïve subsets. Data is representative of n=1 experiments and n>4 mice per treatment group. Statistical analysis was performed using one-way ANOVA. * p<0.05, ** p<0.01, *** p<0.001, **** p<0.0001.

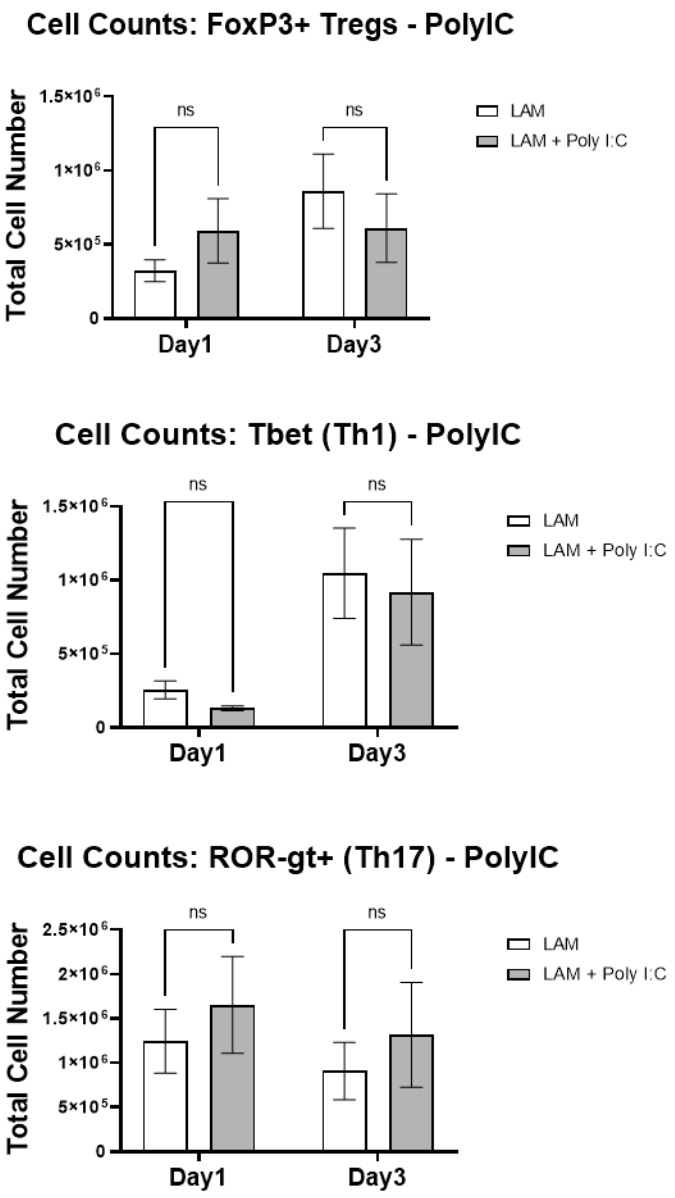

Figure 31. *Helper T Cell populations in response to late intervention intranasal Poly I:C treatment (dosed at 14 days post LAM induction) in LAM lungs.* CD4 helper T cell subsets 1 and 3 days post treatment: total cell numbers of Treg, Th1, and Th17 T Cells. Data is representative of n=1 experiments and n>4 mice per treatment group. Statistical analysis was performed using log-rank test (survival studies). * $p<0.05$, ** $p<0.01$, *** $p<0.001$, **** $p<0.0001$.

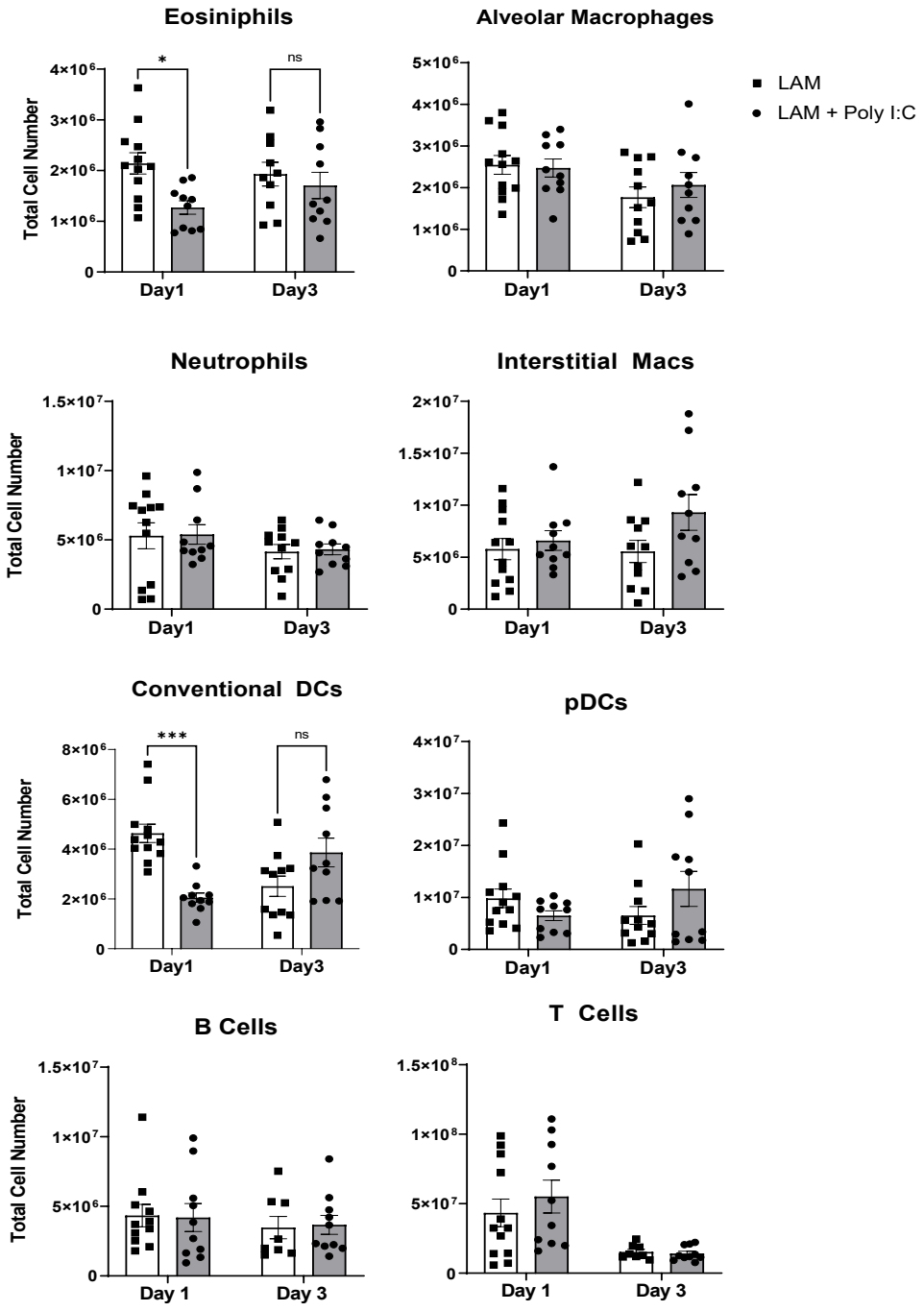

Figure 32. *Immune cell populations in response to late intervention (dosed at 14 days post LAM induction) intranasal Poly I:C treatment in LAM lungs (Day 1 & Day 3 post treatment).* Total cell numbers of granulocytes and antigen presenting cells infiltrating the lungs 1 and 3 days after Poly I:C treatment obtained via flow cytometry. Data is representative of n=2 experiments and n>4 mice per treatment group. Statistical analysis was performed using one-way ANOVA. * $p<0.05$, ** $p<0.01$, *** $p<0.001$.

Discussion

The immune responses we observed with Poly I:C administered during advanced LAM disease mirror results obtained with CpG treatment under similar conditions. One could attribute the lack of immune responsiveness with either TLR agonist to the late intervention and advanced disease stage, however the survival study results show that even with early treatment intervention, Poly I:C fails to reduce LAM nodules or increase survival, suggesting that the immune responses generated at those earlier timepoints are insufficient to alter the course of disease progression like in treatment with CpG. Although Poly I:C has been shown to stimulate protective immune responses in the lungs (211), chronic activation of TLR3 can impair lung function and exacerbate pre-existing disease (212,213).

Another possible explanation for the poor treatment outcomes we observed with Poly I:C could be due to dose. We treated with 10 μg of Poly I:C intranasally. Other research groups doing similar work in mouse lung cancer models have treated with doses in the range of 0.1-10 μg (214,215).

Overall, our findings from these studies suggest that LAM lungs do not respond favorably to Poly I:C adjuvant immunotherapy and that Poly I:C is not effective as hypothesized at activating an immune response in LAM lungs capable of countering the existing immunosuppression. The flow cytometry results are aligned with the survival study and histological data suggesting that immunotherapy with Poly I:C in LAM lungs is not an effective treatment and may actually hinder the efficacy of better alternatives (like in combination therapy).

Appendix III: Tissue Dissociator: Design and Validation

Acknowledgements:

This work was completed with the help of Andrew J. Gregory, John D. Murtagh, Nitay Pavin, Carson Taylor Meyers, Juan Grano de Oro Fernandez, Kaitlyn Moore, and Katharina Maisel. The design and execution was a collaborative effort between researchers in the Maisel Lab and the engineers at the University of Maryland's maker space and fabrication laboratories, Terrapin Works.

This chapter is adapted with permission from:

Amosu, M., Gregory, A. J., Murtagh, J. D., Pavin, N., Meyers, C. T., Grano de Oro Fernandez, J., Moore, K., Maisel, K. Mechanical Dissociation of Tissues for Single Cell Analysis Using a Motorized Device. J. Vis. Exp. (201), e65866, doi:10.3791/65866 (2023).

Introduction:

Single cell analysis has rapidly become crucial for new biomedical discoveries, whether this is for applications like flow cytometry, used to identify different cell types, or single cell sequencing, used to identify genomic or transcriptomic variation between cells (216). To perform such cell isolations from tissues of interest requires mincing dissected tissues and pushing them through a fine cell strainer to filter out connective tissue from the desired cells (**Figure 33A**). Isolating adherent cell types, like dendritic cells or macrophages, or cells from particularly fibrous tissues, requires additional mechanical or enzymatic separation steps (217–219). This process is generally done manually, making it highly time consuming and prone to user variability for assessment of cell yields

and sample viability. Therefore, it is crucial to introduce customizable options for automated tissue dissociation. While some attempts have been made to design such systems, the existing options are not always readily accessible, particularly in academic labs and lower resource settings, largely due to the cost-prohibitive nature of these devices (220). Furthermore, these devices are not always customizable to individual needs of a research group (221). We designed a tissue dissociator device to automate digestion of whole tissues or tissue pieces into single cell suspensions with the aid of digestion enzymes and mechanical disruption. This device can be easily assembled in the lab, placed into heating or cooling chambers for temperature regulation, customized for the required number of tissues to dissociate, and programmed with desired dissociation protocols. Broad use of this device could significantly improve reproducibility in cell extraction protocols and provide a time saving alternative to manual dissociation.

The design allows for simultaneous digestion of up to 12 tissues through an automated process. The device is composed of 12 individual motors wired in parallel and powered by a standard wall plug through an AC/DC adapter with an adjustable voltage dial to control the rotation/speed of the motors. The motors are turning a hex bolt that fits snuggly into the top of the C-tubes. The C-tubes are held in place by downward tension on an acrylic plate that latches on either side to the top plate where the motors are secured (**Figure 33B**). Because the motors are wired in parallel, their speed at any given voltage should not vary much, but the load (the number of C-tubes mounted on the device) will affect speed even when voltage is kept constant. To measure rotations per minute

(rpm), a tachometer has been incorporated using a hall effect sensor and a fixed magnet to one of the motor shafts **(Supp. Figure 1)**. Also included, is a programmable switch to reverse the direction of rotation by reversing the positive/negative charges delivered to the motors. All these features are integrated using coded software (Arduino IDE Software) on an Arduino Nano. Using connected buttons and an LCD panel **(Supp. Figure 2)**, it is possible to create and run saved and custom protocols, automatically reverse the rotational direction at specified times of a protocol, adjust speed using the voltage (**Supp. Figure 3**), and display the current motor speed and time left to complete a programmed protocol (**Supp. Figure 4**).

Methods:

Tissues from 7 to 9-week old female C57BL6/J mice (Jackson Laboratory) were used for these studies. Study protocols were approved by the UMD Institutional Animal Care and Use Committee (IACUC). Single cell suspensions were prepared using both mechanical-enzymatic tissue dissociation with this device and manual-enzymatic tissue dissociation to determine the differences, if any, in cells recovered for downstream applications. The cell preparations were evaluated based on total cell yields per tissue, percent cell viability, and used flow cytometry to compare potential differences in surface marker expression.

Data were analyzed using Graphpad Prism (GraphPad, La Jolla, CA). Unpaired Welch t tests were used to compare pairs of samples or groups with sample sizes n>4 mice representing 2 replicate experiments. Differences were

considered statistically significant when $p < 0.05$. *p<0.05, **p<0.01, ***p<0.001, ****p<0.0001. Error bars represent SEM.

Detailed instructions for fabrication and assembly of this device can be found in the supplementary files.

Protocols

1. Protocol used for manual dissociation, adapted from Maisel K., et al (222):

1.1 Remove dissected tissue and keep in cold cell culture media with 5% fetal bovine serum (FBS).

Note: This protocol is meant for isolation of cells from solid tissues.

1.2 Mince tissue using sharp dissection scissors so that tissue fragments are less than 1 mm in any dimension.

1.3 Transfer minced tissue to a 15 mL conical tube and add 5 mL media.

1.4 Add digestion enzymes according to the tissue and cell types being isolated.

Note: For the presented experiments, the following enzymes were used Collagenase 4 (1 mg/mL), Collagenase D (1 mg/mL), and DNAse (40 µg/mL).

1.5 Incubate on shaker or rocker for 1 hour at 37 ºC with gentle agitation throughout the incubation period.

1.6 Pipette sample up and down 100 times.

1.7 Add EDTA to bring the sample volume to 5 mM concentration.

1.8 Pipette sample up and down 100 times.

1.9 Pipette sample up and down 100 times vigorously.

1.10 Push sample through a 70 µm cell strainer and collect in a 50 or 15 mL tube.

1.11 Spin collected cells down using a centrifuge at 300 x g for 5 minutes at 4 ºC.

1.12 Discard supernatant using a pipette and resuspend cells in 1mL red blood cell lysis buffer.

1.13 Incubate for 1 minute at room temperature.

1.14 Quench lysis buffer with 9 mL cold Phosphate Buffered Saline (PBS).

1.15 Spin collected cells down using a centrifuge at 300 x g for 5 minutes at 4 ºC.

1.16 Discard supernatant using a pipette and resuspend cells in buffer or media.

2. Protocol used for semi-automated mechanical dissociation:

2.1 Remove dissected tissue and keep in cold cell culture media with 5% fetal bovine serum (FBS).

Note: This protocol is meant for isolation of cells from solid tissues.

2.2 Chop tissue using sharp dissection scissors so that tissue fragments are roughly 5 mm in any dimension.

2.3 Transfer to C tube and add 1 mL media.

2.4 Load C tube on device

2.5 Fit the tube holder plate (**Supplementary Figure 1A**) over the D-shaped tube bottoms

2.6 Secure tubes to motor plate by latching tension arms into the acrylic plate (**Supplementary Figure 3**)

2.7 Set a custom program: Forward 30 seconds, Reverse 10 seconds, Loop 4 times

2.7.1 Choose Custom Mode from the Main Menu by pressing the blue button.

2.7.2 In the first custom mode menu, specify the duration of forward rotation by pressing the red button until the value on the screen reads 30 seconds. Push the blue button to select this value and advance to the next menu screen.

2.7.3 In the second custom mode menu, specify the duration of reverse rotation by pressing the red button until the value on the screen reads 10 seconds. Push the blue button to select this value and advance to the next menu screen.

2.7.4 In the third custom mode menu, specify the number of times to repeat selections set in steps 2.7.2- 2.7.3 by pressing the red button until the value on the screen reads 4X. Push the blue button to select this value and begin the program

Note: Custom programs are not retained in the device memory but can be programmed as one of the preset programs for faster operation (device programming instructions provided in Supplemental files).

2.8 Run the custom program at 200 rpm by adjusting the voltage control dial (**Supplementary Figure 3**) until the calculated RPM value in the bottom right corner of the LCD Screen reads 200 (**Supplementary Figure 4**).

2.9 Add digestion enzymes in 4 mL media according to the tissue and cell types being isolated.

Note: for the presented experiments, the following enzymes were used Collagenase 4 (1 mg/mL), Collagenase D (1 mg/mL), and DNase (40 µg /mL).

2.10 Load the C tube on device and repeat steps 2.5-2.8 to run the following program at 200 rpm:

Forward 30 seconds, Reverse 10 seconds, Loop 4 times.

2.11 Transfer device with tubes still loaded to 37 ºC incubator for 45 minutes.

2.12 Load the C tube on device and repeat steps 2.5-2.8 to run the following program at 50 rpm: Forward 270 seconds, Reverse 30 seconds, Loop 9 times.

2.13 Add EDTA to bring the sample volume to a 5 mM concentration.

2.14 Load C tube on device and repeat steps 2.5-2.8 to run the following program at 100 rpm:
Forward 30 seconds, Reverse 10 seconds, Loop 2 times.

2.15 Push sample through a 70 µm cell strainer and collect in a 50 or 15 mL tube.

2.16 Spin collected cells down using a centrifuge at 300 x g for 5 minutes at 4 ºC.

2.17 Discard supernatant using a pipette and resuspend cells in 1mL red blood cell lysis buffer.

2.18 Incubate for 1 minute at room temperature.

2.19 Quench lysis buffer with 9 mL cold Phosphate Buffered Saline (PBS).

2.20 Spin collected cells down using a centrifuge at 300 x g for 5 minutes at 4 ºC.

2.21 Discard supernatant using a pipette and resuspend cells in buffer or media.

Representative Results:

This semi-automated mechanical protocol, is able to replicate results from experiments where cells were processed manually. Cell suspensions prepared using this device vs manual dissociation have comparable cell yields and sample viability across mouse lung, kidney, and heart tissues (**Figure 34A-B**). Populations of immune cells like T cells and dendritic cells were not significantly affected by a difference in isolation protocol (**Figure 34C**). Similarly, analysis of surface marker expression on these immune cell populations show similar frequencies of isolated T cells (**Figure 35A**) and comparable mean fluorescence intensity for antigen presentation marker, MHC-II in dendritic cells (**Figure 35B**) between manual and device isolation.

Discussion:

This device was designed for easy assembly in a research setting to provide single cell suspensions from whole tissues for subsequent single cell analysis. The features, though basic, are enough to meet the needs of researchers in academic settings and beyond. A key benefit of using this device is its potential to improve the preparation of single cell suspensions by reducing variability. In addition, having the ability to process 12+ samples simultaneously could increase sample-to-sample consistency that may be affected by increased time required for manual dissociation protocols. In research institutions and industry settings, devices like this and other commercially available devices allow for faster and customizable tissue processing; however commercial devices are >10 fold the

cost of the device described here, limiting their accessibility particularly for low resource research settings (223,224). In academic laboratories, this device could allow trainees (undergraduate and graduate students) an opportunity to complete more sophisticated research by shortening the time needed to process tissues for in-vivo analyses.

The mechanical dissociation protocol shown here was adapted from a protocol regularly used to isolate immune cells from lung tissues (222). Time consuming manual steps like fine mincing and numerous or vigorous pipetting were substituted with automated mechanical processing, which saved both time and effort required to produce similar results to the manual protocol. This could prove to be ergonomically beneficial for the end user because repetitive pipetting as prescribed in the manual protocol could contribute to the development of neuromuscular conditions like carpal tunnel syndrome.

This semi-automated process can be used to generate cell suspensions for applications including flow cytometry and cell culture. It is important to note that all samples should be kept cold or on ice when not incubating at 37oC, as this could affect cell viability. The enzymes, rotational speeds, and incubation times prescribed in the mechanical protocol may be customized as needed for adaptation to other protocols or desired target cells. However, the minimum and maximum rotational speeds of the device is limited by the specifications of the motors used. For speeds slower than 50 rpm or faster than 200 rpm, motors with a lower or higher maximum speed should be chosen respectively.

Recommendation for Non-Engineering Labs:

This device was built in collaboration with Terrapin Works, the fabrication and prototyping center housed in the Engineering department at the University of Maryland. If available, the mechanical, electrical, and software engineers at any academic institution should find this design relatively easy to assemble. Alternatively, a university's machine shop (if available) or any local mechanical, electrical, and/or software engineering labs may be able to help with the fabrication or advise on additional available resources.

Future Technical Improvements

Software code has not been developed to eliminate the manual voltage dial and automatically adjust the motor speed through programming alone. This is possible, but would require hardware additions including a variable voltage regulator and more sophisticated software to incorporate this feature into the preset and custom program modes.

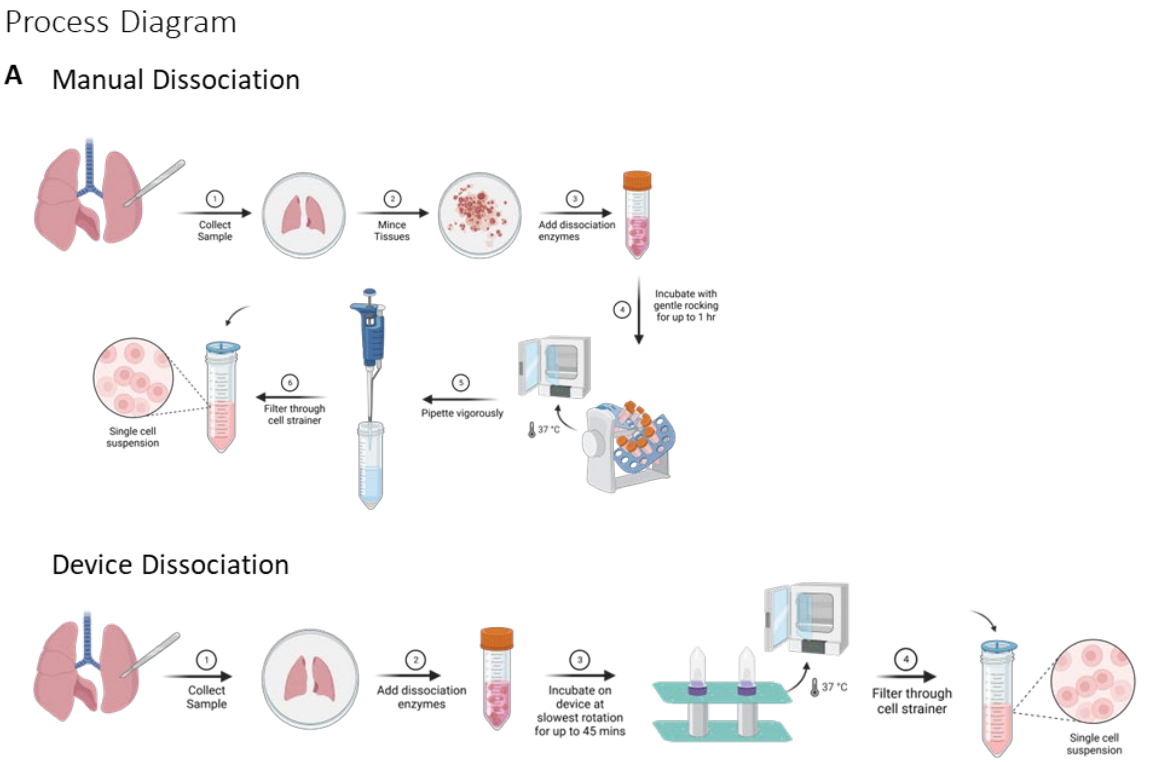

Figure 33.
A) Steps in the process of preparing single cell suspension using simple dissociator device vs manual dissociation.
B) Dissociator device design and features.

This figure is adapted with permission from: *Amosu, M., Gregory, A. J., Murtagh, J. D., Pavin, N., Meyers, C. T., Grano de Oro Fernandez, J., Moore, K., Maisel, K. Mechanical Dissociation of Tissues for Single Cell Analysis Using a Motorized Device. J. Vis. Exp. (201), e65866, doi:10.3791/65866 (2023).*

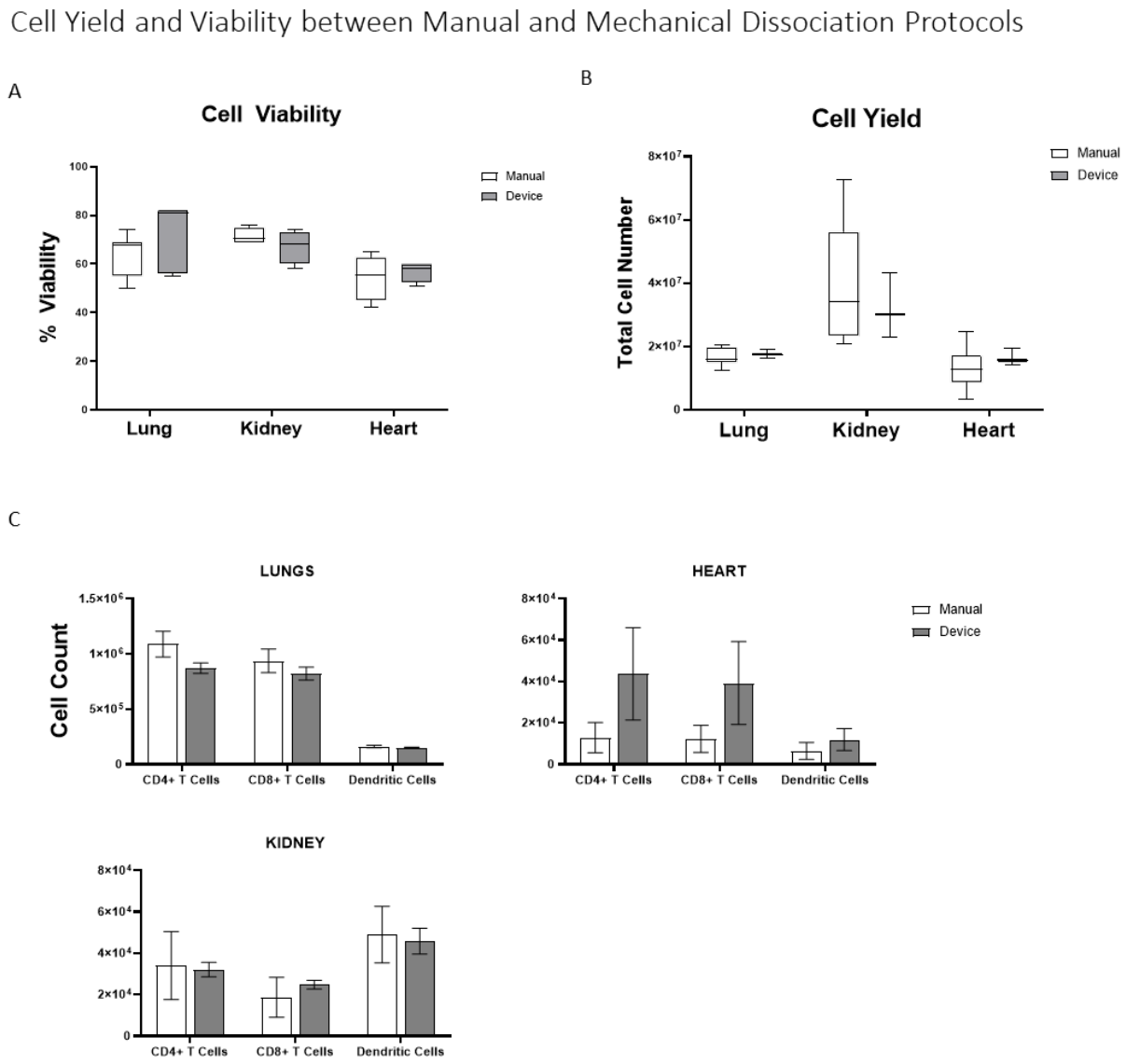

Figure 34.
A) Viability and **B)** yeild of cells from different tissues immediately after preparation of cell suspension counted by hemocytometer before flow staining
C) Cell counts of immune cell populations identified by flow cytometry
Data were analyzed using Graphpad Prism (GraphPad, La Jolla, CA). Unpaired Welch t tests were used to compare pairs of samples or groups. Differences were considered statistically significant when $p < 0.05$. *p<0.05, **p<0.01, ***p<0.001, ****p<0.0001.

This figure is adapted with permission from: *Amosu, M., Gregory, A. J., Murtagh, J. D., Pavin, N., Meyers, C. T., Grano de Oro Fernandez, J., Moore, K., Maisel, K. Mechanical Dissociation of Tissues for Single Cell Analysis Using a Motorized Device. J. Vis. Exp. (201), e65866, doi:10.3791/65866 (2023).*

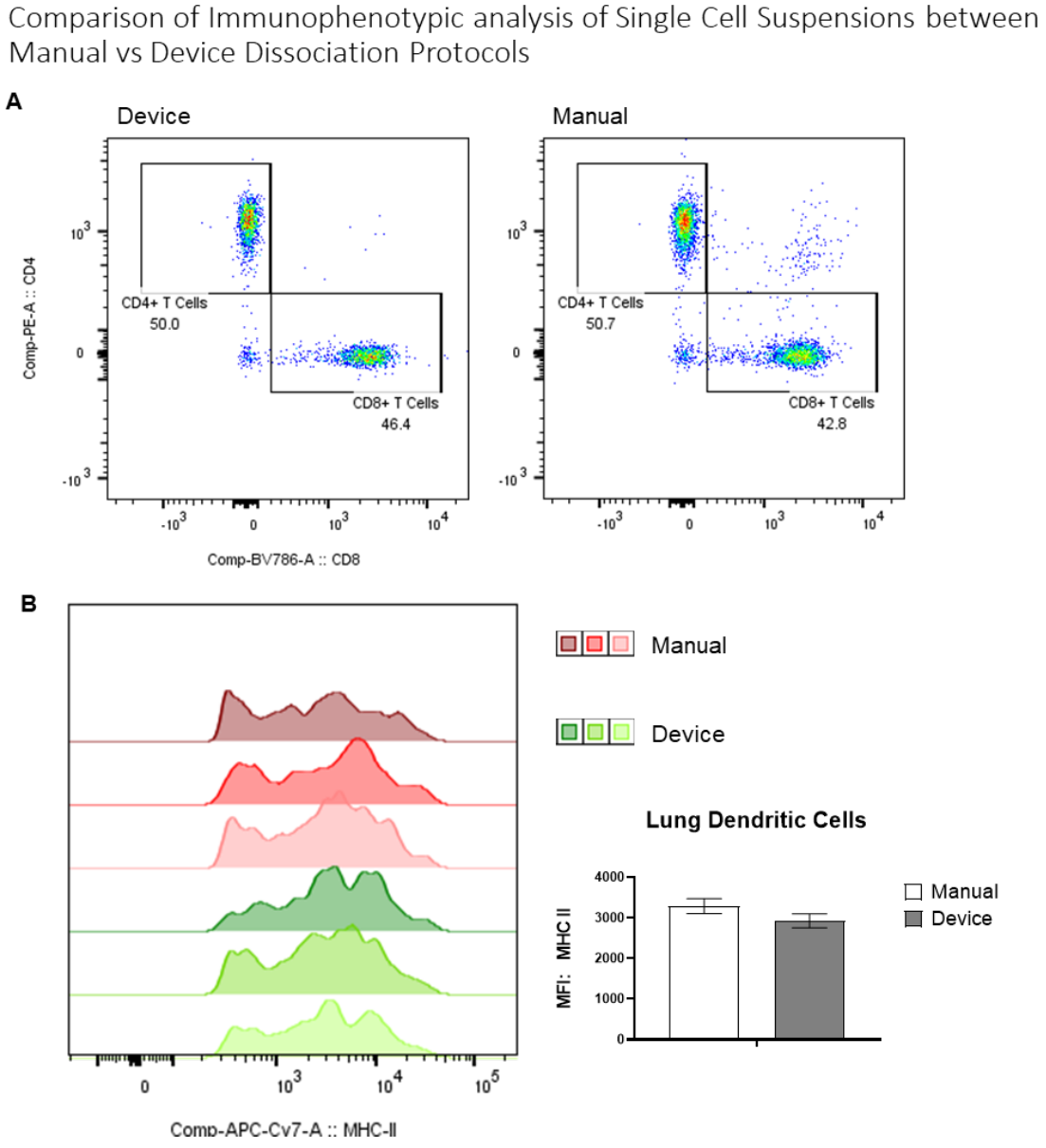

Figure 35. Comparison surface marker expression in single cell suspensions prepared using mechanical dissociator device vs manual dissociation.
A) Lung T Cell populations
B) Mean fluorescence intensity (MFI) of surface MHC-II on lung dendritic cells

This figure is adapted with permission from: *Amosu, M., Gregory, A. J., Murtagh, J. D., Pavin, N., Meyers, C. T., Grano de Oro Fernandez, J., Moore, K., Maisel, K. Mechanical Dissociation of Tissues for Single Cell Analysis Using a Motorized Device. J. Vis. Exp. (201), e65866, doi:10.3791/65866 (2023).*

Supplementary Figure 1.
A) Images of acrylic sheet CAD files
B) Motor/ coupler/ hex bolt / motor spacer unit
C) RPM Sensor
D) Motor wiring

This figure is adapted with permission from: *Amosu, M., Gregory, A. J., Murtagh, J. D., Pavin, N., Meyers, C. T., Grano de Oro Fernandez, J., Moore, K., Maisel, K. Mechanical Dissociation of Tissues for Single Cell Analysis Using a Motorized Device. J. Vis. Exp. (201), e65866, doi:10.3791/65866 (2023).*

Control Panel Assembly

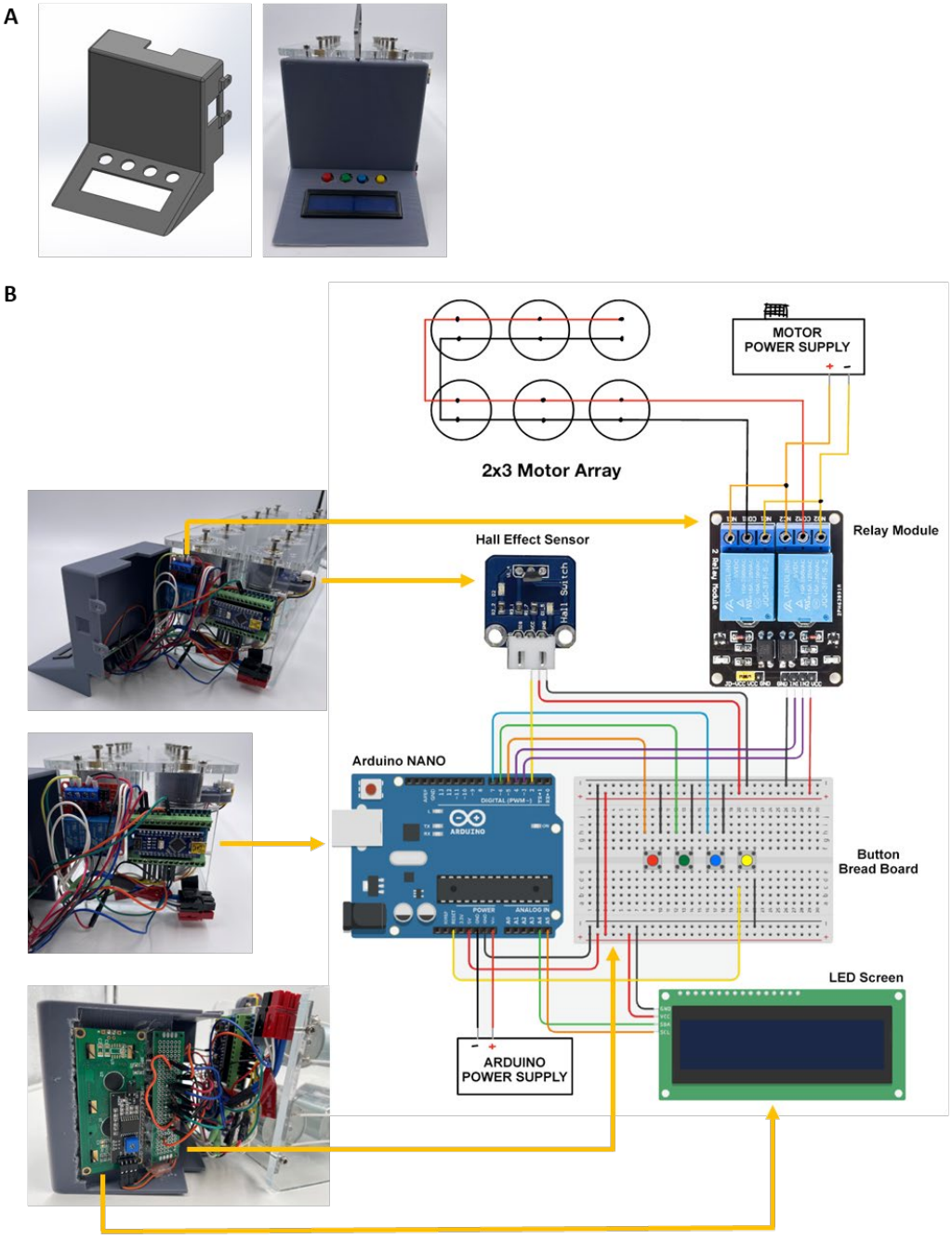

Supplementary Figure 2.
A) Control Panel CAD
B) Control panel / Power Supply wiring diagram
This figure is adapted with permission from: *Amosu, M., Gregory, A. J., Murtagh, J. D., Pavin, N., Meyers, C. T., Grano de Oro Fernandez, J., Moore, K., Maisel, K. Mechanical Dissociation of Tissues for Single Cell Analysis Using a Motorized Device. J. Vis. Exp. (201), e65866, doi:10.3791/65866 (2023).*

Device Operation

A

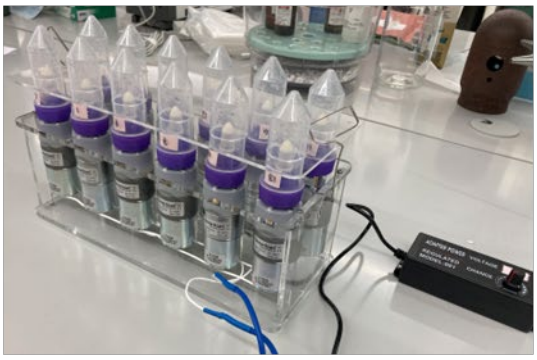

B

Supplementary Figure 3.
A) GentleMacs C Tubes loaded onto device and secured with tube holder plate and tension arms
B) Variable voltage regulator with dial

This figure is adapted with permission from: *Amosu, M., Gregory, A. J., Murtagh, J. D., Pavin, N., Meyers, C. T., Grano de Oro Fernandez, J., Moore, K., Maisel, K. Mechanical Dissociation of Tissues for Single Cell Analysis Using a Motorized Device. J. Vis. Exp. (201), e65866, doi:10.3791/65866 (2023).*

(225)

References

1. Korotcenko L, Schuurmans M, Benden C, Schmitt-Opitz I, Weder W, Inci I. Lung Transplantation for Lymphangioleiomyomatosis: A Single-Center Experience. CHEST. 2017 Oct 1;152(4):A1103.

2. Khawar MU, Yazdani D, Zhu Z, Jandarov R, Dilling DF, Gupta N. Clinical outcomes and survival following lung transplantation in patients with lymphangioleiomyomatosis. The Journal of Heart and Lung Transplantation. 2019 Sep 1;38(9):949–55.

3. Kristof AS. mTOR Signaling in Lymphangioleiomyomatosis. Lymphat Res Biol. 2010 Mar;8(1):33–42.

4. Laplante M, Sabatini DM. mTOR signaling in growth control and disease. Cell. 2012 Apr 13;149(2):274–93.

5. Catherine L. Salussolia, Salussolia CL, Katarzyna Klonowska, Klonowska K, David J. Kwiatkowski, Kwiatkowski DJ, et al. Genetic Etiologies, Diagnosis, and Treatment of Tuberous Sclerosis Complex. Annual Review of Genomics and Human Genetics. 2019 Aug 30;20(1):217–40.

6. Taveira–DaSilva AM, Pacheco–Rodriguez G, Moss J. The Natural History of Lymphangioleiomyomatosis: Markers of Severity, Rate of Progression and Prognosis. Lymphat Res Biol. 2010 Mar;8(1):9–19.

7. Weerakkody Y. Radiopaedia. [cited 2024 Mar 31]. Lymphangioleiomyomatosis | Radiology Reference Article | Radiopaedia.org. Available from: https://radiopaedia.org/articles/lymphangioleiomyomatosis-1?lang=us

8. Taveira-DaSilva AM, Moss J. Clinical features, epidemiology, and therapy of lymphangioleiomyomatosis. Clin Epidemiol. 2015 Apr 7;7:249–57.

9. Sekimoto Y, Suzuki K, Okura M, Hayashi T, Ebana H, Kumasaka T, et al. Uncommon radiologic computed tomography appearances of the chest in patients with lymphangioleiomyomatosis. Sci Rep. 2021 Mar 30;11(1):7170.

10. Li M, Zhu WY, Wang J, Yang XD, Li WM, Wang G. Diagnostic performance of VEGF-D for lymphangioleiomyomatosis: a meta-analysis. J Bras Pneumol. 48(1):e20210337.

11. Vascular Endothelial Growth Factor-D Is Increased in Serum of Patients with Lymphangioleiomyomatosis | Lymphatic Research and Biology [Internet]. [cited 2024 Mar 31]. Available from: https://www.liebertpub.com/doi/10.1089/lrb.2006.4.143?url_ver=Z39.88-2003&rfr_id=ori:rid:crossref.org&rfr_dat=cr_pub%20%200pubmed

12. Glasgow CG, Avila NA, Lin JP, Stylianou MP, Moss J. Serum Vascular Endothelial Growth Factor-D Levels in Patients With Lymphangioleiomyomatosis Reflect Lymphatic Involvement. Chest. 2009 May;135(5):1293–300.

13. Xu W, Yang C, Cheng C, Wang Y, Hu D, Huang J, et al. Determinants of Progression and Mortality in Lymphangioleiomyomatosis. CHEST. 2023 Jul 1;164(1):137–48.

14. Freise J, Klingenberg MS, Fuge J, Welte T. Vascular endothelial growth factor (VEGF) is a predictable marker for FEV1 progression in patients with Lymphangiolyomyomatosis (LAM). European Respiratory Journal [Internet]. 2019 Sep 28 [cited 2024 Mar 31];54(suppl 63). Available from: https://erj.ersjournals.com/content/54/suppl_63/PA3685

15. Jain VV, Gupta OP, Jajoo S, Khiangate B. Recurrent Pneumothorax in a Young Female with Pulmonary Lymphangiomyomatosis: A Case Report and Overview of Literature. J Family Med Prim Care. 2014;3(1):86–8.

16. Oprescu N, McCormack FX, Byrnes S, Kinder BW. Clinical Predictors of Mortality and Cause of Death in Lymphangioleiomyomatosis: A Population-based Registry. Lung. 2013 Feb 1;191(1):35–42.

17. Markers of Cell Proliferation and Expression of Melanosomal Antigen in Lymphangioleiomyomatosis | American Journal of Respiratory Cell and Molecular Biology [Internet]. [cited 2024 Mar 31]. Available from: https://www.atsjournals.org/doi/10.1165/ajrcmb.21.3.3693?url_ver=Z39.88-2003&rfr_id=ori:rid:crossref.org&rfr_dat=cr_pub%20%200pubmed

18. Zhe X, Schuger L. Combined Smooth Muscle and Melanocytic Differentiation in Lymphangioleiomyomatosis. J Histochem Cytochem. 2004 Dec 1;52(12):1537–42.

19. Glasgow CG, Taveira-DaSilva AM, Darling TN, Moss J. Lymphatic Involvement in Lymphangioleiomyomatosis. Ann N Y Acad Sci. 2008;1131:206–14.

20. Goncharova EA, Goncharov DA, Lim PN, Noonan D, Krymskaya VP. Modulation of Cell Migration and Invasiveness by Tumor Suppressor TSC2 in Lymphangioleiomyomatosis. Am J Respir Cell Mol Biol. 2006 Apr;34(4):473–80.

21. Glasgow CG, El-Chemaly S, Moss J. Lymphatics in lymphangioleiomyomatosis and idiopathic pulmonary fibrosis. European Respiratory Review. 2012 Sep 1;21(125):196–206.

22. Yang B, Moss J. Cell survival pathways targeted in rare lung disease affecting women. Sci Adv. 9(19):eadi1215.

23. Prizant H, Hammes SR. Minireview: Lymphangioleiomyomatosis (LAM): The “Other” Steroid-Sensitive Cancer. Endocrinology. 2016 Sep;157(9):3374–83.

24. Pongsuvareeyakul T, Maleki S, DeNardo BD, Dizon DS, Phornphutkul C, Singh K. Sporadic uterine Lymphangioleiomyomatosis (LAM): Report of a unique case arising in the lower uterine segment with short review. Gynecol Oncol Rep. 2021 Jun 17;37:100812.

25. Artoni F, Grützmacher N, Demetriades C. Unbiased evaluation of rapamycin’s specificity as an mTOR inhibitor. Aging Cell. 2023;22(8):e13888.

26. Sarbassov DD, Ali SM, Sengupta S, Sheen JH, Hsu PP, Bagley AF, et al. Prolonged Rapamycin Treatment Inhibits mTORC2 Assembly and Akt/PKB. Molecular Cell. 2006 Apr 21;22(2):159–68.

27. Sarbassov DD, Guertin DA, Ali SM, Sabatini DM. Phosphorylation and Regulation of Akt/PKB by the Rictor-mTOR Complex. Science. 2005 Feb 18;307(5712):1098–101.

28. Delgoffe GM, Kole TP, Zheng Y, Zarek PE, Matthews KL, Xiao B, et al. The mTOR Kinase Differentially Regulates Effector and Regulatory T Cell Lineage Commitment. Immunity. 2009 Jun 19;30(6):832–44.

29. Delaney SP. Modeling and Therapeutic Development for the Tuberous Sclerosis Related Neoplasm Lymphangioleiomyomatosis [Internet]. Université d’Ottawa / University of Ottawa; 2019 [cited 2024 Apr 16]. Available from: http://hdl.handle.net/10393/39810

30. Lu Y, Zhang EY, Liu J, Yu JJ. Inhibition of the mechanistic target of rapamycin induces cell survival via MAPK in tuberous sclerosis complex. Orphanet J Rare Dis. 2020 Aug 17;15:209.

31. El-Hashemite N, Walker V, Zhang H, Kwiatkowski DJ. Loss of Tsc1 or Tsc2 Induces Vascular Endothelial Growth Factor Production through Mammalian Target of Rapamycin1. Cancer Research. 2003 Sep 18;63(17):5173–7.

32. Kenerson HL, Dundon TA, Yeung RW, Yeung RS. Effects of Rapamycin in the Eker Rat Model of Tuberous Sclerosis Complex. Pediatric Research. 2005 Jan 1;57(1):67–75.

33. McCormack FX, Inoue Y, Moss J, Singer LG, Strange C, Nakata K, et al. Efficacy and Safety of Sirolimus in Lymphangioleiomyomatosis. New England Journal of Medicine. 2011 Apr 28;364(17):1595–606.

34. Bissler JJ, McCormack FX, Young LR, Elwing JM, Chuck G, Leonard JM, et al. Sirolimus for Angiomyolipoma in Tuberous Sclerosis Complex or

Lymphangioleiomyomatosis. New England Journal of Medicine. 2008 Jan 10;358(2):140–51.

35. Revilla-López E, Berastegui C, Méndez A, Sáez-Giménez B, Ruiz de Miguel V, López-Meseguer M, et al. Long-term results of sirolimus treatment in lymphangioleiomyomatosis: a single referral centre experience. Sci Rep. 2021 May 13;11(1):10171.

36. Labani-Motlagh A, Ashja-Mahdavi M, Loskog A. The Tumor Microenvironment: A Milieu Hindering and Obstructing Antitumor Immune Responses. Frontiers in Immunology. 2020;11:940.

37. Sun SY. Searching for the real function of mTOR signaling in the regulation of PD-L1 expression. Translational Oncology. 2020 Dec 1;13(12):100847.

38. Yang L, Li A, Lei Q, Zhang Y. Tumor-intrinsic signaling pathways: key roles in the regulation of the immunosuppressive tumor microenvironment. Journal of Hematology & Oncology. 2019 Nov 27;12(1):125.

39. Maisel K, Merrilees MJ, Atochina-Vasserman EN, Lian L, Obraztsova K, Rue R, et al. Immune Checkpoint Ligand PD-L1 Is Upregulated in Pulmonary Lymphangioleiomyomatosis. Am J Respir Cell Mol Biol. 2018 Dec;59(6):723–32.

40. Liu HJ, Lizotte PH, Du H, Speranza MC, Lam HC, Vaughan S, et al. TSC2-deficient tumors have evidence of T cell exhaustion and respond to anti–PD-1/anti–CTLA-4 immunotherapy. JCI Insight. 2018 Apr 19;3(8):e98674.

41. Krymskaya VP. Smooth muscle-like cells in pulmonary lymphangioleiomyomatosis. Proc Am Thorac Soc. 2008 Jan 1;5(1):119–26.

42. Clements D, Dongre A, Krymskaya VP, Johnson SR. Wild Type Mesenchymal Cells Contribute to the Lung Pathology of Lymphangioleiomyomatosis. PLOS ONE. 2015 May 15;10(5):e0126025.

43. Matsui K, K Riemenschneider W, Hilbert SL, Yu ZX, Takeda K, Travis WD, et al. Hyperplasia of type II pneumocytes in pulmonary lymphangioleiomyomatosis. Arch Pathol Lab Med. 2000 Nov;124(11):1642–8.

44. Davis JM, Hyjek E, Husain AN, Shen L, Jones J, Schuger LA. Lymphatic Endothelial Differentiation in Pulmonary Lymphangioleiomyomatosis Cells. J Histochem Cytochem. 2013 Aug;61(8):580–90.

45. Steagall WK, Pacheco-Rodriguez G, Darling TN, Torre O, Harari S, Moss J. The Lymphangioleiomyomatosis Lung Cell and Its Human Cell Models. Am J Respir Cell Mol Biol. 2018 Jun;58(6):678–83.

46. Arbiser JL, Yeung R, Weiss SW, Arbiser ZK, Amin MB, Cohen C, et al. The Generation and Characterization of a Cell Line Derived from a Sporadic Renal Angiomyolipoma. Am J Pathol. 2001 Aug;159(2):483–91.

47. Hilaire C. Lam, Lam HC, Anil J. Trindade, Trindade AJ, Douglas A. Medvetz, Medvetz DA, et al. Abstract A35: Identification of pro-survival rapamycin-dependent microRNA (Rapa-miRs) in tuberous sclerosis complex. Cancer Research. 2013 Oct 1;73.

48. Valianou M, Matthildi Valianou, Erik Y. Zhang, Erik Y. Zhang, Johnson D, Daniel L. Johnson, et al. Combination of Volasertib and Rapamycin Inhibits the Regrowth of TSC2-Deficient Tumors. Cold Spring Harbor Laboratory - bioRxiv. 2022 Nov 3;

49. Dongre A, Clements D, Fisher AJ, Johnson SR. Cathepsin K in Lymphangioleiomyomatosis: LAM Cell–Fibroblast Interactions Enhance Protease Activity by Extracellular Acidification. The American Journal of Pathology. 2017 Aug 1;187(8):1750–62.

50. FAMILIAL RENAL ADENOMAS IN WISTAR RATS - EKER - 1954 - Acta Pathologica Microbiologica Scandinavica - Wiley Online Library [Internet]. [cited 2024 Jan 7]. Available from: https://onlinelibrary.wiley.com/doi/10.1111/j.1699-0463.1954.tb00301.x

51. Hino O, Kobayashi E, Kobayashi E, Youko Hirayama, Hirayama Y, Kobayashi T, et al. Molecular genetic basis of renal carcinogenesis in the Eker rat model of tuberous sclerosis (Tsc2). Molecular Carcinogenesis. 1995 Sep 1;14(1):23–7.

52. Kobayashi T, Youko Hirayama, Hirayama Y, Kobayashi E, Kobayashi E, Kubo Y, et al. A germline insertion in the tuberous sclerosis (Tsc2) gene gives rise to the Eker rat model of dominantly inherited cancer. Nature Genetics. 1995 Jan 1;9(1):70–4.

53. Walker CL, Hunter D, Everitt JI. Uterine leiomyoma in the Eker rat: a unique model for important diseases of women. Genes Chromosomes Cancer. 2003 Dec;38(4):349–56.

54. Shantini D. Gamage, Gamage SD, Eric D. Bischoff, Bischoff ED, Eric D. Bischoff, Bischoff ED, et al. Efficacy of LGD1069 (Targretin), a Retinoid X Receptor-Selective Ligand, for Treatment of Uterine Leiomyoma. Journal of Pharmacology and Experimental Therapeutics. 2000 Nov 1;295(2):677–81.

55. Yang Sun, Sun Y, Chenggang Li, Li C, Kevin M. Marks, Marks K, et al. Abstract LB-129: Evidence from expression profiling, proteomics, metabolomics and FDG-PET of an estrogen-dependent metabolic switch in tuberin-null cells. Cancer Research. 2013 Apr 15;73.

56. Debbie Clements, Clements D, Sarah L Asprey, Asprey SL, Tom McCulloch, McCulloch TA, et al. Analysis of the oestrogen response in an angiomyolipoma derived xenograft model. Endocrine-related Cancer. 2008 Nov 6;16(1):59–72.

57. Li C, Lee PS, Sun Y, Gu X, Zhang E, Guo Y, et al. Estradiol and mTORC2 cooperate to enhance prostaglandin biosynthesis and tumorigenesis in TSC2-deficient LAM cells. J Exp Med. 2014 Jan 13;211(1):15–28.

58. Anya Alayev, Alayev A, Rachel S. Salamon, Salamon RS, Yangying Sun, Sun Y, et al. Effects of Combining Rapamycin and Resveratrol on Apoptosis and Growth of TSC2-Deficient Xenograft Tumors. American Journal of Respiratory Cell and Molecular Biology. 2015 Oct 30;53(5):637–46.

59. Jia Liu, Liu J, Jia Liu, Jun Yuan, Yuan J, Yuan J, et al. miR-124 targets retinoid X receptor α to reduce growth of TSC2-deficient lymphangioleiomyomatosis. Oncology Reports. 2018 Dec 7;41(2):1342–50.

60. Onda H, Lueck A, Marks PW, Warren HB, Kwiatkowski DJ. Tsc2+/– mice develop tumors in multiple sites that express gelsolin and are influenced by genetic background. J Clin Invest. 1999 Sep 15;104(6):687–95.

61. Kobayashi T, Minowa O, Sugitani Y, Takai S, Mitani H, Kobayashi E, et al. A germ-line Tsc1 mutation causes tumor development and embryonic lethality that are similar, but not identical to, those caused by Tsc2 mutation in mice. Proc Natl Acad Sci U S A. 2001 Jul 17;98(15):8762–7.

62. mouse model of TSC1 reveals sex-dependent lethality from liver hemangiomas, and up-regulation of p70S6 kinase activity in Tsc1 null cells | Human Molecular Genetics | Oxford Academic [Internet]. [cited 2024 Jan 7]. Available from: https://academic.oup.com/hmg/article/11/5/525/2901618?login=false

63. mouse model of tuberous sclerosis 1 showing background specific early post-natal mortality and metastatic renal cell carcinoma | Human Molecular Genetics | Oxford Academic [Internet]. [cited 2024 Jan 7]. Available from: https://academic.oup.com/hmg/article/14/13/1839/621075?login=false

64. Goncharova EA, Goncharov DA, Eszterhas A, Hunter DS, Glassberg MK, Yeung RS, et al. Tuberin Regulates p70 S6 Kinase Activation and Ribosomal Protein S6 Phosphorylation: A ROLE FOR THE TSC2 TUMOR SUPPRESSOR GENE IN PULMONARY LYMPHANGIOLEIOMYOMATOSIS (LAM) *. Journal of Biological Chemistry. 2002 Aug 23;277(34):30958–67.

65. Kwiatkowski DJ. Animal Models of Lymphangioleiomyomatosis (LAM) and Tuberous Sclerosis Complex (TSC). Lymphat Res Biol. 2010 Mar;8(1):51–7.

66. Prizant H, Cho SN, DeMayo FJ, Lydon JP, Hammes SR. Uterine-Specific Knockout of TSC2: A Mouse Model for Leiomyoma and LAM. Biology of Reproduction. 2012 Aug 1;87:150–150.

67. Uterine-Specific Loss of Tsc2 Leads to Myometrial Tumors in Both the Uterus and Lungs | Molecular Endocrinology | Oxford Academic [Internet]. [cited 2024 Jan 9]. Available from: https://academic.oup.com/mend/article/27/9/1403/2615090?login=false

68. Goncharova EA, Goncharov DA, Melane Fehrenbach, Fehrenbach M, Khavin I, Ducka B, et al. Prevention of alveolar destruction and airspace enlargement in a mouse model of pulmonary lymphangioleiomyomatosis (LAM). Science Translational Medicine. 2012 Oct 3;4(154).

69. Elena Lesma, Lesma E, Eloisa Chiaramonte, Chiaramonte E, Silvia Ancona, Ancona S, et al. Anti-EGFR antibody reduces lung nodules by inhibition of EGFR-pathway in a model of lymphangioleiomyomatosis. BioMed Research International. 2015 Jan 28;2015:315240–315240.

70. Sandra L. Dabora, Dabora SL, David Neal Franz, Franz DN, Stephen Ashwal, Ashwal S, et al. Multicenter Phase 2 Trial of Sirolimus for Tuberous Sclerosis: Kidney Angiomyolipomas and Other Tumors Regress and VEGF- D Levels Decrease. PLOS ONE. 2011 Sep 6;6(9).

71. Nishant Gupta, Gupta N, Lee Hs, Lee HS, Young Lw, Young LR, et al. Analysis of the MILES cohort reveals determinants of disease progression and treatment response in lymphangioleiomyomatosis. European Respiratory Journal. 2019 Apr 1;53(4):1802066.

72. Sergio Harari, Harari S, Olga Torre, Torre O, Davide Elia, Elia D, et al. Improving Survival in Lymphangioleio-myomatosis: A 16-Year Observational Study in a Large Cohort of Patients. Respiration. 2021 May 27;100(10):989–99.

73. Kai-Feng Xu, Xu KF, Xinlun Tian, Tian X, Yanli Yang, Yang Y, et al. Rapamycin for lymphangioleiomyomatosis: optimal timing and optimal dosage. Thorax. 2018 Feb 2;73(4):308–10.

74. Goldberg HJ, Harari S, Cottin V, Rosas IO, Peters E, Biswal S, et al. Everolimus for the treatment of lymphangioleiomyomatosis: a phase II study. European Respiratory Journal. 2015 Sep 1;46(3):783–94.

75. Yates DH. mTOR treatment in lymphangioleiomyomatosis: the role of everolimus. Expert Review of Respiratory Medicine. 2016 Mar 3;10(3):249–60.

76. Luo C, Zhang YS, Zhang MX, Chen MF, Li Y, Qi L, et al. Everolimus versus sirolimus for angiomyolipoma associated with tuberous sclerosis

complex: a multi-institutional retrospective study in China. Orphanet Journal of Rare Diseases. 2021 Jul 3;16(1):299.

77. Wang Q, Luo M, Xiang B, Chen S, Ji Y. The efficacy and safety of pharmacological treatments for lymphangioleiomyomatosis. Respiratory Research. 2020 Feb 14;21(1):55.

78. Folkerts H, Hilgendorf S, Vellenga E, Bremer E, Wiersma VR. The multifaceted role of autophagy in cancer and the microenvironment. Med Res Rev. 2019 Mar;39(2):517–60.

79. Gozuacik D, Kimchi A. Autophagy as a cell death and tumor suppressor mechanism. Oncogene. 2004 Apr 12;23(16):2891–906.

80. Takamura A, Komatsu M, Hara T, Sakamoto A, Kishi C, Waguri S, et al. Autophagy-deficient mice develop multiple liver tumors. Genes Dev. 2011 Apr 15;25(8):795–800.

81. Sui X, Chen R, Wang Z, Huang Z, Kong N, Zhang M, et al. Autophagy and chemotherapy resistance: a promising therapeutic target for cancer treatment. Cell Death Dis. 2013 Oct;4(10):e838.

82. Altman BJ, Jacobs SR, Mason EF, Michalek RD, MacIntyre AN, Coloff JL, et al. Autophagy is Essential to Suppress Cell Stress and to Allow BCR-Abl-Mediated Leukemogenesis. Oncogene. 2011 Apr 21;30(16):1855–67.

83. Guo JY, Chen HY, Mathew R, Fan J, Strohecker AM, Karsli-Uzunbas G, et al. Activated Ras requires autophagy to maintain oxidative metabolism and tumorigenesis. Genes Dev. 2011 Mar 1;25(5):460–70.

84. Degenhardt K, Mathew R, Beaudoin B, Bray K, Anderson D, Chen G, et al. Autophagy promotes tumor cell survival and restricts necrosis, inflammation, and tumorigenesis. Cancer Cell. 2006 Jul;10(1):51–64.

85. Yosia Mugume, Mugume Y, Zakayo Kazibwe, Kazibwe Z, Diane C. Bassham, Bassham DC. Target of Rapamycin in Control of Autophagy: Puppet Master and Signal Integrator. International Journal of Molecular Sciences. 2020;21(21):8259.

86. Jane Yu, Yu JJ, Andrey A. Parkhitko, Parkhitko AA, Elizabeth P. Henske, Henske EP. Mammalian target of rapamycin signaling and autophagy: roles in lymphangioleiomyomatosis therapy. Proceedings of the American Thoracic Society. 2010 Feb 15;7(1):48–53.

87. Parkhitko A, Myachina F, Morrison TA, Hindi KM, Auricchio N, Karbowniczek M, et al. Tumorigenesis in tuberous sclerosis complex is autophagy and p62/sequestosome 1 (SQSTM1)-dependent. Proc Natl Acad Sci U S A. 2011 Jul 26;108(30):12455–60.

88. Alayev A, Sun Y, Snyder RB, Berger SM, Yu JJ, Holz MK. Resveratrol prevents rapamycin-induced upregulation of autophagy and selectively induces apoptosis in TSC2-deficient cells. Cell Cycle. 2014 Feb 1;13(3):371–82.

89. El-Chemaly S, Taveira-Dasilva A, Goldberg HJ, Peters E, Haughey M, Bienfang D, et al. Sirolimus and Autophagy Inhibition in Lymphangioleiomyomatosis: Results of a Phase I Clinical Trial. Chest. 2017 Jun;151(6):1302.

90. Gupta N, Zhang B, Zhou Y, McCormack FX, Ingledue R, Robbins N, et al. Safety and Efficacy of Combined Resveratrol and Sirolimus in Lymphangioleiomyomatosis. CHEST. 2023 May 1;163(5):1144–55.

91. Valencia JC, Matsui K, Bondy C, Zhou J, Rasmussen A, Cullen K, et al. Distribution and mRNA Expression of Insulin-Like Growth Factor System in Pulmonary Lymphangioleiomyomatosis. Journal of Investigative Medicine. 2001 Sep 1;49(5):421–33.

92. Atochina-Vasserman EN, Abramova E, James ML, Rue R, Liu AY, Ersumo NT, et al. Pharmacological targeting of VEGFR signaling with axitinib inhibits Tsc2-null lesion growth in the mouse model of lymphangioleiomyomatosis. Am J Physiol Lung Cell Mol Physiol. 2015 Dec 15;309(12):L1447–54.

93. Watz* H, Engels* K, Loeschke S, Amthor M, Kirsten D, Magnussen H, et al. Lymphangioleiomyomatosis—presence of receptor tyrosine kinases and the angiogenesis factor VEGF-A as potential therapeutic targets. Thorax. 2007 Jun;62(6):559.

94. Harari S, Elia D, Caminati A, Geginat J, Luisi F, Pelosi G, et al. Late Breaking Abstract - Nintedanib for Lymphangioleiomyomatosis: an open-label phase II study. European Respiratory Journal [Internet]. 2023 Sep 9 [cited 2024 Jan 9];62(suppl 67). Available from: https://erj.ersjournals.com/content/62/suppl_67/OA3274

95. Gao L, Yue MM, Davis J, Hyjek E, Schuger L. In pulmonary lymphangioleiomyomatosis expression of progesterone receptor is frequently higher than that of estrogen receptor. Virchows Arch. 2014 Apr;464(4):495–503.

96. Logginidou H, Ao X, Russo I, Henske EP. Frequent estrogen and progesterone receptor immunoreactivity in renal angiomyolipomas from women with pulmonary lymphangioleiomyomatosis. Chest. 2000 Jan;117(1):25–30.

97. Sun Y, Zhang E, Lao T, Pereira AM, Li C, Xiong L, et al. Progesterone and Estradiol Synergistically Promote the Lung Metastasis of Tuberin-Deficient

Cells in a Preclinical Model of Lymphangioleiomyomatosis. Horm Cancer. 2014 Jul 29;5(5):284–98.

98. Jane Yu, Yu JJ, Victoria A. Robb, Robb VA, Tasha Morrison, Morrison T, et al. Estrogen promotes the survival and pulmonary metastasis of tuberin-null cells. Proceedings of the National Academy of Sciences of the United States of America. 2009 Feb 24;106(8):2635–40.

99. Taylor James R., Ryu Jay, Colby Thomas V., Raffin Thomas A. Lymphangioleiomyomatosis. New England Journal of Medicine. 1990 Nov 1;323(18):1254–60.

100. Yu J, Astrinidis A, Howard S, Henske EP. Estradiol and tamoxifen stimulate LAM-associated angiomyolipoma cell growth and activate both genomic and nongenomic signaling pathways. American Journal of Physiology-Lung Cellular and Molecular Physiology. 2004 Apr;286(4):L694–700.

101. Taveira-DaSilva AM, Stylianou MP, Hedin CJ, Hathaway O, Moss J. Decline in Lung Function in Patients With Lymphangioleiomyomatosis Treated With or Without Progesterone. CHEST. 2004 Dec 1;126(6):1867–74.

102. Lu C, Lee HS, Pappas GP, Dilling DF, Burger CD, Shifren A, et al. A Phase II Clinical Trial of an Aromatase Inhibitor for Postmenopausal Women with Lymphangioleiomyomatosis. Ann Am Thorac Soc. 2017 Jun;14(6):919–28.

103. Statins in Lymphangioleiomyomatosis. Simvastatin and Atorvastatin Induce Differential Effects on tuberous sclerosis complex 2–Null Cell Growth and Signaling | American Journal of Respiratory Cell and Molecular Biology [Internet]. [cited 2024 Apr 2]. Available from: https://www.atsjournals.org/doi/10.1165/rcmb.2013-0203RC?url_ver=Z39.88-2003&rfr_id=ori:rid:crossref.org&rfr_dat=cr_pub%20%200pubmed

104. Krymskaya VP, Courtwright AM, Fleck V, Dorgan D, Kotloff R, McCormack FX, et al. A phase II clinical trial of the Safety Of Simvastatin (SOS) in patients with pulmonary lymphangioleiomyomatosis and with tuberous sclerosis complex. Respiratory Medicine [Internet]. 2020 Mar 1 [cited 2024 Apr 2];163. Available from: https://www.resmedjournal.com/article/S0954-6111(20)30038-X/fulltext

105. Terraneo S, Lesma E, Ancona S, Imeri G, Palumbo G, Torre O, et al. Exploring the Role of Matrix Metalloproteinases as Biomarkers in Sporadic Lymphangioleiomyomatosis and Tuberous Sclerosis Complex. A Pilot Study. Front Med [Internet]. 2021 Apr 26 [cited 2024 Apr 5];8. Available from: https://www.frontiersin.org/articles/10.3389/fmed.2021.605909

106. Ancona S, Orpianesi E, Bernardelli C, Chiaramonte E, Chiaramonte R, Terraneo S, et al. Differential Modulation of Matrix Metalloproteinases-2 and -7 in LAM/TSC Cells. Biomedicines. 2021 Nov 24;9(12):1760.

107. Odajima N, Betsuyaku T, Nasuhara Y, Inoue H, Seyama K, Nishimura M. Matrix metalloproteinases in blood from patients with LAM. Respiratory Medicine. 2009 Jan 1;103(1):124–9.

108. Chang WYC, Clements D, Johnson SR. Effect of doxycycline on proliferation, MMP production, and adhesion in LAM-related cells. American Journal of Physiology-Lung Cellular and Molecular Physiology. 2010 Sep;299(3):L393–400.

109. Chang WYC, Cane JL, Kumaran M, Lewis S, Tattersfield AE, Johnson SR. A 2-year randomised placebo-controlled trial of doxycycline for lymphangioleiomyomatosis. European Respiratory Journal. 2014 Apr 1;43(4):1114–23.

110. Pimenta SP, Baldi BG, Kairalla RA, Carvalho CRR. Doxycycline use in patients with lymphangioleiomyomatosis: biomarkers and pulmonary function response. J bras pneumol. 2013 Feb;39:5–15.

111. Moses Marsha A., Harper Jay, Folkman Judah. Doxycycline Treatment for Lymphangioleiomyomatosis with Urinary Monitoring for MMPs. New England Journal of Medicine. 2006;354(24):2621–2.

112. Araujo MS, Baldi BG, Freitas CSG, Albuquerque ALP, Marques da Silva CCB, Kairalla RA, et al. Pulmonary rehabilitation in lymphangioleiomyomatosis: a controlled clinical trial. Eur Respir J. 2016 May;47(5):1452–60.

113. Le K, Steagall WK, Stylianou M, Pacheco-Rodriguez G, Darling TN, Vaughan M, et al. Effect of beta-agonists on LAM progression and treatment. Proceedings of the National Academy of Sciences. 2018 Jan 30;115(5):E944–53.

114. Weichhart T, Hengstschläger M, Linke M. Regulation of innate immune cell function by mTOR. Nat Rev Immunol. 2015 Oct;15(10):599–614.

115. Giordano A, Avellino R, Ferraro P, Romano S, Corcione N, Romano MF. Rapamycin antagonizes NF-kappaB nuclear translocation activated by TNF-alpha in primary vascular smooth muscle cells and enhances apoptosis. Am J Physiol Heart Circ Physiol. 2006 Jun;290(6):H2459-2465.

116. Gammon JM, Gosselin EA, Tostanoski LH, Chiu YC, Zeng X, Zeng Q, et al. Low-dose controlled release of mTOR inhibitors maintains T cell plasticity and promotes central memory T cells. J Control Release. 2017 Oct 10;263:151–61.

117. Brown J, Wang H, Hajishengallis GN, Martin M. TLR-signaling Networks: An Integration of Adaptor Molecules, Kinases, and Cross-talk. J Dent Res. 2011 Apr 1;90(4):417–27.

118. Awasthi S. Toll-Like Receptor-4 Modulation for Cancer Immunotherapy. Frontiers in Immunology [Internet]. 2014 [cited 2024 Jan 9];5. Available from: https://www.frontiersin.org/articles/10.3389/fimmu.2014.00328

119. Jiang S, Redelman-Sidi G. BCG in Bladder Cancer Immunotherapy. Cancers (Basel). 2022 Jun 23;14(13):3073.

120. Rolfo C, Giovannetti E, Martinez P, McCue S, Naing A. Applications and clinical trial landscape using Toll-like receptor agonists to reduce the toll of cancer. NPJ Precis Oncol. 2023 Mar 8;7:26.

121. Lymphangioleiomyomatosis (LAM. Breathe (Sheff. 2017;13(1):64–71.

122. Singla A, Gupta N, Apewokin S, McCormack FX. Sirolimus for the treatment of lymphangioleiomyomatosis. Expert Opinion on Orphan Drugs. 2017;5(11):907–21.

123. Elia D, Cssandro R, Torre O, Harari S. Long Term Sirolimus therapy for LAM: a real life experience. European Respiratory Journal. 2017;50(suppl 61).

124. Yao J, Taveira-DaSilva AM, Jones AM, Julien-Williams P, Stylianou M, Moss J. Sustained effects of sirolimus on lung function and cystic lung lesions in lymphangioleiomyomatosis. Am J Respir Crit Care Med. 2014;190(11):1273–82.

125. Wu AA, Drake V, Huang HS, Chiu S, Zheng L. Reprogramming the tumor microenvironment: tumor-induced immunosuppressive factors paralyze T cells. Oncoimmunology. 2015;4(7).

126. Tormoen GW, Crittenden MR, Gough MJ. Role of the immunosuppressive microenvironment in immunotherapy. Adv Radiat Oncol. 2018;3(4):520–6.

127. Gonzalez H, Hagerling C, Werb Z. Roles of the immune system in cancer: from tumor initiation to metastatic progression. Genes Dev. 2018;32(19–20):1267–84.

128. Blomberg OS, Spagnuolo L, Visser KE. Immune regulation of metastasis: mechanistic insights and therapeutic opportunities. Dis Model Mech. 2018;11(10).

129. Janssen LME, Ramsay EE, Logsdon CD, Overwijk WW. The immune system in cancer metastasis: friend or foe? Journal for ImmunoTherapy of Cancer. 2017;5(1).

130. Han F, Dellacecca ER, Barse LW, Cosgrove C, Henning SW, Ankney CM, et al. Adoptive T-Cell Transfer to Treat Lymphangioleiomyomatosis. Am J Respir Cell Mol Biol. 2020 Jun;62(6):793–804.

131. Pacheco-Rodriguez G, Kumaki F, Steagall WK, Zhang Y, Ikeda Y, Lin JP, et al. Chemokine-Enhanced Chemotaxis of Lymphangioleiomyomatosis Cells with Mutations in the Tumor Suppressor TSC2 Gene1. The Journal of Immunology. 2009 Feb 1;182(3):1270–7.

132. Mittal P, Wang L, Akimova T, Leach CA, Clemente JC, Sender MR, et al. The CCR2/MCP-1 Chemokine Pathway and Lung Adenocarcinoma. Cancers. 2020 Dec;12(12):3723.

133. Gok Yavuz B, Gunaydin G, Gedik ME, Kosemehmetoglu K, Karakoc D, Ozgur F, et al. Cancer associated fibroblasts sculpt tumour microenvironment by recruiting monocytes and inducing immunosuppressive PD-1+ TAMs. Sci Rep. 2019 Feb 28;9(1):3172.

134. Chang H, Zou Z, Wang Q, Li J, Jin H, Yin Q, et al. Targeting and Specific Activation of Antigen-Presenting Cells by Endogenous Antigen-Loaded Nanoparticles Elicits Tumor-Specific Immunity. Adv Sci. 2020 Jan;7(1):1900069.

135. De Henau O, Rausch M, Winkler D, Campesato LF, Liu C, Cymerman DH, et al. Overcoming resistance to checkpoint blockade therapy by targeting PI3Kγ in myeloid cells. Nature. 2016 Nov;539(7629):443–7.

136. Suek N, Campesato LF, Merghoub T, Khalil DN. Targeted APC Activation in Cancer Immunotherapy to Enhance the Abscopal Effect. Front Immunol. 2019 Apr 2;10:604.

137. Barr TA, Brown S, Ryan G, Zhao J, Gray D. TLR-mediated stimulation of APC: Distinct cytokine responses of B cells and dendritic cells. Eur J Immunol. 2007 Nov;37(11):3040–53.

138. Grassin-Delyle S, Abrial C, Salvator H, Brollo M, Naline E, Devillier P. The Role of Toll-Like Receptors in the Production of Cytokines by Human Lung Macrophages. J Innate Immun. 2020;12(1):63–73.

139. Brignole C, Marimpietri D, Paolo D. Therapeutic targeting of TLR9 inhibits cell growth and induces apoptosis in neuroblastoma. Cancer Res. 2010;70(23):9816–26.

140. Jahrsdorfer B, Weiner GJ. CpG oligodeoxynucleotides as immunotherapy in cancer. Update Cancer Ther. 2008;3(1):27–32.

141. CPG 7909 Injection in Non-Small Cell Lung Cancer [Internet]. Available from: https://ClinicalTrials.gov/sh

142. Cheng Y, Lemke-Miltner CD, Wongpattaraworakul W, Wang Z, Chan CHF, Salem AK, et al. In situ immunization of a TLR9 agonist virus-like particle enhances anti-PD1 therapy. J Immunother Cancer. 2020 Oct 1;8(2):e000940.

143. Gallotta M, Assi H, Degagné É, Kannan SK, Coffman RL, Guiducci C. Inhaled TLR9 Agonist Renders Lung Tumors Permissive to PD-1 Blockade by Promoting Optimal CD4+ and CD8+ T-cell Interplay. Cancer Res. 2018 Sep 1;78(17):4943–56.

144. Reilley MJ, Morrow B, Ager CR, Liu A, Hong DS, Curran MA. TLR9 activation cooperates with T cell checkpoint blockade to regress poorly immunogenic melanoma. Journal for ImmunoTherapy of Cancer. 2019 Nov 26;7(1):323.

145. Sato-Kaneko F, Yao S, Ahmadi A, Zhang SS, Hosoya T, Kaneda MM, et al. Combination immunotherapy with TLR agonists and checkpoint inhibitors suppresses head and neck cancer. JCI Insight. 2017 Sep 21;2(18):e93397.

146. Mangsbo SM, Sandin LC, Anger K, Korman AJ, Loskog A, Tötterman TH. Enhanced tumor eradication by combining CTLA-4 or PD-1 blockade with CpG therapy. J Immunother. 2010 Apr;33(3):225–35.

147. Li T, Hua C, Yue W, Wu J, Lv X, Wei Q, et al. Discrepant antitumor efficacies of three CpG oligodeoxynucleotide classes in monotherapy and co-therapy with PD-1 blockade. Pharmacological Research. 2020 Nov 1;161:105293.

148. Wang Y, Xiang Y, Xin VW, Wang XW, Peng XC, Liu XQ, et al. Dendritic cell biology and its role in tumor immunotherapy. Journal of Hematology & Oncology. 2020 Aug 3;13(1):107.

149. Choi H, Song H, Jung YW. The Roles of CCR7 for the Homing of Memory CD8+ T Cells into Their Survival Niches. Immune Netw. 2020 May 20;20(3):e20.

150. Riol-Blanco L, Sánchez-Sánchez N, Torres A, Tejedor A, Narumiya S, Corbí AL, et al. The Chemokine Receptor CCR7 Activates in Dendritic Cells Two Signaling Modules That Independently Regulate Chemotaxis and Migratory Speed. The Journal of Immunology. 2005 Apr 1;174(7):4070–80.

151. Wherry EJ, Kurachi M. Molecular and cellular insights into T cell exhaustion. Nature reviews Immunology. 2015 Aug;15(8):486.

152. Miyahara Y, Chen H, Moriyama M, Mochizuki K, Kaneko N, Haque ASMR, et al. Toll-like receptor 9-positive plasmacytoid dendritic cells promote Th17 immune responses in oral lichen planus stimulated by epithelium-derived cathepsin K. Sci Rep. 2023 Nov 7;13:19320.

153. Guéry L, Dubrot J, Lippens C, Brighouse D, Malinge P, Irla M, et al. Ag-Presenting CpG-Activated pDCs Prime Th17 Cells That Induce Tumor Regression. Cancer Research. 2014 Nov 13;74(22):6430–40.

154. Su X, Ye J, Hsueh EC, Zhang Y, Hoft DF, Peng G. Tumor Microenvironments Direct the Recruitment and Expansion of Human Th17 Cells. The Journal of Immunology. 2009 Dec 21;184(3):1630–41.

155. Ankathatti Munegowda M, Deng Y, Mulligan SJ, Xiang J. Th17 and Th17-stimulated CD8+ T cells play a distinct role in Th17-induced preventive and therapeutic antitumor immunity. Cancer Immunol Immunother. 2011 Oct 1;60(10):1473–84.

156. Liu H, Ji Y, Ma X, He A, Zhao W, Zhang P, et al. Effects of CpG oligodeoxynucleotides on the differentiation of Treg/Th17 cells. Molecular Immunology. 2021 Apr 1;132:199–208.

157. Yang XO, Nurieva R, Martinez GJ, Kang HS, Chung Y, Pappu BP, et al. Molecular Antagonism and Plasticity of Regulatory and Inflammatory T Cell Programs. Immunity. 2008 Jul 18;29(1):44–56.

158. Downs-Canner S, Berkey S, Delgoffe GM, Edwards RP, Curiel T, Odunsi K, et al. Suppressive IL-17A+Foxp3+ and ex-Th17 IL-17AnegFoxp3+ Treg cells are a source of tumour-associated Treg cells. Nat Commun. 2017 Mar 14;8:14649.

159. Cervantes-Barragan L, Lewis KL, Firner S, Thiel V, Hugues S, Reith W, et al. Plasmacytoid dendritic cells control T-cell response to chronic viral infection. Proceedings of the National Academy of Sciences. 2012 Feb 21;109(8):3012–7.

160. Wu V, Smith AA, You H, Nguyen TA, Ferguson R, Taylor M, et al. Plasmacytoid dendritic cell-derived IFNα modulates Th17 differentiation during early Bordetella pertussis infection in mice. Mucosal Immunol. 2016 May;9(3):777–86.

161. Garon E, Spira AI, Johnson M, Bazhenova L, Leach J, Candia A, et al. Abstract CT224: Phase Ib/II, open label, multicenter study of inhaled DV281, a Toll-like receptor 9 agonist, in combination with nivolumab in patients with advanced or metastatic non small cell lung cancer (NSCLC). Cancer Research. 2019 Jul 1;79(13_Supplement):CT224–CT224.

162. Valkenburg KC, de Groot AE, Pienta KC. Targeting the tumour stroma to improve cancer therapy. Nat Rev Clin Oncol. 2018 Jun;15(6):366–81.

163. Wang LCS, Lo A, Scholler J, Sun J, Majumdar RS, Kapoor V, et al. Targeting fibroblast activation protein in tumor stroma with chimeric antigen

receptor T cells can inhibit tumor growth and augment host immunity without severe toxicity. Cancer Immunol Res. 2014 Feb;2(2):154–66.

164. Chen M, Xiang R, Wen Y, Xu G, Wang C, Luo S, et al. A whole-cell tumor vaccine modified to express fibroblast activation protein induces antitumor immunity against both tumor cells and cancer-associated fibroblasts. Sci Rep. 2015 Sep 23;5:14421.

165. Wen Y, Wang CT, Ma TT, Li ZY, Zhou LN, Mu B, et al. Immunotherapy targeting fibroblast activation protein inhibits tumor growth and increases survival in a murine colon cancer model. Cancer Sci. 2010 Nov;101(11):2325–32.

166. Clements D, Miller S, Babaei-Jadidi R, Adam M, Potter SS, Johnson SR. Cross talk between LAM cells and fibroblasts may influence alveolar epithelial cell behavior in lymphangioleiomyomatosis. American Journal of Physiology-Lung Cellular and Molecular Physiology. 2022 Feb;322(2):L283–93.

167. Babaei-Jadidi R, Dongre A, Miller S, Castellanos Uribe M, Stewart ID, Thompson ZM, et al. Mast-Cell Tryptase Release Contributes to Disease Progression in Lymphangioleiomyomatosis. Am J Respir Crit Care Med. 2021 Aug 15;204(4):431–44.

168. Trujillo G, Meneghin A, Flaherty KR, Sholl LM, Myers JL, Kazerooni EA, et al. TLR9 Differentiates Rapid from Slowly Progressive Forms of Idiopathic Pulmonary Fibrosis. Sci Transl Med. 2010 Nov 10;2(57):57ra82.

169. Zhong S, Cui Y, Liu Q, Chen S. CAR-T cell therapy for lung cancer: a promising but challenging future. J Thorac Dis. 2020 Aug;12(8):4516–21.

170. Non-Small Cell Lung Cancer Treatment (PDQ®)–Health Professional Version - NCI [Internet]. 2022 [cited 2023 Feb 2]. Available from: https://www.cancer.gov/types/lung/hp/non-small-cell-lung-treatment-pdq

171. Du Y, Guo M, Wu Y, Wagner A, Perl AK, Wikenheiser-Brokamp K, et al. Lymphangioleiomyomatosis (LAM) Cell Atlas. Thorax. 2023 Jan;78(1):85–7.

172. Aric Huang, Aric Huang, Chad Groer, Chad E. Groer, Ruolin Lu, Ruolin Lu, et al. Glatiramer Acetate Complexed with CpG as Intratumoral Immunotherapy in Combination with Anti-PD-1. Molecular Pharmaceutics. 2022 Oct 25;

173. Mohammed M. Milhem, Milhem MM, Yousef Zakharia, Zakharia Y, Diwakar Davar, Davar D, et al. O85 Durable responses in anti-PD-1 refractory melanoma following intratumoral injection of a toll-like receptor 9 (TLR9) agonist, CMP-001, in combination with pembrolizumab. Journal for ImmunoTherapy of Cancer. 2020 Apr 1;8.

174. Mona Yazdani, Yazdani M, Mahdi Hatamipour, Mahdi Hatamipour, Behrang Alani, Alani B, et al. Liposomal gp100 vaccine combined with CpG ODN sensitizes established B16F10 melanoma tumors to anti PD-1 therapy. Iranian Journal of Basic Medical Sciences. 2020 Aug 1;23(8):1065–77.

175. Ohtani M, Nagai S, Kondo S, Mizuno S, Nakamura K, Tanabe M, et al. Mammalian target of rapamycin and glycogen synthase kinase 3 differentially regulate lipopolysaccharide-induced interleukin-12 production in dendritic cells. Blood. 2008 Aug 1;112(3):635–43.

176. Weichhart T, Costantino G, Poglitsch M, Rosner M, Zeyda M, Stuhlmeier KM, et al. The TSC-mTOR Signaling Pathway Regulates the Innate Inflammatory Response. Immunity. 2008 Oct 17;29(4):565–77.

177. Amiel E, Everts B, Freitas TC, King IL, Curtis JD, Pearce EL, et al. Inhibition of Mechanistic Target of Rapamycin Promotes Dendritic Cell Activation and Enhances Therapeutic Autologous Vaccination in Mice. The Journal of Immunology. 2012 Sep 1;189(5):2151–8.

178. Boor PPC, Metselaar HJ, Mancham S, van der Laan LJW, Kwekkeboom J. Rapamycin has suppressive and stimulatory effects on human plasmacytoid dendritic cell functions. Clin Exp Immunol. 2013 Dec;174(3):389–401.

179. Esfahani K, Al-Aubodah TA, Thebault P, Lapointe R, Hudson M, Johnson NA, et al. Targeting the mTOR pathway uncouples the efficacy and toxicity of PD-1 blockade in renal transplantation. Nat Commun. 2019 Oct 17;10(1):4712.

180. Li H, Li X, Liu S, Guo L, Zhang B, Zhang J, et al. Programmed cell death-1 (PD-1) checkpoint blockade in combination with a mammalian target of rapamycin inhibitor restrains hepatocellular carcinoma growth induced by hepatoma cell-intrinsic PD-1. Hepatology. 2017 Dec;66(6):1920–33.

181. Cheng Y, Wang C, Wang H, Zhang Z, Yang X, Dong Y, et al. Combination of an autophagy inhibitor with immunoadjuvants and an anti-PD-L1 antibody in multifunctional nanoparticles for enhanced breast cancer immunotherapy. BMC Med. 2022 Oct 28;20(1):411.

182. Gu F, Hu C, Cao W, Li C, Xia Q, Gao Y, et al. Tumor Microenvironment Multiple Responsive Nanoparticles for Targeted Delivery of Doxorubicin and CpG Against Triple-Negative Breast Cancer. Int J Nanomedicine. 2022;17:4401–17.

183. Zhang M, Fang Z, Zhang H, Cui M, Wang M, Liu K. Reversing tumor immunosuppressive microenvironment via targeting codelivery of CpG ODNs/PD-L1 peptide antagonists to enhance the immune checkpoint blockade-based anti-tumor effect. European Journal of Pharmaceutical Sciences. 2022 Jan 1;168:106044.

184. Taveira-DaSilva AM, Moss J. Optimizing treatments for lymphangioleiomyomatosis. Expert Rev Respir Med. 2012 Jun;6(3):267–76.

185. Szwed A, Kim E, Jacinto E. Regulation and metabolic functions of mTORC1 and mTORC2. Physiol Rev. 2021 Jul 1;101(3):1371–426.

186. Foster DA, Toschi A. Targeting mTOR with rapamycin: One dose does not fit all. Cell Cycle. 2009 Apr 1;8(7):1026–9.

187. Bai Y, Xu R, Zhang X, Zhang X, Hu X, Li Y, et al. Differential Role of Rapamycin in Epidermis-Induced IL-15-IGF-1 Secretion via Activation of Akt/mTORC2. Cellular Physiology and Biochemistry. 2017 Jul 26;42(5):1755–68.

188. Chen XG, Liu F, Song XF, Wang ZH, Dong ZQ, Hu ZQ, et al. Rapamycin regulates Akt and ERK phosphorylation through mTORC1 and mTORC2 signaling pathways. Mol Carcinog. 2010 Jun;49(6):603–10.

189. Toschi A, Lee E, Xu L, Garcia A, Gadir N, Foster DA. Regulation of mTORC1 and mTORC2 Complex Assembly by Phosphatidic Acid: Competition with Rapamycin. Mol Cell Biol. 2009 Mar;29(6):1411–20.

190. Kolesnichenko M, Hong L, Liao R, Vogt PK, Sun P. Attenuation of TORC1 signaling delays replicative and oncogenic RAS-induced senescence. Cell Cycle. 2012 Jun 15;11(12):2391–401.

191. Huang J, Manning BD. A complex interplay between Akt, TSC2 and the two mTOR complexes. Biochem Soc Trans. 2009 Feb;37(Pt 1):217–22.

192. Yang G, Murashige DS, Humphrey SJ, James DE. A Positive Feedback Loop between Akt and mTORC2 via SIN1 Phosphorylation. Cell Reports. 2015 Aug 11;12(6):937–43.

193. Gayatri MB, Gajula NN, Chava S, Reddy ABM. High glutamine suppresses osteogenesis through mTORC1-mediated inhibition of the mTORC2/AKT-473/RUNX2 axis. Cell Death Discov. 2022 Jun 7;8(1):277.

194. Goncharova EA, Goncharov DA, Li H, Pimtong W, Lu S, Khavin I, et al. mTORC2 Is Required for Proliferation and Survival of TSC2-Null Cells ▿. Mol Cell Biol. 2011 Jun;31(12):2484–98.

195. Nobuhide Higashino, Higashino N, Yoshiaki Koma, Koma Y ichiro, Masayoshi Hosono, Hosono M, et al. Fibroblast activation protein-positive fibroblasts promote tumor progression through secretion of CCL2 and interleukin-6 in esophageal squamous cell carcinoma. Laboratory Investigation. 2019 Jan 25;99(6):777–92.

196. Xuyang Wen, Wen X, Xiaoping He, He X, Feng Jiao, Jiao F, et al. Fibroblast Activation Protein-α-Positive Fibroblasts Promote Gastric Cancer Progression and Resistance to Immune Checkpoint Blockade. Oncology Research. 2017 Apr 14;25(4):629–40.

197. Zicheng Deng, Zicheng Deng, Zicheng Deng, Zicheng Deng, Deng Z, Gregory T. Kalin, et al. Nanoparticle Delivery Systems with Cell-Specific Targeting for Pulmonary Diseases. American Journal of Respiratory Cell and Molecular Biology. 2020;64(3):292–307.

198. McCright J, Naiknavare R, Yarmovsky J, Maisel K. Targeting Lymphatics for Nanoparticle Drug Delivery. Front Pharmacol. 2022 Jun 3;13:887402.

199. McCright J, Skeen C, Yarmovsky J, Maisel K. Nanoparticles with dense poly(ethylene glycol) coatings with near neutral charge are maximally transported across lymphatics and to the lymph nodes. Acta Biomaterialia. 2022 Jun 1;145:146–58.

200. Hotz C, Bourquin C. Systemic cancer immunotherapy with Toll-like receptor 7 agonists. Oncoimmunology. 2012 Mar 1;1(2):227–8.

201. Biswas SK, Lopez-Collazo E. Endotoxin tolerance: new mechanisms, molecules and clinical significance. Trends in Immunology. 2009 Oct 1;30(10):475–87.

202. Yeo SJ, Yoon JG, Hong SC, Yi AK. CpG DNA Induces Self and Cross-Hyporesponsiveness of RAW264.7 Cells in Response to CpG DNA and Lipopolysaccharide: Alterations in IL-1 Receptor-Associated Kinase Expression. The Journal of Immunology. 2003 Jan 15;170(2):1052–61.

203. Tsukada K, Kitazawa T, Fukushima A, Okugawa S, Yanagimoto S, Tatsuno K, et al. Macrophage tolerance induced by stimulation with Toll-like receptor 7/8 ligands. Immunology Letters. 2007 Jul 31;111(1):51–6.

204. Naqvi I, Giroux N, Olson L, Morrison SA, Llanga T, Akinade TO, et al. DAMPs/PAMPs induce monocytic TLR activation and tolerance in COVID-19 patients; nucleic acid binding scavengers can counteract such TLR agonists. Biomaterials. 2022 Jan 28;121393.

205. Butcher SK, O'Carroll CE, Wells CA, Carmody RJ. Toll-Like Receptors Drive Specific Patterns of Tolerance and Training on Restimulation of Macrophages. Front Immunol. 2018;9:933.

206. Kwok SK, Lee JY, Park SH, Cho ML, Min SY, Park SH, et al. Dysfunctional interferon-alpha production by peripheral plasmacytoid dendritic cells upon Toll-like receptor-9 stimulation in patients with systemic lupus erythematosus. Arthritis Res Ther. 2008;10(2):R29.

207. Bourquin C, Hotz C, Noerenberg D, Voelkl A, Heidegger S, Roetzer LC, et al. Systemic Cancer Therapy with a Small Molecule Agonist of Toll-like Receptor 7 Can Be Improved by Circumventing TLR Tolerance. Cancer Research. 2011 Jul 28;71(15):5123–33.

208. Broad A, Kirby JA, Jones DEJ, Applied Immunology and Transplantation Research Group. Toll-like receptor interactions: tolerance of MyD88-dependent cytokines but enhancement of MyD88-independent interferon-β production. Immunology. 2007;120(1):103–11.

209. Forte G, Rega A, Morello S, Luciano A, Arra C, Pinto A, et al. Polyinosinic-polycytidylic acid limits tumor outgrowth in a mouse model of metastatic lung cancer. J Immunol. 2012 Jun 1;188(11):5357–64.

210. Yi L, Sun D, Han Q, Liu Z, Zeng Z, Wu Y, et al. Interferon regulatory factor 3 mediates Poly(I:C)-induced innate immune response and apoptosis in non-small cell lung cancer. International Journal of Oncology. 2018 May 1;52(5):1623–32.

211. Zhao J, Wohlford-Lenane C, Zhao J, Fleming E, Lane TE, McCray PB, et al. Intranasal Treatment with Poly(I·C) Protects Aged Mice from Lethal Respiratory Virus Infections. J Virol. 2012 Nov;86(21):11416–24.

212. Stowell NC, Seideman J, Raymond HA, Smalley KA, Lamb RJ, Egenolf DD, et al. Long-term activation of TLR3 by Poly(I:C) induces inflammation and impairs lung function in mice. Respiratory Research. 2009 Jun 1;10(1):43.

213. Antonelli LRV, Rothfuchs AG, Gonçalves R, Roffê E, Cheever AW, Bafica A, et al. Intranasal Poly-IC treatment exacerbates tuberculosis in mice through the pulmonary recruitment of a pathogen-permissive monocyte/macrophage population. J Clin Invest. 2010 May 3;120(5):1674–82.

214. Jeon SG, Oh SY, Park HK, Kim YS, Shim EJ, Lee HS, et al. TH2 and TH1 lung inflammation induced by airway allergen sensitization with low and high doses of double-stranded RNA. Journal of Allergy and Clinical Immunology. 2007 Oct 1;120(4):803–12.

215. She L, Alanazi HH, Yan L, Brooks EG, Dube PH, Xiang Y, et al. Sensing and signaling of immunogenic extracellular RNAs restrain group 2 innate lymphoid cell-driven acute lung inflammation and airway hyperresponsiveness. PLOS ONE. 2020 Jul 30;15(7):e0236744.

216. Wiegleb G, Reinhardt S, Dahl A, Posnien N. Tissue dissociation for single-cell and single-nuclei RNA sequencing for low amounts of input material. Frontiers in Zoology. 2022 Nov 12;19(1):27.

217. Weiskirchen S, Tag CG, Sauer-Lehnen S, Tacke F, Weiskirchen R. Isolation and Culture of Primary Murine Hepatic Stellate Cells. In: Rittié L,

editor. Fibrosis: Methods and Protocols [Internet]. New York, NY: Springer; 2017 [cited 2023 May 3]. p. 165–91. (Methods in Molecular Biology). Available from: https://doi.org/10.1007/978-1-4939-7113-8_11

218. The isolation and characterization of endothelial cells from juvenile nasopharyngeal angiofibroma. ABBS. 2022 Apr 20;856–8.

219. Burja B, Paul D, Tastanova A, Edalat SG, Gerber R, Houtman M, et al. An Optimized Tissue Dissociation Protocol for Single-Cell RNA Sequencing Analysis of Fresh and Cultured Human Skin Biopsies. Frontiers in Cell and Developmental Biology [Internet]. 2022 [cited 2023 May 3];10. Available from: https://www.frontiersin.org/articles/10.3389/fcell.2022.872688

220. McBeth C, Gutermuth A, Ochs J, Sharon A, Sauer-Budge AF. Automated Tissue Dissociation for Rapid Extraction of Viable Cells. Procedia CIRP. 2017 Jan 1;65:88–92.

221. Welch EC, Yu H, Barabino G, Tapinos N, Tripathi A. Electric-field facilitated rapid and efficient dissociation of tissues Into viable single cells. Sci Rep. 2022 Jun 24;12(1):10728.

222. Maisel K, Hrusch CL, Medellin JEG, Potin L, Chapel DB, Nurmi H, et al. Pro-lymphangiogenic VEGFR-3 signaling modulates memory T cell responses in allergic airway inflammation. Mucosal Immunol. 2021 Jan;14(1):144–51.

223. Karmakar T, Banerjee S, Brahma S, Dey D, Radhakrishnan V, Chandy M, et al. A Pilot Study to Determine the Utility of Automated Tissue Dissociator for Flowcytometry Based Evaluation of Hematolymphoid Tumor Tissue Biopsies. Indian J Hematol Blood Transfus. 2022 Apr 1;38(2):403–10.

224. Montanari M, Burattini S, Ciacci C, Ambrogini P, Carloni S, Balduini W, et al. Automated—Mechanical Procedure Compared to Gentle Enzymatic Tissue Dissociation in Cell Function Studies. Biomolecules. 2022 May;12(5):701.

225. Amosu, M., Gregory, A. J., Murtagh, J. D., Pavin, N., Meyers, C. T., Grano de Oro Fernandez, J., Moore, K., Maisel, K. Mechanical Dissociation of Tissues for Single Cell Analysis Using a Motorized Device. J. Vis. Exp. (201), e65866, doi:10.3791/65866 (2023).